BIOCOMPATIBILITY AND SURFACE MODIFICATIONS OF PEEK AND PEEK / CARBON FIBRE COMPOSITES

Thesis submitted in accordance with the requirements of the University of Liverpool for the degree of Doctor in Philosophy by

SARAH RUTH SMITH

December 1990

Institute of Medical and Dental Bioengineering

ACKNOWLEDGEMENTS

Thanks to Professor Dave Williams and Dr. Roger "style victim" Turner for being patient and helpful supervisors, for prompt reading of my thesis drafts... .... and for some decent lunches. Mega thanks to everyone at ICI for help with sample preparation, surface treatments, trace element analysis and differential scanning calorimetry; I am particularly grateful to Andy Pearson and Marie O'Neil for enlivening the work. For putting up with me in the workshop but principally for "bike fixing", thanks to Jim "Oh no not you again" Blackhurst. I am indebted to Debs Haggarty for histological assistance, to Jan Chesters for the herbal tea (and SEM advice), to Dr. Pattie Doherty and Dr. Kamal for surgical support, to Dr. Rach Williams for the XPS and to John "mental giant" Hunt for being incredible fun to nag, hassle & generally annoy (also for being a minor whizz at image analysis). Thanks to the Composites Boys for practical help and adopting me as a member of their tea club. I am grateful to the Bone Research Group for being generous with their time and allowing me to use their facilities. For sewing, sweets and general mothering I am grateful to "Prof" Feeney.

Turtle thanks to Diane "flippin' Nora" Gunn, Paula "hungry" Walsh and Jane "telephonist" Wakeman for many a good laugh. Especial thanks to Janie for the bicycle and the cod liver oil pills (I'm sure they swung the balance). Finally I acknowledge the love and support of my parents and my brother and sister.

I am grateful to the Science and Engineering Research Council (SERC) and ICI Advanced Materials for funding this research as a SERC-CASE studentship.

ABSTRACT

The aim of this thesis was to investigate, as possible orthopædic materials, a family of polymers based on polyetheretherketone (PEEK). The materials studied were PEEK 450G, D150CA30 (30% chopped carbon fibre reinforced PEEK) and APC2 (68% by weight continuous carbon fibre reinforced PEEK). These materials provide a range of elastic moduli, dependent upon the volume fraction and arrangement of the carbon fibre. It is assumed that the lower elastic moduli of such materials, and especially the matching of modulus to that of bone, will overcome the problem of aseptic loosening of orthopædic devices. Surface modifications were also examined as a means of improving implant fixation by the production of a surface which is active in promoting cell attachment and spreading.

The biocompatibility of the materials was assessed both *in vitro* and *in vivo* with respect to mechanical and physiological properties. The tensile and flexural strength, flexural modulus, and microhardness of the materials was determined. Although some minor changes were seen after ageing, no repeatable trend was obtained which would indicate a deterioration in the mechanical properties. The interfacial shear strength and stiffness of APC2 rods implanted intraosseously was estimated from push-out tests. The results indicated a strength of attachment developed similar to that reported in the literature for metallic and ceramic coated devices. Intramuscular implantation showed little inflammatory reaction to the materials with the typical reaction being the formation of a fibrous capsule at the material/tissue interface at all time periods examined - from 7 weeks to 9 months. Implantation into rat femur showed the materials to be osteoconductive with very close apposition of bone tissue to the implant surface at 6 months. The bone response was examined using backscattered electron imaging (BEI) and light microscopy. Areas of remodelling associated with the material edge were distinguished using BEI. The cytotoxicity of the materials was examined using solid and extracted forms. A primary and a secondary cell line were used and three quantitative cytotoxicity tests performed: the MB test (cell number), the MTT test (cell respiration), and the ^{3}H-Tdr test (cell proliferation). Cell growth up to the edge of the material was also assessed qualitatively using a direct contact assay. The materials were found to be non-cytotoxic as compared to controls (medical grade polyethylene and PVC containing 4% lead stearate). Stimulation of human neutrophils by powdered PEEK was measured using a chemiluminescence assay; the results obtained were inconclusive. The adhesion of cells onto the material surface was examined using SEM. All the test material surfaces (as received) were found to support both primary and secondary cell adhesion.

PEEK and APC2 surfaces were modified using glow discharge treatments to encourage cell adhesion and spreading. The surface wettability was modified using Ar, O_2, HFP & HFB plasmas and surface roughness induced using an O_2 plasma etching technique. SEM of cells on the material surfaces in conjunction with image analysis was used to assess the *in vitro* response to the modified materials. Increased cell adhesion and spreading were seen on the roughened (O_2 plasma etch) and more wettable (Ar and O_2) substrata in the presence of serum. In the absence of serum, the more hydrophobic substrata were seen to be more attractive to cell adhesion although not necessarily cell spreading. The *in vivo* response to the modified materials was studied during the early wound healing stage using immunohistochemical stains together with image analysis, although attempts to correlate these observations with the *in vitro* studies were not successful.

CONTENTS

1.1 Review of the use of materials in orthopædics

Since the introduction of aseptic surgical processes by Lister towards the end of the nineteenth century, alloplastic materials of all types have been implanted into the body to fulfil a variety of functions ranging from simple support during healing to active physiological roles. Presently, tissues as diverse as the blood vessel, cornea, heart valve, and femoral head can be successfully replaced.

Orthopædic surgery especially, has made use of implant materials with the fixation of fractures being one of the most common and oldest applications of materials in surgery. Metal wires, screws, and metal plates fixed to bone by screws, have been used to internally fixate fractures since the late nineteenth century. In 1890 Thomas Gluck, a German surgeon was implanting joints fashioned from ivory into the hip, finger and thumb of soldiers injured in the Crimean war. Realising that loosening of the joint prosthesis due to inadequate fixation was a major complication, he tried using a "bone glue" composed of colophony, pumice, and plaster of Paris to secure the implants. Inadequate fixation of implants to bone is still a major reason for prosthesis failure.

Conditions of the musculoskeletal system requiring replacement or augmentation by materials can be congenital (congenital dysplasia of the hip, where the hip socket is not normally modelled); developmental (scoliosis); traumatic (fractures); degenerative (osteoarthritis, where excessive erosion of the cartilage surface associated with excess bone formation at the margins of the joint leads to gradual loss of function because of pain and stiffness); or neoplastic (either benign, such as occurring in Jaffes disease, or malignant,

such as a Ewing tumour seen in children with osteosarcoma).

Materials used in orthopædic surgery include metals, ceramics and polymers with the successful outcome of operation resting on the correct choice of material, prosthesis design and surgical technique. It is clearly necessary for the material to perform the required mechanical function and be biologically compatible, that is to say it must be a 'biocompatible' material. Biocompatibility has been defined as the ability of a material to perform with an appropriate host response in a specific application (Williams, 1987a). The concept of biocompatibility as applied to the choice of materials in the orthopædic field is one which has only recently been systematically applied. Failure of the early prosthetic and fixation devices was due to a combination of non biocompatible materials and poor surgical technique. The materials chosen were either mechanically inadequate, or provoked an intense inflammatory response due to material toxicity. The introduction of alloys based on stainless steel and cobalt in the 1920s and 1930s led to the design of prostheses which were more corrosion resistant with improved mechanical properties.

The use of arthroplastic techniques employing implant materials to relieve joint pain, has been suggested to be one of the main surgical advances of recent years (Lee, 1981). Few materials have been found to be both biologically compatible and mechanically adequate. In the 1920s, Smith-Peterson used first a glass and then a celluloid cup to cover the reshaped head of the femur in an attempt to provide a new bearing surface. The glass proved too brittle and the celluloid generated too much foreign body reaction. A Bakelite version was tried in 1937, and again proved unsatisfactory. Acrylic cups were implanted by Harmon, and acrylic femoral heads sometimes with a metal stem, by Judet; however the resin was too brittle to withstand the load and shattered. In 1943, Moore and Bohlman designed a complete upper femur (shaft, head and neck)

(shaft, head and neck) for use in a patient with a malignant giant cell tumour. This design, where the load is transmitted through the femoral neck with an intramedullary stem to prevent rotation of the prosthesis, was the forerunner of the Moore femoral prosthesis introduced in 1951. These femoral head prostheses were successful for treating subcapital fractures of the hip, and avascular necrosis of the femoral head, especially when the acetabulum is well preserved. The stems were press-fitted for fixation with large fenestrations in the proximal portion of the stem to encourage fixation by tissue.

Unfortunately, the Moore prosthesis is unsuitable for treating chronic osteoarthritis, a condition affecting a vast proportion of the older population. In this condition, where there is excessive wear of the acetabular cup and erosion of the femoral head both components of this ball and socket joint should be replaced. The first "total hip replacements" (THR), where components were provided for both articulating surfaces were carried out by Wiles in 1938 and consisted of a stainless steel acetabular cup held in place by screws and a femoral component secured by a bolt. Prostheses of this design were never successful for very long, mainly because sufficiently inert materials were not available, the fixation of the components to the bone was inadequate and there was excessive wear of the ball on the edge of the cup.

The idea of a total hip replacement was pursued by McKee in Norwich who used a cobalt-chrome, metal on metal, modified Thompson design in the 1950s. Screws were used for fixation with the inevitable problems of loosening suffered by all designs of the same period.

1.2 Fixation of implants using cement

Gluck may be thought of as being ahead of his time in trying to solve the problem of fixation using a "bone glue" and it was not until 1951 that the idea was reintroduced by Haboush. Unfortunately the hip dislocated shortly after surgery and the technique was not pursued again until 1960, when Charnley used a self-curing methyl methacrylate (Charnley, 1960). The polymethylmethacrylate or PMMA has a dual role; fixation, by mechanically keying into irregularities on the surface of the two parts to be bonded, and load transmission, through the prosthetic component into the femur.

Initially a cemented metallic femoral stem with a small 22mm head bearing against a press-fitted socket was used with the socket fabricated from polytetrafluoroethylene (PTFE). However, severe wear of the PTFE was experienced and the uncemented components soon loosened leading Charnley to switch to cemented sockets made from ultra high molecular weight polyethylene (UHMWPE). By this time, the McKee-Farrar type of total hip replacement, involving metallic femoral and acetabular components was also being cemented in place; although it has a higher coefficient of friction, less wear is experienced than in the Charnley combination. More recently, the cement has also been loaded with gentamicin in an attempt to overcome problems of infection associated with joint replacement (Garvin, 1988). The gentamicin impregnated cement was found to reduce the infection rate.

The knee joint is also prone to arthritis and components for the knee appeared around 1940 with mould arthroplasties being performed by Smith-Peterson, Aufranc and Campbell. To overcome severe knee arthritis, hinges were introduced from about the 1950s. The Walldius and the Shiers hinge were two popular designs with the Walldius constructed of first acrylic and then cobalt-chrome alloy and the Shiers being made from stainless steel

(Girzadas, 1968). Although useful for many patients, the removal of a large amount of bone, loosening and infection led to the development of more conservative approaches to knee prostheses. Unicompartmental metallic prostheses where one side of the knee is left with normal cartilage were developed by McKeever and MacIntosh (MacIntosh, 1958). About 10 years after introducing cemented metal-plastic hips, Charnley introduced a knee prosthesis based on this same combination (Gunston, 1971). Developments for other joints postdated those of the hip and knee. Metallic hinges for the elbow and finger joints were used from the early 1950s, and suffered from the same problems of loosening as non-cemented hip and knee components. In the mid 1960s, silastic spacers for the finger joint were independently developed by Swanson and Niebauer.

1.3 Aseptic loosening of cemented implants

Aseptic loosening of cemented prosthetic components is the major long term complication of total joint replacement. The problem is minimized with older and more sedentary patients, with a total hip replacement expected to function satisfactorily for between 10 and 15 years. However, this time period is reduced in younger patients as their continued growth and increased activity leads to greater stress on the prosthesis, inevitably producing loosening. The problem is related to the use of cement and to the use of high modulus materials such as stainless steel and cobalt chrome alloys.

1.3.1 Cement related problems

Although successful in the fixation of joint prostheses, and especially the total hip replacement, PMMA does have problems associated with use which lead to loosening of the implant. Polymerization is an exothermic reaction

which must take place *in situ*; if polymerization is incomplete, the toxic monomer may adversely affect the local tissue response. The heat given out causes necrosis of tissue at the place of insertion and there can be an acute drop in blood pressure leading to the possibility of cardiac arrest.

The physiological response to bulk PMMA is the formation of a fibrous tissue membrane (Johanson, 1987) reflecting mechanical, chemical, and thermal induced trauma. When retrieved from loosened prostheses and examined, this interface membrane is seen to be thickened and to contain a pronounced monocyte-macrophage infiltration, with formation of giant cells (Bullough, 1988). Particulate PMMA generated by micromotion or strains experienced by the loaded cement-bone interface has been shown to have an inflammatory effect *in vitro* by stimulating the release, by mononuclear cells, of bone resorbing mediators such as interleukin-1, tumour necrosis factor, and prostaglandin E_2 (Herman, 1989; Horowitz, 1986). *In vivo*, osteoclastic activity has been found to be increased around areas associated with particulate PMMA (Jasty, 1986).

PMMA has been shown to age mechanically thereby compromising its mechanical suitability for such a highly loaded environment. Decreases in the flexural modulus (Looney, 1986) and short term increases in creep strain (Chwirut, 1984) have been reported. Laboratory controls have been compared to PMMA specimens implanted for periods ranging from 15 days to 8 years and found the test samples to exhibit a decrease in compressive strength and Young's modulus (Fernandez-Fairen, 1983).

There are also problems in using cemented components in the revision of failed primary cemented joint replacements. The loss of bone associated with such failed implants leaves the surgeon with a femur characterized by lack of cancellous bone and a sclerotic, smooth walled, highly vascular appearance.

Under these conditions it is impossible to achieve the microinterlock between PMMA and host bone necessary for long term fixation (Krause, 1982).

1.3.2 Material modulus related problems

The modulus of metallic materials used in cemented prostheses is approximately 10 times that of bone as the Young's modulus for Co-Cr-Mo alloy is 220 GPa as compared to 20 GPa for cortical bone. This mismatch of modulus between the bone and the implant serves to shield the bone from physiological levels of stress; the bone is under-loaded and resorption takes place resulting in a porotic structure. There is no longer close apposition between the bone and the implant and loosening can occur. Such alloys also undergo corrosion producing an adverse tissue reaction and a deterioration in mechanical properties, especially fatigue strength (Cahoon, 1978).

The titanium alloy Ti-6Al-4V, was introduced in the early 1980s as a low modulus, biocompatible orthopædic material (Albrektsson, 1981). Unfortunately it suffers from poor wear resistance and has been reported to be especially susceptible to abrasive wear by particles of acrylic cement (McKellop, 1981). Clinically, severe osteolysis induced by metallic wear debris leading to loosening has occurred. Upon revision, black staining of the soft tissues adjacent to the failed implant, a blackened fibrous membrane at the interface and giant cells and histiocytes containing metallic debris have been seen (Lombardi, 1989; Agins, 1988). Recently, the wear and fatigue properties of titanium alloys have been improved using a surface treatment known as ion implantation where nitrogen or oxygen ions are implanted into the surface, increasing the hardness and reducing the wear of the alloy (Buchanan, 1987).

1.3.3 Cementless designs

To overcome the above problems and produce more permanent joint prostheses, cementless designs incorporating lower modulus materials are being investigated. Apart from the goal of long term interface stability, cementless components offer several potential advantages over cemented ones including reduced operating time, reduced initial trauma to the endosteal bone surfaces, reduced volume of synthetic material, and improved ease of revision.

For a cementless total hip replacement to be successful there must be firm attachment of the prosthesis, ideally to bony tissue. The modulus mismatch between implant and bone should be reduced to a minimum to reduce remodelling. The femoral stem component must be of an adequate size to enable the transfer of load to bone with the minimization of local stresses and motion, thereby reducing bone resorption and avoiding remodelling in the long term.

Fixation of cementless prostheses may be achieved in several ways; by using pins and plates with the associated problems of stress concentration and loosening, by achieving an interference fit, by the ingrowth of either bony or fibrous tissue into surface pores or by the direct apposition of bone onto the implant.

All of these designs require a close geometric fit between the femoral component and supporting bone for successful function. Despite the importance of this fact, few published studies have examined endosteal geometry in sufficient detail for use in the design of components. A recent study by Noble (1988) disputes the reasoning that implant design may be based upon relationships derived from periosteal morphology or that an accurate fit may be selected on the basis of the reamed diameter of the medullary canal. His group reasons that femoral components must

accommodate substantial variability as there is a wide range of endosteal morphology, and therefore one basic design of femoral stem is not compatible with optimal performance of a cementless total hip replacement (THR). Customized implants have been produced using quantitative computed tomography sizing methods in conjunction with computerized stem design programs (Robertson, 1987).

1.4 Porous coated prostheses

Experimental work in the early 1970s established satisfactory bone ingrowth into microporous chrome-cobalt alloy and fibremesh titanium (Engh 1983). It was found that bond strength exceeded PMMA/bone bond strength after only 5 weeks. The success of these experiments led to the design of porous surfaced THR prostheses. The surfaces used in orthopædics are constructed from metals, polymers and ceramics. A porous coating is defined as a 3-D interconnecting array of pores; as distinct from an irregular surfaced (textured) implant. It is generally found that an interconnecting pore size of around 100-200μm is optimal for tissue ingrowth irrespective of the material. The difference in behaviour of porous coatings is found in their influence on the adaptive remodelling of bone around the implant.

1.4.1 Metallic coatings

Metallic porous coatings which have been investigated include cobalt-chromium and titanium. Either powder-made or fibre-made porous coatings can be used with the surface produced by a sintering technique. The first porous cobalt-chromium prostheses had sintered microspheres of cobalt-chromium alloy approximately 100μm in diameter, yielding an equivalent pore size. Early designs had stems that were fully coated. The postoperative results

were not good; of the patients who still had a hip in place, 50% had developed a radiolucent line around the prosthesis at 6 months and demonstrated sclerosis around the prosthesis tip at 1 year. This was due to stress shielding as a result of bony ingrowth into the distal part of the femoral component (Cameron, 1982). Later prosthetic designs have limited the coating to the proximal two-thirds, and subsequently the proximal third of the stem, to ensure loading of the proximal femur and to facilitate removal. Acetabular cup components with a similar cobalt-chrome coating have been available since the early 1980s and have three spikes for initial stabilization, for example the Harris-Galante prosthesis.

1.4.2 Ceramic coatings

Ceramic materials are generally too brittle to be used as bulk implant materials in load support situations, but have been applied to metallic components as porous coatings. Both aluminium oxide and calcium phosphates have been used, with calcium phosphates such as hydroxyapatite being particularly attractive because of their excellent biocompatibility. Most (Jarcho, 1981) histologic studies report direct bony contact between hydroxyapatite and host bone with little tendency to form a soft tissue encapsulation of the materials; under these circumstances, hydroxyapatite is described as an osteoconductive material. It has been suggested that there is chemical bonding between the bone and the ceramic (Hench, 1978). Bioactive ceramics are a family of ceramics which contain glassy phases and are said to encourage direct bone bonding. The necessary precursor to bonding is a surface reaction that releases Ca^{2+}, P^{4+} and Na^{+} ions and produces a water rich gel on the implant surface. The best known of these materials is Bioglass 45S5 developed by Hench and coworkers.

1.4.3 Polymeric coatings

Porous polymer coatings on metallic prosthesis cores have been developed recently using coatings such as porous polysulfone (Richards), porous high-density polyethylene (Johnson & Johnson), and porous carbon-fibre reinforced PTFE (Proplast by Vitek). All of these coatings are undergoing clinical trial but the most extensive human trials have been with Proplast. Tullos (1984) reported 36% failures in a series of 47 hips followed for an average of 37 months. Examination of 5 retrieved prostheses revealed failure through the Proplast coating which was ingrown with fibrous tissue. The tensile strength of Proplast is reported to be about 1MPa and it was concluded that the coating had insufficient strength to withstand normal weight bearing loads.

1.4.4 Problems associated with porous coatings

The fixation of cementless prostheses by bony ingrowth is the subject of much debate. Retrieval studies have found ingrowth to be limited, with only a fraction of the acetabular and femoral surfaces being fixed in this way (Haddad, 1987). In a retrieval study of devices with a porous coating, Cameron (1986) failed to show bone growth in any of a series of femoral components, although they had functioned well for up to 6 years. Clinical success, therefore, is not necessarily indicative of bone ingrowth. A study by Cook et al. (1988) reported definite evidence of bone ingrowth within the pores of 18 out of 22 femoral stems, however, only 5 out of the 22 stems demonstrated ingrowth of bone into more than 5% of the available pore volume. The problems of porous coated devices have been related to the surgical precision required to obtain bone ingrowth, the careful selection of prosthesis size to ensure maximal fit, the stress shielding effects of certain designs, the necessity for immediate stability, and the unknown clinical

consequences of metal ion release from the metallic porous surfaces (Spector, 1987). As an alternative to porous coated cementless designs, press-fitted devices with textured articulating surfaces are becoming popular. Townley (1988) has described the successful modification of both hip and unicompartmental knee components. Sharp edged, bone penetrating, striated surfaces designed to provide both immediate mechanical stability and subsequent permanent interface fixation through linear bone ingrowth were provided. Lord (1988), Judet (1978) and Andrew (1985) have reported success using uncemented devices with surface irregularities, rather than an interconnecting porosity, that do not meet the design parameters determined to be optimal for bone ingrowth.

1.5 Low modulus materials

Different design criteria guide the selection of materials for the bulk and surface of the device. Initially, strength and corrosion resistance were the most important criteria governing the selection of materials for femoral stems, with stainless steel being superseded by the more corrosion resistant cobalt-chrome alloys. The introduction of noncemented devices has led to the reassessment of the importance of material stiffness in femoral design. In cementless devices the stress shielding effect of high modulus materials is more pronounced as there is no longer a cement interface spreading the load perceived by the bone, resulting in extensive bone loss. Titanium alloys were introduced as low modulus materials with a modulus of approximately 100GPa, half that of the cobalt-chrome alloys, but it is likely that even titanium does not have a sufficiently low modulus to allow for the fabrication of stems that are flexible enough to yield near normal bone remodelling especially in femurs with large canals (Poss, 1988). To find materials having a low modulus, but which are

still strong enough to function in a load bearing situation, orthopædic surgeons have turned to advanced engineering polymers and composites.

1.6 Polymers in orthopædics

A variety of polymers is used clinically; acrylic resins as bone cement and as contact lenses, polyetherurethanes and polyethylene terephthalate as artificial arteries and polyethylene as the acetabular component in THR. Polysulfone, epoxy resin, and polyetheretherketone are under investigation as orthopædic prosthetic materials. The tissue response to polymers will vary according to the polymer chemical composition and tissue environment. The wound healing response follows a recognized pattern with the acute inflammatory response initiated by the release of complement, platelets, and clotting factors. Neutrophils then migrate into the wound site followed by monocytes which differentiate into macrophages. Small blood vessels, and fibroblasts which secrete collagen will eventually infiltrate the area. If an implant is placed, the first reaction will be the deposition of proteins; this pattern of deposition may affect the sequence of wound healing. If a material is biologically 'inert', the physiological response will be the formation of a collagen capsule, effectively isolating the material from the surrounding tissue.

1.6.1 Polymer degradation

Degradation in the physiological environment may occur via; micromotion at the material/tissue interface leading to the production of wear particles, the leaching of soluble plasticizers, the oxidative actions of enzymes released by cells, or hydrolysis due to swelling. The technique used to sterilize the implant may also have a degradative effect. Some polymers have a melt temperature (Tm) below that used for steam sterilization or a glass transition temperature

(Tg) near that of sterilization; melting or a change in the crystal structure may occur with a concomitant change in mechanical properties. Sensitivity to gamma irradiation at the levels used for sterilization (2.5Mrad) can result in a change in colour, crosslinking or embrittlement, again leading to a change in mechanical properties.

The production of wear particles due to micromotion between two adjacent or articulating surfaces has been seen with bone cement, UHMWPE (Amstutz, 1985) and PTFE. In all cases the wear particles invoked an inflammatory response not seen with the bulk materials. The particles may stimulate or be phagocytosed by cells such as neutrophils and macrophages, with the concomitant release of hydrolytic enzymes or oxygen radicals which may degrade the polymer. Soluble factors such as leukotrienes may also be released; these may stimulate osteoclastic bone resorbing activity.

Plasticizers and additives are generally low molecular weight compounds added to polymers to lower the Tg, thereby making the polymers more ductile and easier to process. If these compounds are leached from the polymer, there will be an increase in elastic modulus and a decrease in toughness. Mould release agents are used to aid removal of the polymers from moulds and if not removed from the surface may leach at a later date. Water may act as a plasticizing agent, if absorbed by the polymer, leading to an increase in flexibility. If gross swelling occurs, unexpected constriction of tissue may ensue.

Polymers are viscoelastic materials whose deformation is dependent on temperature and rate of loading, as well as applied load. Although generally regarded as a negative characteristic, as creep may lead to failure at stresses below the yield stress, the viscoelastic nature of polymers has been utilised in the design of a fixation plate to reduce stress shielding. A stainless steel

fixation plate backed with Silastic was found to reduce porosity and remodelling occurring under the plate when implanted in canines for 27 weeks (Korvick, 1989). As part of an orthopædic appliance, polymers will be subject to cyclical loading possibly leading to fatigue failure. Stress corrosion whereby a material in a hostile environment rapidly decays due to the combined action of stress and the environment may result in cracking and fatigue failure.

1.7 Use of composites

Polymer composites embodying a fibre or powder filled resin matrix have been recently introduced into orthopædic surgery. A composite material has been defined as that consisting of two or more physically distinct and mechanically separable materials, made by mixing the separate materials in such a way that the dispersion of one material in the other can be done in a controlled way to achieve optimum properties. Bone is a natural composite material consisting of collagen fibres in an inorganic matrix. The synthetic matrices used show good resistance to corrosion and attack in the physiological environment, but alone, would not be able to support physiological loading. Fibres have very high strength and modulus but this is only developed in very fine, brittle fibres, with diameters in the range of 7-15μm. Together, a composite may be developed which has properties superior to the properties of the individual components; a material having superior corrosion resistance with good mechanical properties. The fibres used may be in a chopped or a long, continuous form. Chopped fibres may be aligned or randomly orientated whilst the long fibres can form a laminate structure with the plies oriented according to the modulus required. In this way, the modulus of the composite may be matched to that of the bone it is supporting and an isoelastic hip prosthesis produced. Fibres and particles used include carbon and glass whilst

matrices under investigation include polysulfone (PS), polyetheretherketone (PEEK), epoxy resin, polyethylene and carbon.

1.7.1 Degradation of composites

The mechanisms of *in vivo* degradation of composites are similar to those of the polymers outlined above. If the composite is heat sensitive, differential expansion between fibre and resin can lead to internal stresses which may lead to cracking under load. Absorption of water can affect the intralaminar and interlaminar shear properties by causing degradation of the matrix-fibre interface; this may lead to debonding of the fibre from the matrix and possibly delamination in laminar structures. The geometry of the diffusion path is dependent on the fibre arrangement and volume fraction, and wicking can occur rapidly along the interface. The diffusion processes and hence the deterioration are increased in the presence of applied stress. The fibres may also be susceptible to the physiological environment, for example, glass fibre is susceptible to water leaching of the soluble oxides K_2O and Na_2O. This leaching results in surface pits and reduction of strength and may affect the host response. Leaching of sizing agents used to ensure adhesion of the carbon and glass fibres to the matrix may also occur.

1.7.2 Composites used in orthopædic prostheses

At present, carbon reinforced UHMWPE bearing components are used as the tibial component in knee prostheses, supposedly to improve the wear and creep properties of the polyethylene. However, recent studies by Wright (1988) analyzing surface damage of retrieved carbon fibre reinforced and unreinforced polyethylene, suggest that carbon reinforcement offers no advantage over unreinforced UHMWPE as an articulating surface. The increase in modulus

caused by the addition of carbon fibres was shown to increase the contact pressures and other stresses that are associated with surface damage more than it increased strength.

A carbon fibre reinforced carbon (CFRC) hip prosthesis has been developed by Christel (1987) and coworkers. The stem is made of CFRC with an alumina ceramic head and an UHMWPE cup. The CFRC material has an open porosity which can be filled with bone and can therefore be used as a noncemented implant. A clinical trial is under way with no reported complications thus far.

Osteopænia and periosteal resorption are seen with high modulus fracture fixation plates for the same reason as in joint prostheses. Upon removal of the device, the weakened bone is vulnerable to refracture for several weeks. Ideally fixation devices would have sufficient stiffness to facilitate fracture healing whilst allowing bone to carry higher stresses during remodelling. Several researchers have investigated various composite systems for use in this situation. Graphite fibre methylmethacrylate resin has been favourably compared to stainless steel plates in the repair of radial osteotomies (Woo, 1974), and its properties under dry/wet conditions have been examined (Ekstrand, 1989). Fractures of the human tibia have been fixed using carbon fibre reinforced epoxy resin plates (Tayton, 1982). A carbon fibre reinforced carbon composite has been investigated by Adams (1984). Short carbon fibre reinforced nylon 6-10 and polyester plates having elastic moduli approximately half that of bone have been satisfactorily used to fix canine fractures (Gillett 1985). The mechanical properties of a carbon fibre reinforced polysulphone composite plate have been recently been investigated with a view to its use as a spine plate (Wenz, 1989). Biocompatible orthopædic polymer is a resorbable composite developed by Skondia et al. (1987) as a bone filling material. If reinforced with polyamide 6, it is strong enough for load bearing applications,

and is being considered for use as an intramedullary rod. Finite element analysis (2D) has been used to design a collarless prosthesis which has maximum stiffness at the core and lower stiffness at the bone-implant interface. A carbon fibre core was envisaged surrounded by a hydroxyapatite - polyethylene outer shell (Shirandami, 1990). Polyetheretherketone, a thermoplastic matrix fabricated by ICI filled with carbon fibres is another composite system suggested for use as an orthopædic material. Preliminary *in vivo* (Williams, 1987b) and *in vitro* (Wenz, 1990) toxicity testing has been reported and the material found to be non-toxic. Recently, Brown et al (1990) reported the effect of short term ageing on the fracture toughness and flexural strength properties of a chopped carbon fibre filled PEEK composite in comparison to similar thermoplastic composites. The PEEK composite was found to be superior to the polysulphone and polybutylene terephthalate composites examined. Mechanical and biocompatibility evaluation of PEEK/carbon composites has also been performed by Spector (1990). The properties evaluated were found to be superior to PS/carbon composites examined simultaneously. PEKEKK (polyetherketoneetherketoneketone) is a similar resin to PEEK also being investigated as an orthopædic material. Cytotoxicity assays using the agar overlay test show the resin and PEKEKK/carbon composites to be non-toxic (McMillin, 1990). Further investigation of PEEK based composites forms the basis of this thesis.

1.8 Aims of thesis

The first part of this thesis is concerned with a detailed examination of the biocompatibility of PEEK, chopped carbon fibre reinforced PEEK (D150CA30), and long carbon fibre reinforced PEEK (APC2). The toxicity of the materials both *in vitro* and *in vivo*, and the degradation of the mechanical properties by long term ageing has been examined.

The interface between the implant material and bone has been recognized as influential in the successful fixation of orthopædic devices. The exact components of the interface which are significant are not known, but material factors thought to be important are surface chemistry and morphology. By chemically or physically modifying the surface of an implant material, optimal bony tissue integration or apposition may be obtained. This would provide an alternative method of fixation to cement or mechanical fastening, without the drawbacks associated with the use of either technique. To influence the interfacial reaction between the test materials and tissue, the surface chemistry and morphology of the PEEK materials were modified using plasma techniques. Cell culture and implantation assays were used in conjunction with image analysis to assess the effect.

In summary, the aims of this thesis were to assess the biocompatibility of PEEK based materials; and to examine the impact of surface modifications on interfacial reactions.

2.1 PEEK

The materials used in the study are based on poly(aryl-ether-ether-ketone), PEEK, a semicrystalline, thermoplastic resin introduced in 1981 by ICI under the trade name of Victrex. A thermoplastic resin derives its strength from the inherent properties of the monomer units and the very high molecular weight; unlike thermosetting resins, such as the epoxies, which are stabilized by crosslinks. As a thermoplastic, PEEK is melt processable and can be converted into a range of shapes using a variety of fabrication techniques including extrusion and injection moulding. The resin is produced in the form of a powder which for ease of processing is formed into granules using an extrusion technique, whereby the powder is fed into a heated barrel, extruded as a solid lace and chopped into granules. To produce components the granules are injected at temperature and pressure into the desired mould.

A variety of unreinforced grades of PEEK are available: PEEK 150, an easy flow grade which has a low melt viscosity making it especially suitable for metal coating and composites production; PEEK 380, a medium viscosity grade suitable for film, monofilament and wire coating; PEEK 450, a general purpose grade for injection moulding; and speciality formulations for bearings applications. The PEEK 450 grade was used as the unfilled polymer in this study; different grades were used in the composites. PEEK has a wide variety of applications: as insulation of high performance wires and cables in the marine, nuclear, oil well, electronics and aerospace industries; as bearings for the automotive industry; and as the resin matrix for composite structures used in the aerospace industry.

2.1.1 Morphology

Morphologically, PEEK has been shown to consist of two phases; an amorphous phase of entangled molecular chains and an ordered crystalline phase where spherulites may be seen (Blundell, 1983). The level of crystallinity is approximately 30% in commercially available grades. This microstructure is dependent on the processing conditions of the polymer and influences the mechanical and physical properties. To ensure homogeneity, commercial PEEK products have been designed to be insensitive, as regards the degree of crystallinity and spherulite size, towards a wide range of processing conditions. They have a high nucleation density (number of spherulites per unit volume) meaning that slight variations in the processing conditions do not affect the microstructure; consequently, the product has reproducible and therefore reliable properties. This is particularly important if PEEK is to be used as an orthopædic, load bearing implant, which may be processed several times before the finished product is made.

2.1.2 Mechanical properties

The mechanical properties of commercial grades of PEEK are well documented. Under load, unreinforced PEEK exhibits yielding indicating its ductility, with tensile elongation of 50% at room temperature. Data sheet values for mechanical properties of the 450G grade at room temperature are; tensile yield stress = 92 MPa, tensile modulus = 3.6 GPa, flexural strength = 170 MPa, and flexural modulus = 3.6 GPa (ICI, 1988). PEEK exhibits good creep, fatigue and wear properties; all necessary considerations for a material to be used in a bearing application under cyclical loading, as for instance in the case of a replacement hip joint.

2.1.3 Environmental resistance

The aromatic rings of the polymer molecules (Figure 2a) hinder molecular rotation resulting in a fairly rigid chain, imparting high temperature stability.

Figure 2a : Structure of PEEK

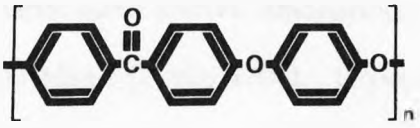

The glass transition temperature, T_g of the amorphous phase, at which the chains start to disentangle and the polymer becomes less viscous, occurs at around 143°C. The crystalline phase melts at T_m=334°C, resulting in an amorphous, viscous liquid (Blundell, 1983). The continuous use temperature is 200°C (Attwood, 1981). PEEK exhibits good environmental resistance in comparison to other aromatic thermoplastics. This has been attributed to its crystalline structure. At room temperature the only solvent it is soluble in is concentrated sulphuric acid (Attwood, 1981). At elevated temperatures, PEEK grades are affected by exposure to strong acids and alkalis; both causing a loss of tensile strength. Acids can cause embrittlement but have little effect on stiffness. Under stress, the integrity of the polymer can be reduced; for example under a 3% strain rate for 1 hour, acetone can induce crazing.

The solubility of water in PEEK has been examined by many workers. Grayson et al (1987) reported the uptake to be 0.44% at 35°C and 0.55% at 95°C. The solubility following sorption and resorption was found to be the same indicating the morphology of the resin to be unappreciably altered by the sorption-desorption-resorption cycle. Hot water immersion at 200°C for periods of time up to 2500 hours produced an initial increase in tensile and flexural properties followed by a decrease to equilibrium for tensile strength and a continued decrease in flexural strength (ICI, 1990).

As a component of a medical device, PEEK would have to be sterilized before use; conventionally using either steam or gamma irradiation. Repeated steam cycles at 138°C have been shown to increase the tensile strength by approximately 10 MPa over 250 cycles, each cycle lasting 3.5 minutes (ICI, 1990). Irradiation experiments have shown amorphous PEEK to be resistant to attack up to a dose of 1000 Mrad (Yoda, 1984). Experiments on PEEK having a 15% crystallinity level found an increase of 1% in elastic modulus at a dose of 5000 Mrad (Nguyen, 1987). It is clear that commonly used medical sterilization techniques would not have a detrimental effect on the morphology or mechanical properties of PEEK.

2.2 PEEK / Carbon composites

PEEK may be reinforced with either glass or carbon fibres to produce a composite material benefitting from the corrosion resistance of the matrix and the superior strength and stiffness of the reinforcing fibres (Turner, 1986). The fibre may be either chopped or continuous. Two carbon fibre reinforced PEEK materials were used in this study; D150CA30, "an easy flow grade" injection moulded material containing 30% chopped carbon fibres, and APC2, containing 61% carbon fibres (volume fraction) in the continuous form. The volume fraction of carbon fibres in APC2 may be varied by interleaving the laminar structure of APC2 with neat PEEK resin obtaining different material properties. The sources of carbon fibre used in the fabrication of each composite are different; Hercules Magnamite AS4 carbon fibre is used in APC2 and Courtaulds XAS in D150CA30.

The structure and properties of the fibre-matrix interface play a major role in the mechanical and physical properties of composite materials. Stresses are communicated from the matrix to the fibres via the interface; there must therefore be strong adhesion between the fibres and the matrix. The carbon fibres used in D150CA30 are specially coated (sized) to enhance the chemical bonding between the fibre and the PEEK, and to ease processing. Etching techniques have shown the carbon fibre surfaces to act as nucleating sites, with spherulitic growth emerging from the fibre surface before initiation takes place in the matrix (Peacock, 1986). SEM micrographs of APC2 fracture surfaces show ductile PEEK layers covering the carbon fibres indicating the strong adhesion between fibre and matrix (Cogswell, 1983).

2.2.1 Strength anisotropy

In the injection moulded D150CA30 composite, flexural modulus is increased from 3.6 GPa to 14.1 GPa and the tensile strength is increased from 92 MPa to 211 MPa (ICI, 1985). Unlike the unreinforced matrix, the strength properties of D150CA30 are anisotropic. Anisotropy occurs in the injection moulding of D150CA30 granules (produced by mixing fibres with the PEEK powder and extruding) where fibres can be aligned in the direction of melt flow. It has been shown that fibres in the outer or skin layers of the material are aligned in the direction of flow whilst those in the core are transversely aligned (Bozarth, 1987). The properties in flexure will be dominated by the skin, as the strain is a maximum at the surface in bending. A unique value for stiffness or strength will not exist; moulding thickness and gate geometry will have an overriding influence. The thinner the moulding the more dominant the effect of skin layers.

Continuous carbon fibre reinforced PEEK samples also exhibit strength anisotropy, but due to the lay up design and not moulding technicalities. A laminate structure is built up from individual plies cut from pre-impregnated (pre-preg) tapes consisting of a single ply of continuous carbon fibres in the PEEK matrix. Single plies may be compression moulded together under heat and pressure with the plies layed up, or orientated, as desired; thereby achieving different mechanical properties. The tensile strength of APC2 may vary from 80 MPa to 2130 MPa for unidirectionally layed up test specimens depending on the direction of test. The lower value is for a test conducted at 90° to the fibre direction whereas the high value is obtained if the test is conducted in the same direction, 0°, as the fibres. The tensile modulus varies from 8.9 GPa to 134 GPa, flexural strength from 137 MPa to 1880 MPa and flexural modulus from 8.9 GPa to 121 GPa, again depending on the orientation of test (ICI, 1986). Components fabricated from APC2 can therefore be designed to achieve specific strengths and stiffnesses. This would be a distinct improvement in orthopaedic prosthesis design, where mis-match of moduli between implant and bone leads to stress shielding, bone resorption, and prosthesis loosening.

2.2.2 Environmental resistance

The environmental resistance of the carbon fibre composites is similar to that of the unreinforced PEEK matrix. The composites will be most vulnerable to environmental attack at the interface between the matrix and the carbon fibre, with a further weak point being the interlaminar interface in the APC2 composites. The strength of the interlaminar interface may be measured using fracture toughness measurements, which are a measure of the ability of the material to resist defect initiation and propagation. A study by Wang (1989)

showed that the fracture toughness of APC2 was unaffected by moisture absorption. Water absorption by D150CA30 is estimated to be less than that of the PEEK matrix, at 0.06% for 24 hours immersion at room temperature (ICI, 1985). The effect of environmental ageing on mechanical properties of short carbon fibre reinforced PEEK is variable depending on the orientation of the test. Measurements on mechanical properties taken parallel to the fibre orientation show little effect of ageing; however, measurements taken in the direction where matrix characteristics are dominant show a greater effect.

The excellent environmental resistance and mechanical properties of PEEK and composites based on this resin, make it an ideal candidate material for orthopædic prostheses. The fabrication of components from thermoplastic based composites is faster than that of thermoset based composites such as carbon fibre reinforced epoxies. A range of resins and composites is available allowing the tailoring of the prosthesis to the precise requirements. Specially formulated bearing grades may be used for situations such as the replacement of a femoral head where the implant will be subject to a bearing stress. The flexural strength and modulus of a fracture fixation plate can be optimised by varying the carbon fibre content and lay up of the material. The prospect of uncemented, low modulus total hip replacements having a longer service life may be realised using prostheses based on PEEK composite systems.

3.1 Introduction

The evaluation of materials intended for use in medical devices should include both general screening, and testing directed towards the end use of the material. In the past, mechanical properties were used as the main basis for selecting orthopædic materials, with little consideration given to the disruptive effect materials might have on the body. This distorted approach to material choice with undue emphasis on the functional properties of materials, led to the failure of implants due to adverse local and systemic tissue reactions arising from material corrosion. The introduction of appropriate *in vivo* and *in vitro* test procedures has led to an improvement in the success rate of prostheses. The effect of the physiological environment on the material's properties as well as the effect of the material on the host must be investigated. The mechanical properties of the material may be affected by the absorption of water, the leaching of low molecular weight additives, or wear caused by micromotion between the tissue and the implant. The material may prove to be toxic to the host via the leaching of soluble toxins, or the production of irritating wear particles. Even if non-toxic, the material surface or the leachate may invoke abnormal cellular responses; a stimulatory effect may lead to excessive proliferation, or, adhesion of cells to the surface of the material may be inhibited.

Guidelines for testing material biocompatibility are given by standards bodies such as the American Society for Testing Materials (ASTM), British Standards Institution (BSI), US Pharmacopoeia (USP), and the US Food and

Drug Administration (FDA); however, these standards do not incorporate quantitative test procedures for analysing the tissue or cell reaction to the implant.

3.1.1 Methods used to study the host-material interaction *in vivo*

Common tests used to assess biomaterial toxicity *in vivo* include the rabbit intramuscular implantation test, the mouse systemic injection test and the rabbit intracutaneous injection test; all forming part of USP guidelines for material assessment. In the intramuscular implantation test, strips of the test material are implanted and the tissue reaction examined at 7 days. The systemic injection test involves extraction of the material for a maximum period of 72 hours at 50°C in saline, ethanol and cottonseed oil; organs are then examined for toxic symptoms up to 72 hours after injection. The extracts can also be examined by injecting small volumes (200µl) intracutaneously into rabbits. The reactions to the materials are all assessed qualitatively and materials ranked according to certain parameters. All of these tests measure the acute toxicity of the material by gross microscopical examination of tissue, relying on the expertise of the observer in identifying cells morphologically.

It is known that the host response to a non-toxic non-degradable material is commonly the formation of a collagen capsule, but the events leading to capsule formation and the constituents of adjacent tissue can be modified by the material implanted. More detailed information on the local cell population can be obtained using enzyme histochemistry, or immunohistochemistry. In both cases either frozen or low-temperature resin embedded tissue sections are used to avoid destruction of the heat labile enzymes or cell membrane antigens. Using a combination of staining techniques, quantitative information on the type, number and even activation level of cells involved in the inflammatory

response to a particular material may be obtained. Good preservation of the interface between material and tissue is necessary for accurate, reproducible results to be obtained using these histological techniques. The removal of biomaterials too hard to be sectioned in situ leads to disruption of this interface, introducing error into the measurements. Materials which cannot be thin-sectioned using traditional glass, steel or tungsten-carbide knives, must be embedded in resin and thick sections cut on a diamond wheel. These sections must then be ground down to the required thickness. Electrochemical dissolution has been used to degrade metallic implants in situ, thus retaining an intact interface; although it is not known whether the method affects enzymes or cell markers required for specific identification.

An alternative approach to examining the tissue reaction to a material is to place the material within a cage or chamber that is implanted, from which samples of the tissue exudate can be removed at regular intervals without sacrifice of the animal. The porosity of the cage can be varied to inhibit the entrance of cells or proteins of various sizes. Enzymes, cells, and proteins present in the exudate can be quantitatively analysed using various biochemical techniques. A cage implant system has been used by Marchant et al (1983) to follow the *in vivo* degradation of a biodegradable hydrogel. Eriksson (1988) has described the use of titanium and PTFE chambers which allow removal of exudate enabling assessment of early wound healing.

The systemic dissemination of corrosion products can be followed by collection and examination of urine, faeces and blood from test animals. Trace element analysis can be performed using mass spectrometry techniques such as inductively coupled mass spectrometry (ICPMS); if radiolabels are incorporated into degradable polymers, their rate of breakdown and route can be analysed.

3.1.2 Methods used to study the host-material interaction *in vitro*

There is increasing public opposition to the use of animals for the basic screening of chemicals and cosmetics and it is widely thought that their use should be minimized in medical and pharmaceutical situations; *in vivo* experiments are also expensive and time consuming. For these reasons, appropriate *in vitro* methods of assessing acute material toxicity are becoming more popular. The use of cell cultures to assess material toxicity is based on the hypothesis that leachable, toxic chemicals that alter normal metabolic processes of cells *in vivo* will produce concomitant cytopathological changes in cells in culture.

In vitro tests utilise organ, or more usually cell cultures to ascertain the effect of the material on one aspect of cell morphology or function. The populations of cells may be derived from tissue by chemical or mechanical disaggregation, and are defined as either primary (diploid) or secondary (aneuploid) cells. Primary lines originate directly from tissue, whereas secondary lines arise from tumours or the transformation of a primary line. Primary lines retain more morphological and functional characteristics of the cell *in vivo*, but are difficult to maintain and have a finite life time. Secondary or established lines are easier to maintain and may be passaged many hundreds of times before mutating and changing their characteristic growth rates and morphology; however, they possess an abnormal chromosome number and therefore retain fewer *in vivo* characteristics. Differences between cells *in vitro*, and *in vivo*, arise because of the lack of nervous and endocrine stimulation and the dissociation of cells from a 3-dimensional geometry, although cellulose sponges are being used as growth substrata which will retain specific cell interactions. *In vitro* tests cannot approximate the complexity of interactions in the living animal, but they can provide essential information on

the intrinsic toxicity of pure materials, composites, powders and extracts. The information can be used in computer programmes which simulate the *in vivo* toxicokinetics of chemicals from molecular structure - activity models.

Cytotoxicity may be assessed using both qualitative and quantitative methods. The simplest method is to incubate the material in either solid or extracted form with the cells and examine the cultures using light microscopy. Comparison of the cell morphology to that of control cultures will enable an estimation of material toxicity to be made. Procedures such as the agar overlay (Guess, 1965) and the direct contact test (Johnson, 1983) based on qualitative ranking using light microscopy are commonly used in biomaterial assessment. Monolayers of cells are incubated with the solid material, separated by a layer of agar in the overlay test, and examined for signs of cell death or deterioration after 24 hours.

The use of dyes which distinguish between viable and non-viable cells can be used in conjunction with the above tests, to reduce the observer bias. Dye exclusion tests examine the integrity of the cell membrane after exposure to test substances, identifying non-viable cells as those which have lost the ability to exclude stain. However, a lack of correlation between dye exclusion methods and other ways of assessing cell viability has been found (Bhuyan, 1976) and they are known to give a high number of false positives. Qualitative examination of cellular morphology is useful when evaluating material biocompatibility, especially if high power electron microscopy is combined with light microscopy, but tests of this nature are open to observer bias and give no information as to the non-cytotoxic effect a material may be having on cell metabolism. Quantitative evaluation of cellular metabolic activity is required to improve the reproducibility of results and enable comparisons to be made

between materials and laboratories. In this way, the numbers of animals used in toxicity testing may be reduced.

Radiolabelled metabolites are widely used in a quantitative manner to investigate specific aspects of the interaction between a material and cell metabolism. Common radiolabelled metabolites include: ^{51}chromium, released upon cell lysis; tritiated thymidine, incorporated into the cell during proliferation; and radiolabelled proline, taken up during protein synthesis. The information obtained is accurate, but strict safety regulations must be observed with their use making them more inconvenient than non-radioactive methods.

The agar diffusion test has been modified by examining the incorporation by living cells of fluoresceindiacetate. This reagent is metabolized into fluorescein by hydrolysis of the acetate endings of the molecule. This remains in the viable cell and emits a green light upon ultraviolet excitation. The high contrast produced allows for the possibility of video-digitizing and quantitative analysis of the results (Schmalz, 1985). The light production of luminescent bacteria after exposure to material extracts has been used to assess material toxicity and was found to be more sensitive than USP *in vivo* acute toxicity tests (Burton, 1986).

Recently, semi-automated tests which rely on the production of coloured products by intact cellular enzymes, or the incorporation of a coloured compound by viable cells have become popular. The optical density of the coloured product, if rendered soluble, can be measured using a spectrophotometer. If the assay can be performed in a microtitre plate, microplate spectrophotometers can be used, enabling 96 assays to be simultaneously performed using small volumes of reagents (250µl). Serial dilutions of the test extract can be tested and the concentration which produces 50 percent inhibition, the IC50, determined. The test extract IC50 can be

compared to that of known chemical toxins to give a measure of relative toxicity. Total cellular protein can be measured in this way using kenacid blue, a reagent which reacts with protein in cells imparting a blue colour. Healthy, growing cells contain more protein than dead ones; consequently, control cultures will be dark blue. Neutral red is a vital dye taken up and stored by living cells but not by dead ones. The amount of dye retained by the cells is an indication of the number of living cells. It has been shown to give comparable results to those obtained using the Draize ocular irritancy test (Hockley, 1986).

The integrity of the respiratory chain can be monitored using methylthiazolyldiphenyl tetrazolium, or MTT. This tetrazolium salt is reduced to a blue formazan salt by the action of respiratory enzymes such as succinate dehydrogenase. The optical density of the coloured product can be measured using a spectrophotometer and is, presuming equal activation levels of all cells, an estimation of the number of viable cells in the population. A technique based on the use of MTT was first published by Mosmann (1986) as a method of assessing cell proliferation in response to various lymphokines. Modifications of this method have been used in further lymphokine assays (Denizot, 1986) and in comparison with clonogenic assays to assess the efficacy of anti-cancer drugs (Carmichael, 1987). Recently, it has been used as an acute toxicity test to screen soluble synthetic polymers (Sgouras, 1990).

The tests described above are generally only useful for evaluating *in vitro* cytotoxicity of extracts or solid materials. Quantitative examination of the effect of powdered biomaterials on cell activity requires the use of phagocytic cells such as neutrophils and macrophages, although tritiated thymidine uptake by human lymphocytes has been used to assess the toxicity of simulated wear particles from materials used in orthopædic prostheses (Pizzoferrato, 1983).

Neutrophils and macrophages may be stimulated to release superoxide and hydrogen peroxide when their cell membrane is perturbed by activating agents. Together with a marked increase in oxygen consumption, this coordinated sequence of actions is known as the oxidative or respiratory burst. The products of oxygen reduction are formed on the external and internal surface of the cell and mediate microbicidal, cytotoxic and cytolytic effects of these phagocytic cells. They may also degrade polymeric materials. Phagocytosis occurs with stimulation of receptors on the cell surface and the transport of particulate material into the cell, if particles are of a small enough size. If the material cannot be digested eg. asbestos, the material resides in the cells resulting in persistent activation and a chronic inflammatory response with ensuing tissue damage. If the particles are too large to be ingested, the material surface may still stimulate the phagocytes causing a respiratory burst. Methods used to follow the respiratory burst include microtitre based assays such as the reduction of nitrobluetetrazolium by O_2^- (Pick, 1986), and techniques based on measuring the chemiluminescence associated with metabolic activation of the hexose monophosphate shunt (Allen, 1976).

3.2 Biocompatibility assessment of PEEK materials

The PEEK materials are intended to function under load bearing conditions in close apposition to bony tissue. Accordingly, protocols were designed to ascertain: the acute toxicity of the materials in solid, extracted and powdered form, sub chronic toxicity, the adhesion of cells to the material surface and the maintenance of mechanical properties.

3.2.1 *In vivo* assessment

The toxicity of the solid materials was assessed *in vivo* by implantation in soft tissue for 7 weeks, 3, 4, and 9 months and in hard tissue for 6 months and 3 months. Muscle, although not an intended site of material use, has a more extensive blood supply than bone and will display a greater inflammatory response. The specimens were removed from the muscle, which was then embedded in wax and examined using routine histological stains. The implant specimens were examined using scanning electron microscopy (SEM).

The bone specimens were embedded in an acrylic resin, and examined using backscattered electron imaging. Backscattered electrons are produced by collision of electrons with atomic nuclei rather than with electrons, as for secondary electron imaging (SEI). There is little energy loss, but the direction of the emergent electron is changed. Unlike SEI, the contrast obtained is dependent on the atomic number of elements present; the higher the atomic number, the higher the fraction of backscattered electrons produced. Better contrast is also obtained using higher accelerating voltages than with SEI eg. 25kV rather than 15kV. Energy loss may occur due to scattering of electrons by surface topography and so the block surface was polished to reduce this error.

To obtain more information regarding the bone/material interaction throughout the bone specimen, thick sections (300μm) were cut and examined using transmitted light microscopy. Thin sections (1μm) were also obtained from the 3 month implantation period specimen.

3.2.2 Cytotoxicity testing

Cytotoxicity testing was performed using fibroblasts of both primary (human gingival) and secondary (M^cCoys) origin. A primary line was used because although established cell lines are easier to maintain, it has been suggested that diploid cells show increased sensitivity to toxic challenge depending on the cell line and the toxin (Feigal, 1985). Cytotoxicity was tested qualitatively and quantitatively using ultrahigh molecular weight polyethylene (UHMWPE) as the negative control and polyvinyl chloride containing 4% lead stearate (PVC_{lead}) as the positive control. UHMWPE was chosen for the negative control as it is widely used as the acetabular cup component of hip prostheses. It was introduced by Charnley in the late 1960s and has been successfully used in total hip replacement ever since.

Qualitative tests examined the effect of close contact of the material with cells using light and electron microscopy. In the direct contact assay, the effect of water soluble leachates released in a short time period from the materials was examined using light microscopy. Any inhibition of cell growth can be seen as a zone around the material where no cells are present. The ability of the material surface to support cell growth and maintain normal cell morphology was examined using scanning electron microscopy.

The effect of the test materials on cell viability, proliferation and attachment was quantitatively assessed using extracted, solid and powdered forms of the material. Extracts made at 37°C and 80°C were tested using MTT, MB and ^{3}H-Tdr assays and solid discs were tested using MTT and MB assays.

The MTT assay was used to assess cell viability by measuring the amount of formazan produced by the reduction of the tetrazolium salt, MTT, after incubation with material extracts or solid for 72 hours. The uptake of ^{3}H thymidine (^{3}H-Tdr) by the replicating DNA of cells in the S phase is a conventional measure of cell proliferation. Cells were exposed to material extracts for 72 hours and then incubated with ^{3}H-Tdr for 6 hours before being harvested onto glass fibre mats. These were dried, placed in scintillation fluid and counted. A culture which is being stimulated to proliferate will have a higher proportion of cells in the S phase at any one time and there will be a concurrent increase in the uptake of ^{3}H-Tdr leading to higher counts of radioactivity being recorded.

Cell number was assessed using the staining of cell cytoplasm via methylene blue (MB) (Harvey, 1986). The quantity of stain adsorbed depends solely on the quantity of cytoplasm present regardless of whether the cells are viable or not. Presuming that all non viable cells were removed by vigorous washing the assay was used to clarify the results from the MTT assay, where the results may be interpreted in terms of changes in activation or cell number. By comparison with the MB assay it was possible to determine whether significant differences in cellular response to the materials were due to different numbers of cells being present or different levels of stimulation.

The effect of powdered PEEK resin on human polymorphonuclear leukocyte activity was measured using a chemiluminescence assay. The particle size used was 40μm - too large for phagocytosis by the cells, but any stimulatory effect

of the surface may still be measured. The chemiluminescent emission of the cells was amplified using 5-amino-2,3-dihydro-1,4-phthalazinedione (luminol) and the response measured using a chemiluminometer. The positive control used was zymosan - a polysaccharide cell wall extract of yeast. When opsonized, by incubation in serum, it is capable of activating the alternative pathway of the complement system. This phenomenon is based on the interaction of complement receptor type C3 expressed on the surface of PMNs, with C3b present on the surface of opsonized zymosan particles.

Trace element analysis of extracts obtained at 80°C was performed using inductively coupled mass spectrometry (ICPMS).

3.2.3 Physiological ageing of materials

The mechanical properties of the materials are detailed in data sheets obtainable from ICI. However, it was necessary to perform some basic mechanical testing as part of biocompatibility assessment as: no standard deviations are reported with the data, the tests were designed to show maximum strengths rather than weaknesses, and the ageing experiments were carried out for short time periods under non-physiological conditions.

As an orthopædic device, the material will be subjected to compressive, tensile, torsional, shear and bending forces; dependent on specific application. In the case of the hip joint it has been shown that the joint is subject to oscillatory loading which may reach seven times the body weight. A replacement joint must be able to withstand such forces in a physiological environment without deterioration of mechanical properties. Degradation of the material's mechanical properties may occur through wear, the leaching of low molecular weight plasticizers, and the absorption of water and lipids; all possibly leading to fatigue failure.

Within the scope of this study, simple mechanical tests were chosen which emulated some aspect of the complex *in vivo* loading situation to which an orthopædic device might be subjected. Tensile and flexural stress-strain tests give an indication of the strength and toughness of a material where toughness is defined as the ability of a material to absorb energy before breaking. The elastic modulus is a measure of the ability of the material to resist deformation when loaded in the elastic region and is the ratio of applied stress to resulting strain. Microhardness testing is considered to be a nondestructive means of characterizing materials which reveals information about polymer microstructure and some aspects of mechanical behaviour.

The design of the *in vitro* tests modelled physiological conditions as closely as possible. The incubate used was phosphate buffered saline (PBS), a salt solution used as the basis of a growth medium for cells and which is balanced to provide a physiological pH and osmotic pressure. Two incubation temperatures were used; 37°C to mimic physiological conditions and 80°C to provide a more stressful environment which might accelerate any aging effects. Where appropriate, British standards were adhered to and are stated in the text.

The tensile and flexural strengths of the materials were measured after; *in vivo* ageing for 6 months, *in vitro* ageing in phosphate buffered saline (PBS) for 6, 12 and 18 months at 37°C and 80°C, and autoclaving. Flexural modulus and microhardness measurements were made at sequential periods on samples incubated at 37°C and 80°C. Vickers microhardness was measured, where the resistance of a material to indentation by a diamond indentor under load is evaluated. Preliminary experiments were done using a push-out test to assess the strength of attachment between bone and the materials after 6 months intraosseous implantation. After testing, the fractures surfaces of the specimens

were examined using SEM for evidence of fibre pull out or delamination - indicating degradation of the fibre - matrix bond.

The crystal structure of the matrix of PEEK and APC2 flexure specimens aged for 18 months at 80°C was examined using differential scanning calorimetry. Changes in the crystallinity of the matrix may occur through absorption of water, or leaching of plasticizers. These may lead to crosslinking, producing branches and side groups which can reduce the mobility of the polymer chains thus preventing chain folding and close packing.

4.1 Test materials

The test materials used were polyetheretherketone (PEEK), grade 450G, PEEK with 30% short carbon fibre reinforcement (D150CA30), and PEEK with 61% by volume long carbon fibre reinforcement (APC2); all obtained from ICI Advanced Materials at Wilton. PEEK and D150CA30 were obtained preformed as 3mm thick plaques produced by injection moulding. APC2 was compression moulded using 6 x 2" and 8 x 6" moulds in an 8" press. Unidirectional pre-preg sheets of APC2 were cut to size from a roll of pre-preg tape. Plies were laid up in the desired orientation to provide the required thickness: 8 plies giving a 1mm thick sheet and 24 plies a 3mm thick sheet. The lay up of plies was balanced and symmetrical about the neutral axis (or centre line) of the sheet, such that a resin rich face was outermost at both sides of the mould. In this way, bowing due to differential thermal contraction on cooling was avoided. The laid up stack was then placed between sheets of high temper aluminium foil (0.1mm thick) pretreated by spraying with Freekote FRP mould release agent. This sandwich was placed into the hot platen press preheated to 400°C. The moulding cycle varied according to the mould size but consisted of a preheating period at a pressure of 2 te where thermal equilibrium between the resin and the fibres was achieved, followed by a consolidation period of high pressure, 6 te, for a shorter period of time. The temperature throughout the moulding cycle was 400°C. For the 6 x 2" mould, the preheat period was 15 minutes followed by a consolidation period lasting 5 minutes.

For the 6 x 8" mould, the preheat period was extended to 30 minutes and the consolidation period to 15 minutes. The moulding cycle was completed in each case by air cooling the platens to 300°C followed by water cooling until the mould could be safely handled.

4.2 Control materials

The control materials used in the *in vitro* toxicity work were ultra high molecular weight polyethylene, UHMWPE, (Goodfellows) and polyvinylchloride containing 4% lead stearate, PVC_{lead}, (ICI Runcorn). The UHMWPE was obtained as a sheet of thickness 3mm, but the PVC_{lead} was obtained as a powder and moulded into rectangular sheets at a temperature of 180°C.

4.3 *In vivo* assessment of host response

The animals used in all the implantation experiments were black and white hooded Lister rats of the Liverpool strain which have been bred in-house for more than 30 years. The animals were anæsthetized with small animal Immobilon (Reckitt & Coleman), diluted 1:1 in sterile distilled water, at a dosing level of 0.1ml per 100g body weight. The appropriate area of the animal was then shaved. After closure of the external wound an acrylic spray dressing, Nobecutane (Astra Pharmaceutica), was applied to the wound area. This reduced the risk of infection and stopped the animal interfering with the sutures. The animals were revived using Revivon (Reckitt & Coleman) at a dose of 0.05ml per 100g body weight.

4.3.1 Intramuscular implantation

Two specimen geometries were used: a rod of dimensions 5mm length x 3mm width, and 5mm diameter discs. The discs were punched from 1mm thick plaques previously machined down from an original thickness of 3mm, whilst the rods were machined from 3mm thick plaques. The machining produced a rough surface finish in comparison to the 'as moulded' surface. The samples were cleaned by ultrasonication in Lipsol detergent, rinsed 6 times in double distilled deionized water (SDDD) and steam sterilized for 20 minutes under 20 lbs pressure.

Test materials were implanted bilaterally into the dorso-lumbar muscle region with a maximum of two specimens implanted in each side. A single incision approximately 2cm long and 3cm from the tail was made on the midline. The skin was separated from the muscle fascia by blunt scissor dissection and an incision of approximately 0.5cm length made in the muscle. Implant pockets were created using a blunt probe and the implants carefully placed. Two specimens of each material were implanted for each time period. The incision was closed with a double tie of Dexon 2/0 gauge polyglycolic acid suture material (Davis and Geck) and the external wound closed by interrupted sutures with silk (Mersilk). Four time periods were used: 7 weeks, 3 months, 4 months, and 9 months. Two samples of each test material were implanted for examination at each time period. Early implants were rod shaped but these were replaced by discs for the longer time periods (4 and 9 months) to increase the surface area of the test material in contact with the tissue. The animals were sacrificed by carbon dioxide asphyxiation and muscle tissue processed either for wax sections (2, 3, and 4 months specimens) or frozen sections (9 month specimens).

For wax histology, tissue blocks containing the implants were excised and placed immediately into 10% neutral formol buffered saline for 48 hours. The implants were removed after fixation as this process hardens tissue. Even so, they did not slip easily out of the collagen capsule but had to be carefully teased out; especially at the earlier time periods. The blocks were dehydrated and infiltrated with paraffin wax using an automatic processor, and then embedded by hand. Thin sections were cut (5μ) on a stainless steel knife and stained using haematoxylin and eosin (H & E), and van Giesen stains following standard histological procedures (Bancroft & Stevens, 1977). H & E stain identifies cell cytoplasm as pink and cell nuclei as purple; different cell types may be identified with experience but the stain is not cell specific. The van Giesen stain enables the observer to clearly identify the collagen capsule, staining it red in comparison with muscle which is stained yellow. Sections from tissue where APC2 had been implanted were also stained with Perls' stain (Bancroft & Stevens, 1977) which identifies hæmosiderin by the formation of blue deposits of Prussian Blue.

For frozen sections, the implants were removed prior to freezing and the tissue blocks secured onto cryostat chucks (Bright) using cryoembed (Bright). The blocks were then gently lowered into a cardice/isopentane mixture at -70°C and allowed to freeze. They were stored at -70°C and sectioned using a cryostat (Bright 5030). H & E and van Giesen staining was performed using standard techniques.

Upon removal, the implants were placed into neutral formol buffered saline to fix any adhering proteins or collagenous tissue. When required for SEM, they were dehydrated in 70% and then 100% ethanol (1 day each) and air dryed before being mounted on aluminium SEM stubs and gold coated.

4.3.2 Intraosseous implantation

Rod shaped implants of approximately 3mm length x 2mm diameter were machined out of the test materials leaving a rough finish on the surface. The specimen dimensions were measured to 0.1 of a millimetre using a micrometer to enable the correct choice of drill to be made. Specimens were cleaned and sterilized in the same manner as those for intramuscular implantation.

Ten implants, four PEEK and three of each of the composites, were placed into the femurs of male black and white hooded Lister rats of the Liverpool strain aged between 5 and 6 months. A longitudinal incision was made along the anterolateral side of the femur and the femur exposed by blunt dissection through the fascial layers of the muscle. The bone was cleaned of periosteum using a periosteal elevator. A 1mm drill was used to create a hole, the size of which was gradually increased to that desired by using increasing sizes of drill, usually up to 1.8mm maximum. During operation the drill and bone was constantly cooled using sterile saline and a periosteal elevator was used underneath the bone as a support and to protect the underlying muscle from damage. The implants were tapped into place and retained by an interference fit. One implant was placed bilaterally in each animal. The animals were allowed full weight-bearing immediately after surgery.

After a period of 6 and 3 (1 x PEEK) months, the animals were sacrificed by cervical dislocation and the femurs removed. Each femur was trimmed, using a carborundum disc, to a length of approximately 1.5cm containing the implant and fixed in 10% neutral buffered formol saline for 48 hours. They were then dehydrated to absolute ethanol from 50% ethanol/water through 70% ethanol/water and 90% ethanol/water, each step lasting 48 hours. After dehydration, they were placed in xylene for 6 hours to remove any remaining lipids. An acrylic resin, Osteobed (Polysciences), was used for infiltration and

embedding. The infiltration schedule was: 100% Osteobed for 7 days, 7 days in 100% resin containing 1% benzoyl peroxide activator, 7 days in 100% resin containing 2.5% activator. All infiltration was done at 20°C under vacuum in soda glass universals. The specimens were embedded at 35°C in a fresh preparation of resin containing 2.5% activator. The polymerization of the resin took between 1 and 2 days. The universals were refrigerated for 30 minutes and then cracked and the glass removed to leave the embedded specimen.

A Polycut microtome (Reichert & Jung) was used to trim the blocks parallel to the long axis of the bone (longitudinally) until the outer surface of tissue was removed, revealing the implant face transcortically.

The blocks were secured to Historesin specimen adaptors (LKB) using Bostik adhesive and polished on a dental polishing machine using water soluble diamond pastes (Hyprez, Engis Ltd) ranging from a size of 6μm, through 1μm to 0.25μm. When ready for SEM examination, the specimens were removed from the specimen adaptors, secured to the SEM specimen holder using colloidal graphite (Emscope), and coated with graphite. The resin was stable under the electron beam and no specimen damage was seen. A Robinson RDEM II backscattered electron detector was used to obtain backscattered electron images (BEI) of the block surface using an accelerating voltage of 25 kV.

After SEM examination, the graphite coating was polished off and the blocks were sectioned at 300μm using a diamond saw (Buehler). These thick sections were examined using transmitted light.

The 3 month PEEK block was further sectioned on the Polycut microtome to obtain 1μm sections. These were stained with toluidine blue which will stain any basophilic structures enabling identification of hæmatopoietic cells in the bone marrow and bone cells (Bancroft & Stevens, 1977).

4.4 *In vitro* toxicity assessment

Two fibroblastic cell lines were used for the assessment of the materials: a primary line obtained from human gingiva, HGFs, and a secondary line (Flow Laboratories) of murine origin, M^{c}Coys. The primary line was maintained in DMEM medium (Flow Laboratories) supplemented with 10% foetal calf serum (Gibco) and 1% antibiotic-antimycotic solution (Gibco) in a humidified 5% CO_2 / 95% air atmosphere at 37°C. The secondary line was maintained in 199M medium (Gibco) with the same supplements and in the same atmosphere as the primary cells. Both the cell lines are adherent and when required for use were detached from the culture flasks (Falcon) using trypsin-EDTA (Gibco) in PBS (without divalent cations). The medium was removed from the flasks and a few mls of trypsin-EDTA added. The flasks were reincubated for 3 to 4 minutes at 37°C and the enzyme removed. The cells were then dislodged by the gentle pipetting of medium over them. Cell counts were performed using a hæmocytometer.

The materials were tested in the form of 5mm and 10mm diameter discs of thickness 1mm and as rectangular strips 70 x 10 x 3mm (for extraction). The discs were obtained as for the *in vivo* work, resulting in two distinct surfaces; a rough machined surface and a smoother as-moulded surface. The moulded surface was always presented to the cells, with identification being aided by a scratch mark on the rougher side. The materials were cleaned by sonication in Lipsol biological detergent and rinsed 6 times in sterile double distilled deionized water.

4.4.1 Direct contact assay

Discs of diameter 10mm were secured, machined side face down, to the bottom of wells of a 6 well plate (Linbro) using silastic adhesive (Dow Corning). The adhesive was left to cure for 1 hour before subconfluent $M^{C}Coy$ fibroblast-like cells were added to a concentration of $3x10^5$ cells/well. To verify that there was no toxic effect due to the adhesive, a control well containing only adhesive and a well with no adhesive was seeded with cells. The growth of cells was examined after 24 hours using an inverted phase contrast microscope (Leitz) and photomicrographs prepared.

4.4.2 Scanning electron microscopy

Discs of diameter 10mm and 5mm were secured to wells of either a 6 (Linbro), 24 (Falcon), or 96 well plate (Falcon). Discs punched from plastic tissue culture (Tc) petri dishes (Falcon) were used as a further control material. Silastic adhesive was used to affix the 10mm but not the 5mm discs. $M^{C}Coy$ fibroblast-like and HGF cells were seeded onto the material surface at different concentrations depending on the area of well used. The first experiments were done in 6 well plates using high cell concentrations, later it was realized that such high concentrations were not necessary and the cell numbers were reduced. For the microtitre plate, cells were seeded at $2.5x10^4$ cells/well; for the 24 well plate, cells were seeded at $1.5x10^5$ cells/well; and for the 6 well plate, cells were seeded at $1x10^6$ cells/well. Cell attachment was examined 90 minutes, 24 and 48 hours after seeding.

After each time period the supernatant from the wells was removed and the material surfaces were washed with excess buffer to remove unattached cells. Originally, a 0.1M sodium cacodylate buffer, pH7.4, was used (Sigma) but due to COSHH regulations this was changed to a 0.1M phosphate buffer at pH7.4.

The phosphate buffer working solution consisted of 47.5cm^3 solution A, 202.5cm^3 solution B and 250cm^3 distilled water; where solution A was made by adding 13.8g sodium dihydrogen phosphate to 500cm^3 distilled water, and solution B by adding 14.2g disodium hydrogen orthophosphate to 500cm^3 distilled water.

Two washing steps of 10 minutes each were used, during which time the plate was reincubated. The cells were then fixed for 1 hour in 2.5% gluteraldehyde (Emscope) diluted in the appropriate buffer. The fixative was replaced with buffer and the plate stored at 4°C.

When required for examination the samples were dehydrated through a series of alcohols: 70% methanol/water twice, 90% methanol/water twice and 100% methanol twice. Each dehydration step lasted 10 minutes. After dehydration, the samples were dried using a critical point dryer. The methanol in the cells was replaced with liquid carbon dioxide (CO_2) which was heated until it reached its critical point where it vaporized, leaving the samples dry.

After drying, the samples were affixed onto labelled, aluminium stubs (Agar Aids) using Bostik adhesive which was left to cure overnight. They were then gold coated using a sputter coater (Emscope) to stop them charging under the electron beam and examined using a JEOL JSM 35-C scanning electron microscope, with an electron beam energy of 15kV. For each sample, the entire surface was scanned before representative areas were chosen and photographed.

4.4.3 Extraction technique

Both test and control materials were extracted. The sample shape used was a rectangular strip 7cm x 1cm x 0.3cm. Three such strips were extracted together giving a total area of 56.4 cm^2. Acid washed and sterilized borosilicate glass culture tubes with screw lids containing PTFE liners (Corning) were used as the extraction containers (ASTM standard guidelines F619-79), with 20ml of sterile double distilled deionized (SDDD) water as the extractant. The samples were cleaned by sonication with Lipsol biological detergent, rinsed 6 times with SDDD water and then placed aseptically into the extractant. The samples were agitated continuously on a blood roller for one month at either 37°C or 80°C and the extracts stored at 4°C. Control tubes containing SDDD water were included at each temperature. Three extractions were performed, with each extract being tested with both primary and secondary cells using at least two of the cytotoxicity tests at any one time.

When required the extracts were filtered to ensure sterility and then used to formulate a 1x strength cell growth medium from a 10x strength source. Supernatant was removed from cells which had been seeded the previous day at $1x10^4$ cells/well and replaced with extract medium at 100µl/well. Cells were seeded using a 12 well multipipette to minimize pipetting errors and the same plate design used for each assay; in this way reproducibility between testing times was maximised. Each extract was added to five microtitre wells enabling all the extracts from both temperatures and controls to be tested on the same microtitre plate. The microtitre plates were incubated at 37°C for 72 hours and then processed according to the assay being performed. The MTT, proliferation and MB assays were performed simultaneously.

4.4.4 Trace element analysis of the extracts

Inductively coupled mass spectrometry (ICPMS) was used to obtain a trace element analysis of the extracts and control. Any leaching from the materials would be more pronounced at 80°C and so extracts obtained at this temperature were analysed. ICPMS is a very sensitive analytical tool giving a measurable signal at 0.1ppb in undiluted aqueous solutions. The machine used was a VG Plasmaquad ICPMS and each test solution had 100ppb of indium added as an internal standard.

4.4.5 MTT assay

Using a modified version of the procedure described by Denizot (1986) the optimal incubation time for the cells with the MTT was found to be 4 hours. Supernatant was discarded from each well and replaced with 50µl of filter sterilized MTT (Sigma) at 1mg/ml in the appropriate medium (without foetal calf serum or phenol red) for 4 hours at 37°C. At the appropriate time the MTT was flicked off and the plates blotted. Isopropanol (100µl) was added to each well and the plate agitated on a shaker to aid dissolution of the formazan crystals. The optical density (OD) of each well was read immediately on a Dynatech Multiwell scanner at 570nm. A reference wavelength of 670nm was used to correct for background interference.

The relationships between OD, cell concentration and population growth were ascertained in order for the assay to be optimised for the cell lines and test systems used. Cells were seeded at required concentrations into flat-bottomed microtitre plates (Falcon) in 200µl of the appropriate medium. To verify the straight line relationship between cell concentration and OD, the microtitre plates were centrifuged at 1000rpm for 5 minutes immediately after seeding and the supernatant discarded. They were then analysed using the

procedure described above. To assess changes in OD with population growth, cells were seeded at initial concentrations of $1x10^4$, $5x10^4$, and $1x10^5$ cells/well and MTT assays performed at regular periods for 7 days.

Both extracts and solid discs were tested using the MTT assay. The extracts (100µl) were added to cells seeded the previous day at $1x10^4$cells/well and incubated for 72 hours before performing the assay.

To test the solid surface, 5mm discs of the test materials were placed in microtitre wells, machined side face down, and $1x10^4$ M^{C}Coy fibroblast-like cells seeded into the well in 150µl of medium. After 72 hours incubation, the supernatant was removed and the plate processed as above. After removal of the MTT the discs were moved to fresh wells, and 100µl isopropanol added to the wells containing material, (A), the wells the materials were removed from, (B), and control wells with cells only, (C). After dissolution of the formazan crystals, the materials were discarded enabling the ODs of all the wells to be read. A mean of the ODs of all wells B was taken and this figure subtracted from that obtained from the control wells, C. In this way an OD reading was obtained for an area of tissue culture plastic equivalent to the area of test material used, permitting a comparison between results from tissue culture plastic and the test materials.

4.4.6 Proliferation assay

Cells were seeded into flat bottomed microtitre plates at a density of $1x10^4$ cells/well in 200µl of medium and left to stabilize overnight. The supernatant was replaced with 100µl of test extract and the cells then incubated for 72 hours. After this time period, 1µCi of ^{3}H-Tdr (Amersham) in 10µl of medium was added to each well and the plates re-incubated for a further 6 hours. The supernatant in each well was then replaced with 100µl of trypsin-EDTA in PBS

(without divalent cations) and after 10 minutes incubation at 37°C the cells were harvested onto glass filter mats (Dynatech) using a Minimash 2000 cell harvester (Dynatech). The filtermats were dried overnight at room temperature, carefully punched out and placed into 4ml of Optiphase Safe scintillation fluid (LKB).

Each sample was counted for 10 minutes on the tritium channel of a Packard tri-carb scintillation counter with external standardization.

4.4.7 Methylene blue technique

After removing the medium from each well the cells were fixed for 5 minutes in methanol (100µl/well). This was removed and the fixed layer of cells stained with 100µl of 0.1% methylene blue in 10mM borate buffer, pH 8.5. Excessive stain was removed by washing each well 3 times with 200µl of 10mM borate buffer pH 8.5. The plate was then blotted and the stain dissolved in 100µl of acid alcohol solution (20% ethanol in 0.1M HCl). A plate shaker was used to achieve full dissolution of the methylene blue and the plate read on a Dynatech Multiwell scanner at 670nm. A reference filter of wavelength 410nm was used to correct for background interference.

The relationship between OD and cell number was ascertained by seeding a range of cell densities and performing the assay. The extracts were tested by adding 100µl of each one to cells seeded the previous day at $1x10^4$cells/well. The plates were then incubated for 72 hours before the assay was carried out as described above. Discs of the test material were tested in a similar manner to those tested using the MTT assay. M^{c}Coy cells were seeded into wells containing the discs (moulded side face up) at $1x10^4$ cells/well in 150µl medium and incubated for 72 hours. Control wells with cells only were seeded at the same time. After incubation, the supernatant was

removed and the wells processed as described above. Before adding acid alcohol, the discs were moved to fresh wells. A mean OD reading for an area of well equivalent to the area of the disc was obtained in the same way as for the MTT assay.

4.4.8 Chemiluminescence assay

Two PEEK powders 150P and 380P were obtained from ICI Wilton Advanced Materials. The 150P grade has a lower molecular mass and more end groups than the 380P grade. The powders were sieved to separate particles of different sizes; most particles were found to be in the 40 to 50μm sieve and therefore particles of this size were used. PVC_{lead} powder from which the solid toxic control was fabricated, and 5μm PTFE powder (Goodfellows) were also used.

Heparinized venous blood was collected from healthy volunteers and the erythrocytes removed, by coagulation with dextran 110, as they interfere with the chemiluminescence signal. The PMNs were isolated by centrifugation of plasma and white blood cells with Ficoll-Paque (Pharmacia) at 1200rpm for 25 minutes. Remaining erythrocytes in the PMN fraction obtained from centrifugation were lysed by shaking with 1ml of sterile distilled water for 30 seconds. The resulting PMNs were transferred to 10mls of Hanks buffered saline solution (phenol red free) (Gibco) containing 10mM MOPS (Sigma) (HBSS/MOPS).

The test powders were opsonized by adding 20mg of powder to 2mls of human serum and incubating this mixture for 30 minutes at 37°C. During incubation, the mixtures were vortex mixed 5 times for 1 minute each. The opsonized powders were washed 3 times in HBSS to ensure removal of excess serum and then stored at -70°C until required. The positive control, zymosan

A (Sigma) was opsonized at 0.2mg/ml of human serum in the same way as above.

To ensure that the PEEK powders would not lyse the cells at the concentrations used, a range of concentrations of 380P powder and cells was incubated for 30 minutes on a blood roller and the cells observed under a light microscope. The concentrations used varied from 1mg/ml to 5mg/ml. Upon observation, the cells were seen to be healthy after incubation with all concentrations of powder. The highest concentration examined, 5mg/ml, was used in order to magnify any response. This concentration was also used for the PVC_{lead} and PTFE powder.

PMNs were obtained as described above and resuspended at a final concentration of $2x10^6$ cells/ml in phenol red free HBSS/MOPS. Each powder was vortex mixed before 500µl of powder/buffer mixture was added to 500µl cells giving a final concentration of 5mg/ml of test powder. To this reaction mixture, 100µl of luminol (Sigma) was added and the suspension read immediately. Subsequent readings were taken every few minutes. Inbetween readings, the cuvettes were placed on a blood roller at 37°C. The positive control was opsonized zymosan (500µl at 0.2mg/ml added to 500µl of cells) which was read first to check the system was working. The negative control was HBSS/MOPS with no zymosan or test powders.

4.5 Ageing of the materials

Black and white hooded Lister rats of the Liverpool strain were used for *in vivo* ageing as described previously. Test specimens were cleaned and sterilised before use. In each animal, one flexural specimen and two tensile specimens were implanted bilaterally. In total, 12 samples of each material were implanted, with retrieval after 6 months. Rods of APC2 of nominal dimensions 3 mm x 2 mm were implanted into rat femurs using the surgical technique described previously for intraosseous implantation. Each specimen was accurately measured to enable precise drilling of the hole. The implants were stabilized by an interference fit as for the toxicity testing regime. Originally, four specimens were implanted however results were only obtained from two. One animal suffered a fractured femur some time after surgery, but the injury was not noticed until sacrifice. The second femur fractured during the test.

For *in vitro* ageing, specimens were aged in 20mls of Dulbecco's phosphate buffered saline (PBS) (Gibco) at 37°C to mimic physiological temperatures, and 80°C to accelerate any deterioration in mechanical properties. They were also autoclaved for 20 minutes at 120°C under 20lbs of pressure to assess the mechanical response after sterilising.

4.6 Mechanical testing

Test specimens were cut from unidirectional 24 ply compression moulded plaques of APC2 and injection moulded plaques of P450G and D150CA30. To place the materials under the maximum stress, samples were tested in the weakest direction; transversely to the direction of melt flow for injection moulded samples and 90° to the fibre orientation for unidirectional laminates.

Tensile test specimens were machined using a tungsten carbide router on a pantograph. The size and geometry of the specimen was chosen so that the

same specimens could be used for both *in vivo* implantation and *in vitro* ageing. Dumbbell shaped specimens of 35mm total length, with a gauge length of 10mm were chosen. Rough edges were smoothed off before sterilization. Tensile strength (Ts) was calculated from:

$$Ts = \frac{F}{b \times h}$$

where F is the force recorded at breaking point
b is the specimen width
h is the specimen thickness

Flexural specimens were machined from test plaques using a steel bandsaw for PEEK and D150CA30 and a diamond saw for APC2. Specimen geometry was in accordance with BSI regulations BS 2782: Part 10: Method 1005:1977 EN 63. A span to depth ratio of 20:1 was used where the span is the distance between supports. A three-point bending rig was used to measure ultimate flexural strength and flexural modulus. Flexural modulus was tested using a sub-critical load of 20kN (less than 10% of the breaking load for each material) retesting the same samples every time. Flexural stress (Fs) and modulus (E_b) were calculated from:

$$Fs = \frac{3 \times F \times L}{2 \times b \times h^2}$$

$$E_b = \frac{L^3}{4 \times b \times h^3} \times \frac{\Delta F}{\Delta d}$$

where F is the force at breaking point
L is the span
b is the specimen width
h is the specimen thickness
$\Delta F / \Delta d$ is the gradient of the force-deflection curve in the initial linear region

Specimen width and thickness were measured to an accuracy of 0.01 mm using digital calipers (RS). Both the tensile and the transverse flexural tests were performed on either an Instron model 1185, or a JJ Lloyd M5K mechanical tester using crosshead speeds and load cells as indicated in the results. The fracture surfaces were gold coated and examined using a JEOL JSM 35-C SEM.

Vickers microhardness measurements were performed on flexural modulus specimens using a Zeiss MHP microhardness rig attached to a Zeiss microscope according to manufacturers instructions. Two specimens were chosen at random from each material group and temperature, and were tested before ageing and then retested at selected time periods. To improve reproducibility between test periods the same surface was tested each time with 10 random measurements being taken. All of the determinations were performed at room temperature, using a contact time of 10 seconds and a load of 100g for PEEK and D150CA30, and 200g for APC2.

The maximum load required to push the APC2 rods out of bone was measured, using a push out tester adapted from the three point bend rig, on the Instron 1185 tester. A 5kN load cell and a crosshead speed of 1mm/min were used. A pin of diameter 1.5mm and length 50mm was attached to the loading nose of the rig and a support plate with a 3mm hole placed directly underneath it. The hole acted as a guide when the specimen was being pushed out. The bone was removed from the animal and trimmed down to a length of 15mm to 20mm with the specimen in the middle. The bone was not fixed but kept moist with saline solution and tested immediately. The specimen was not seen to protrude through either end of the drill hole although the top could be seen at one cortex. Difficulty was had in maintaining the orientation of the push out pin to the bone as the angular

geometry of the rat femur meant that initial contact with the specimen would nearly always result in twisting of the bone. Results were achieved using a vacuum sealant as a support at either end of the bone. During testing the bone was constantly re-wetted using saline solution. From the load-displacement trace the interfacial shear strength and stiffness were calculated by estimating the maximum area of bone / implant contact as being dependent on the length of the implant rod.

4.7 Differential scanning calorimetry

Differential scanning calorimetry (DSC) was used to measure any changes in the polymer structure due to chemical aging. The test material and a reference (empty sample pan) are heated at a uniform rate and the power to heat each measured. This will be the same until a change in the sample takes place. If the change is exothermic, eg. due to the heat of crystallization, the heating power to the test material will be decreased; but if it is endothermic, eg. due to melting, the power to the test material will momentarily increase. A servo-system immediately increases the power input to either sample or reference to maintain both at the same temperature. The difference between the power needed to heat the sample and that needed to heat the reference is measured.

DSC scans were made on surface layers of PEEK 450G and APC2 aged *in vitro* for 18 months in PBS at 80°C and compared to those obtained from unaged samples. The scanning rate used was 20°C/minute on a Perkin-Elmer DSC4 machine.

5.1 Intramuscular implantation

Materials were implanted intramuscularly into rats and retrieved after 7 weeks, 3, 4 and 9 months. Little inflammatory reaction to the materials was seen at any of these time periods; the characteristic response was a thin fibrous capsule containing predominantly fibroblasts and fibrocytes. The fibrocyte is a mature fibroblast identified by its narrow spindle shaped nucleus, in contrast to the plump nucleus of a fibroblast.

Figures 5.1a, i-iii show the fibrous capsule seen at the implant site after 7 weeks implantation with D150CA30 (i), PEEK (ii) and APC2 (iii). In this case the implant was rod shaped. Fibrocollagenous tissue was seen associated with all the implant sites. This tissue is a normal component of the inflammatory response to any procedure and is composed of remnants of the wound healing reaction: dead inflammatory and muscle cells, small blood vessels, and occasional inflammatory cells such as macrophages and lymphocytes. Fatty tissue, identified by its lacy appearance, was seen at the implant site of all materials and is clearly shown in figure 5.1a,i. Figure 5.1a,iii shows carbon particles associated with the implant site of APC2; this was typical for the implant site of the composite materials at all time periods and is shown at 9 months in Figure 5.1b, iii. The carbon particles had a yellow-green tinge associated with them. Hæmosiderin, a breakdown product of hæmoglobin stains yellow in H & E stain and may be identified positively using Perls' stain. However, when sections were stained using Perls' stain to identify hæmosiderin, these areas were not found to coincide with the carbon particles.

The sections were then examined using polarized light and it could be clearly seen that the colour was due to refraction of light by carbon particles.

After 3 and 4 months implantation little change was seen in the host response to the materials. At 4 months, a fibrous capsule containing fibroblasts and fibrocytes could still be seen associated with the implant site of each material as is shown in Figure 5.1a,iv (PEEK) and 5.1b,i (APC2) and ii (PEEK). Fatty tissue is shown in Figure 5.1b,i & ii; in general this tissue was more noticeable with the composite materials than with PEEK.

At 9 months a difference between the response of the host to the composite materials and to the unfilled resin was found. A very thin capsule was seen at the PEEK implant site, with muscle cells adjacent to the collagen layer and no fatty or fibrocollagenous tissue imposed between (Figure 5.1b, iv). In contrast, the fibrous capsule surrounding the composite materials was more cellular and fibrocollagenous tissue was still seen (Figure 5.1b, iii).

There was little change in the inflammatory response to the material between 3 and 9 months; at 9 months a distinct capsule was still seen. This may be due to the difference in implant shape used. Rod shaped specimens were used at 7 weeks and 3 months whereas disc shaped implants were used at 4 and 9 months. The larger surface area of the disc may have increased the stimulation time of the inflammatory cells, thus lengthening the time of healing.

The non-inflammatory nature of the materials was further confirmed upon examination of the implant surface using SEM. No attached cells were found and very little adherent tissue debris was seen.

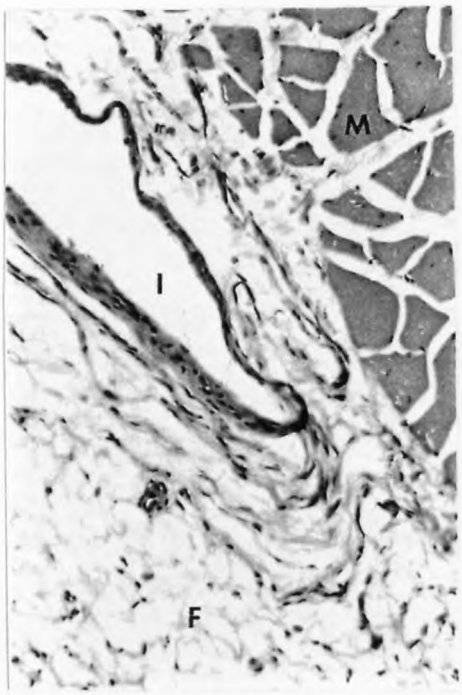

i) x500

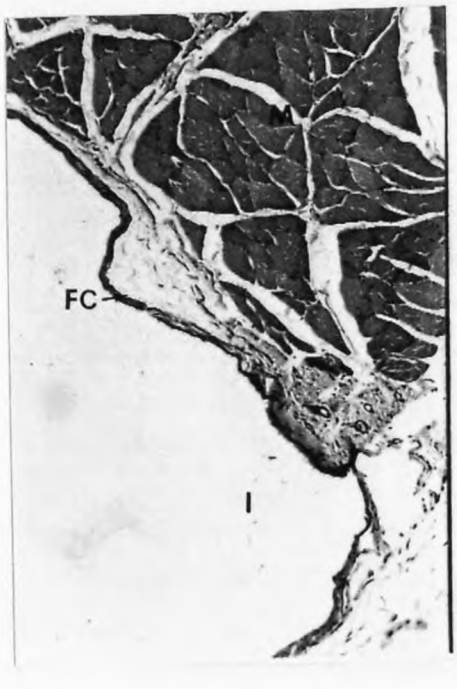

ii) x250

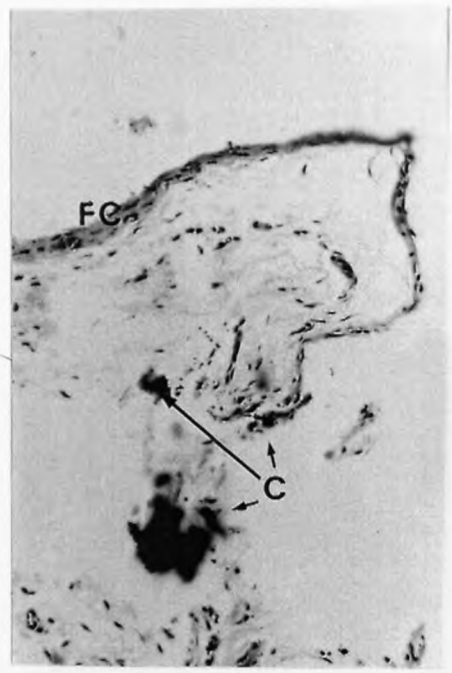

iii) x500

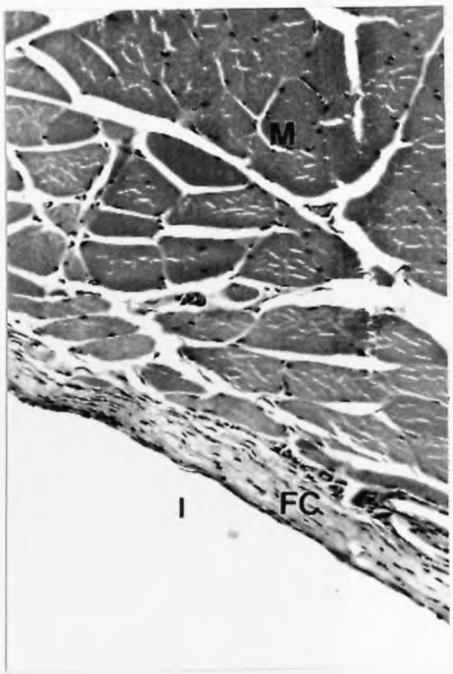

iv) x500

Figure 5.1a: Intramuscular implantation. Light micrographs showing implantation site of D150CA30 (i), PEEK (ii) & APC2 (iii) 7 weeks post-implantation; and PEEK (iv) 4 months post-implantation. Carbon particles (C), fatty tissue (F), fibrous capsule (FC), implant space (I), muscle (M). Haematoxylin & eosin stain.

i) x500

ii) x250

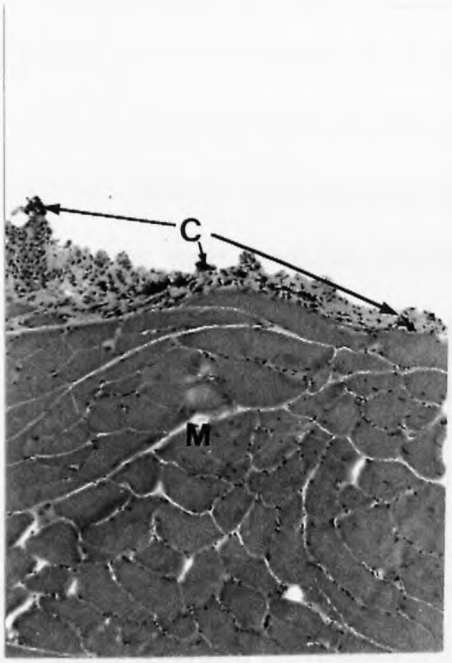

iii) x250

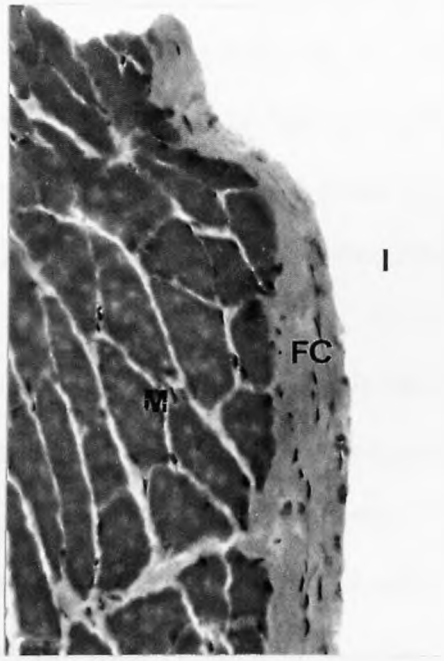

iv) x800

Figure 5.1b: Intramuscular implantation. Light micrographs showing implantation site of APC2 (i) & PEEK (ii) 4 months post-implantation; and APC2 (iii) & PEEK 9 months post-implantation. Carbon particles (C), fatty tissue (F), fibrous capsule (FC), implant space (I), muscle (M). Haematoxylin & eosin stain.

5.2 Intraosseous implantation

The rod used for implantation were machined out of plaques; this gave a rough surface as can be seen in Figure 5.2a, i-iii.

Backscattered electron images of areas adjacent to an APC2 implant, in place for 6 months, are shown in figures 5.2b, i-vi. A distinct darker grey band was seen adjacent to the implant, indicating a lower density of bone mineral in this area (Figure 5.2b, i-iii, v & vi). This band was only seen in association with the implant (Figure 5.2b, iv). At the periosteal edge, furthest away from the implant a darker band was again found (Figure 5.2b, v). The black oval shaped spots in the bone are presumed to be lacunae - small cavities which house osteocytes - rather than Haversian canals as these are not present in the rat femur. Striations were clearly seen in some micrographs (Figure 5.2b, vi) and may represent collagen fibres. In the marrow space, a thin spur of bone was seen to surround the implant at most places (Figure 5.2b, v).

Both reversal and arrest cement lines were seen; a cement line is a collagen poor area usually demarcating areas of remodelling. Reversal lines may be identified by their irregular, crooked appearance in contrast to the smooth even appearance of arrest lines.

In areas of close contact between the material edge and the bone, the edge of the bone tissue adjacent to the implant was seen to 'outline' the edge of the carbon fibres (Figures 5.2c, i & ii) taking on a jagged appearance. Gaps between the material and the implant were seen and here the bone edge was smoother, although the banding was still seen (Figure 5.2b, ii & vi and Figure 5.2c, ii). The presence or absence of gaps may be purely artefactual, due to uneven shrinkage of the resin during processing. However, if the gaps were introduced during processing, the edge of the bone would be expected to be

more uniform in appearance. The nature of any tissue or other substance in the gaps could not be discerned from the electron images.

Distinct bands of differing mineral density were not seen with PEEK and D150CA30 implant materials implanted for 6 months (Figure 5.2c, iii-v). Figure 5.2c, iv shows the even bone morphology seen extending from the implant to the far cortical edge. The appearance is similar to that of the cortical bone at a distance from the APC2 implant as shown in Figure 5.2b, iv. In areas of extremely close contact between the implant and the bone, the bony edge was seen to follow the shape of the material edge closely (figure 5.2c, v).

Figure 5.2c, vi shows a backscattered image of a PEEK rod implanted for 3 months. An area of lower mineral density containing a higher proportion of lacunae was seen adjacent to the implant. More lacunae were seen at the material edge than with the APC2 6 month implant. Both arrest and reversal lines were seen demarcating the boundary between differing mineral densities although only an arrest line is shown in the micrograph.

Only one block was examined for each material type using BEI, as air bubbles were present in the surface layers of the others. However, all the blocks (3 samples of each material type at 6 months, and 1 PEEK block at 3 months) were sectioned and examined using transmitted light. Although the sections were 300μm thick, useful images were obtained and it was possible to focus on osteocyte lacunae at different depths through the section. The implants were seen to be surrounded by a thin spur of bony tissue at all levels throughout the bone. Sections of the bottom cortex showed good healing of the drill hole with only a faint circular outline remaining.

Some of the osteocyte lacunae and canaliculi appeared black resembling little spiders. These 'stained' lacunae were in general more closely associated with the implant material. At first it was thought that this appearance was due to

contamination of the surface by a lubricant used on the sectioning device. However, the microscope used allowed limited optical sectioning by focusing through the section, and black lacunae were seen at depths throughout the section. As they were seen with the unfilled resin PEEK as well as the carbon fibre filled APC2 and D150CA30, the appearance could not be due to absorption of carbon. 'Spidery' osteocytes were on sections which had not been examined using BEI and so were unlikely to be related to the graphite coating used.

The 3 month PEEK specimen was further sectioned with the implant in place. Unfortunately, the material was displaced on retrieval of the thin sections. However, the implant site was preserved and the space can be seen in Figure 5.2d, ii & iii. A portion of the bony spur described above can also be seen. It is similar in appearance to the cortical bone as can be seen by comparison with Figure 5.2d, i, which shows cortical bone adjacent to marrow tissue at a site distant to the implant. The black spidery osteocyte lacunae described above can be clearly seen in Figure 5.2d, iv.

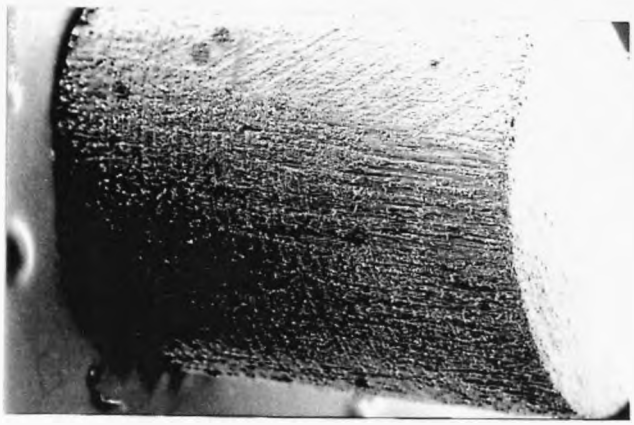

i) x34

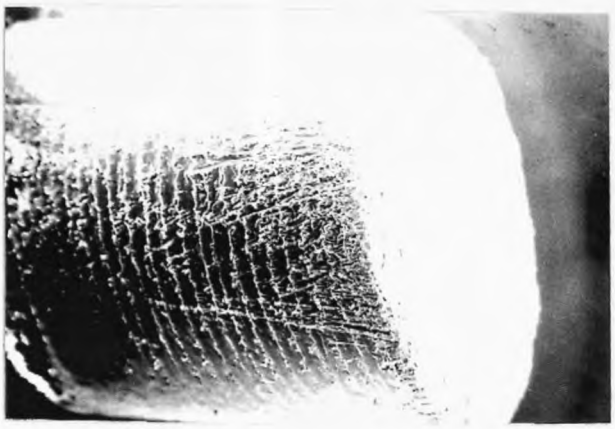

ii) x34

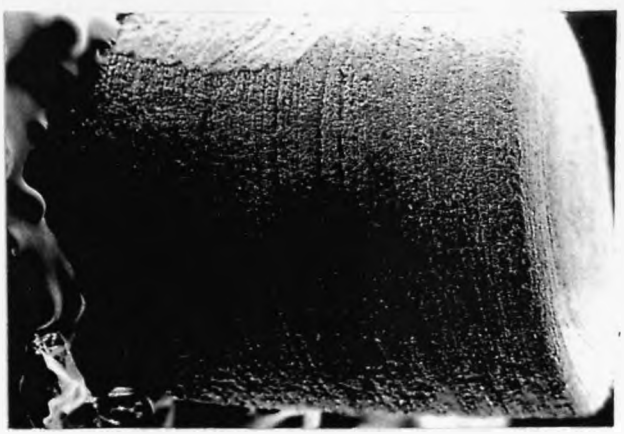

iii) x34

Figure 5.2a: Intraosseous implantation. Material surfaces prior to implantation, APC2 (i), PEEK (ii) & D150CA30 (iii).

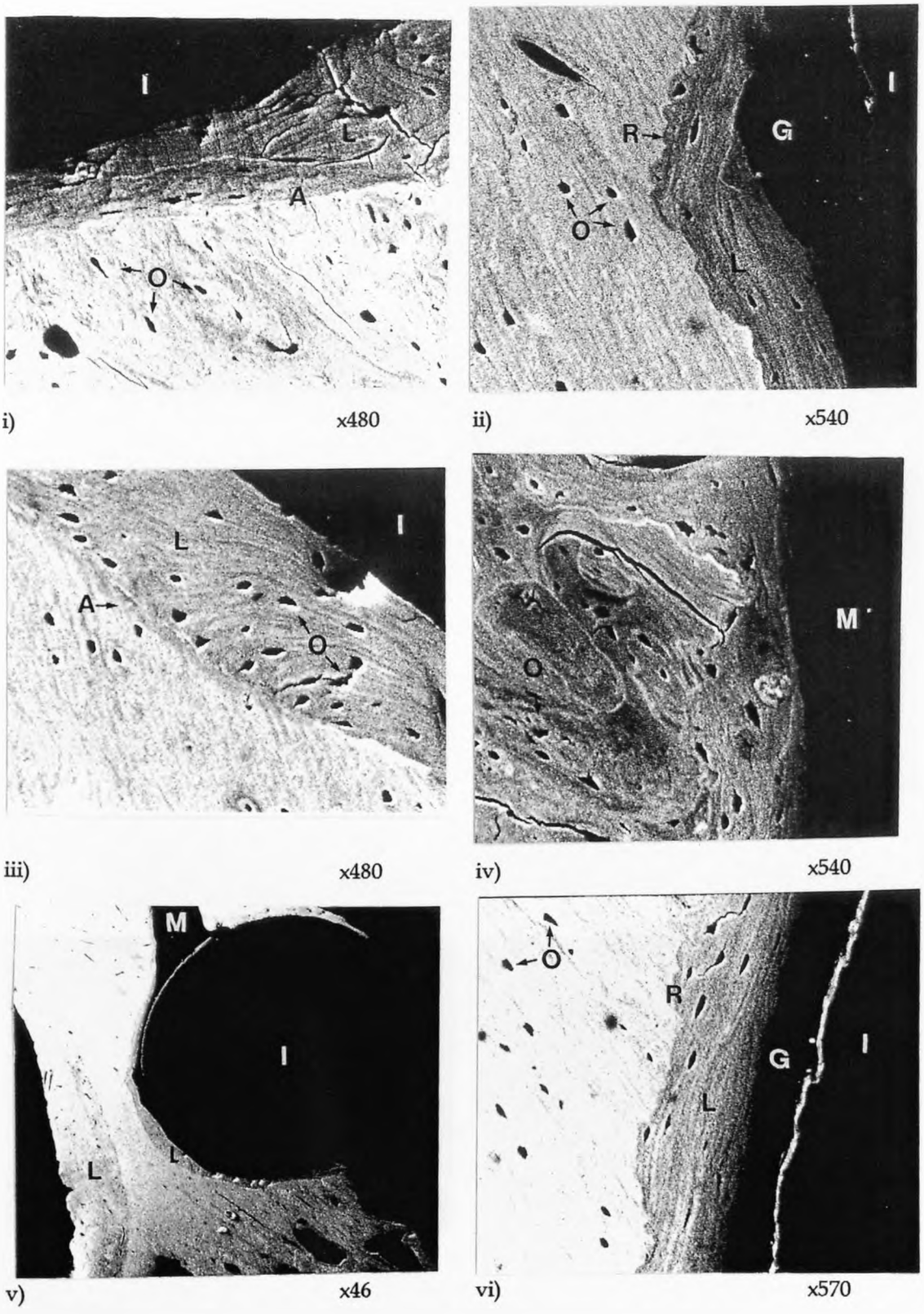

Figure 5.2b: Intraosseous implantation. Backscattered electron images of APC2 in femoral bone 6 months post-implantation. Arrest line (A), gap between implant and bone (G), implant (I), areas of lower mineral density (L), marrow space (M), osteocyte lacunae (O), reversal line (R).

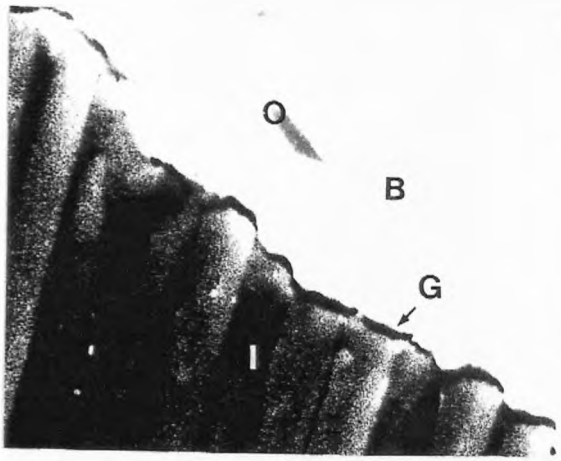

i) x1800

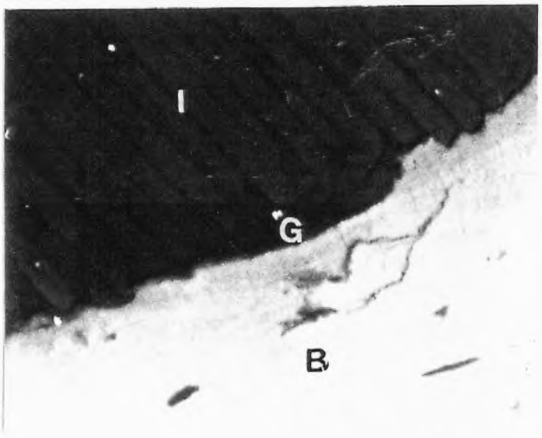

ii) x830

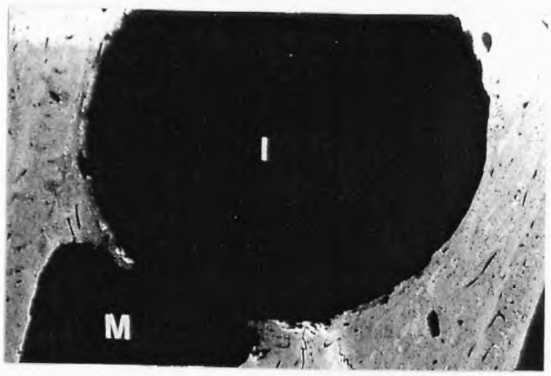

iii) x50

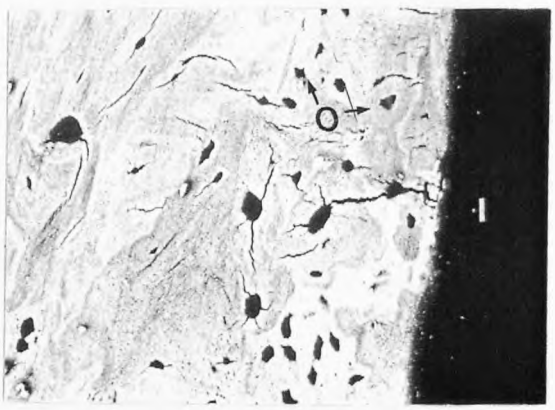

iv) x450

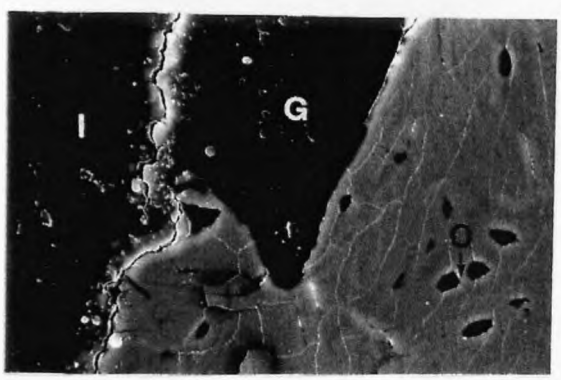

v) x470

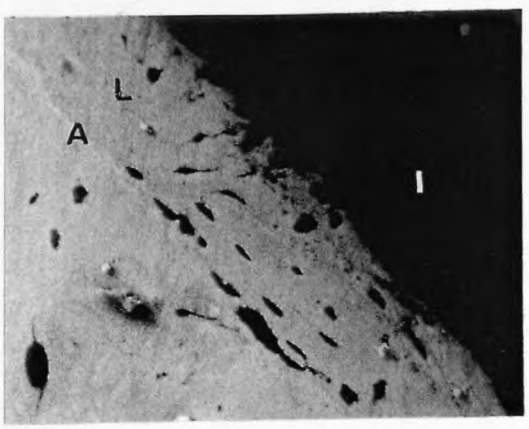

vi) x790

Figure 5.2c: Intraosseous implantation. Backscattered electron images of APC2 (i & ii), D150CA30 (iii, iv & v) in femoral bone 6 months post-implantation; and PEEK (vi) 3 months post-implantation. (v is a secondary electron image). Arrest line (A), bone (B), gap between implant and bone (G), implant (I), area of lower mineral density (L), marrow space (M), osteocyte lacunae (O).

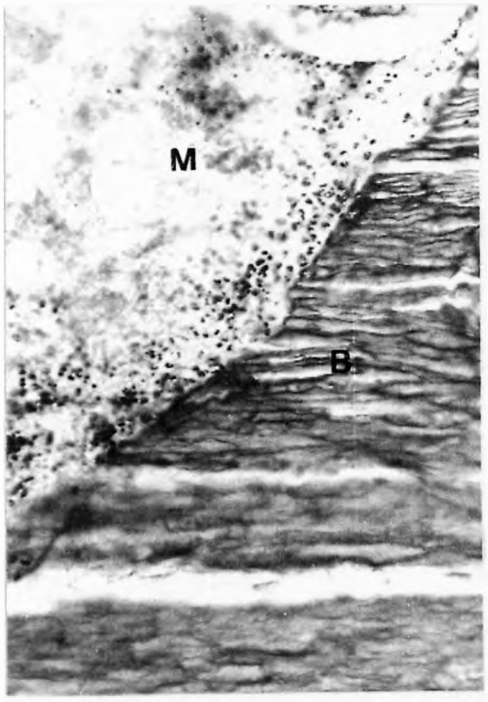

i) x630

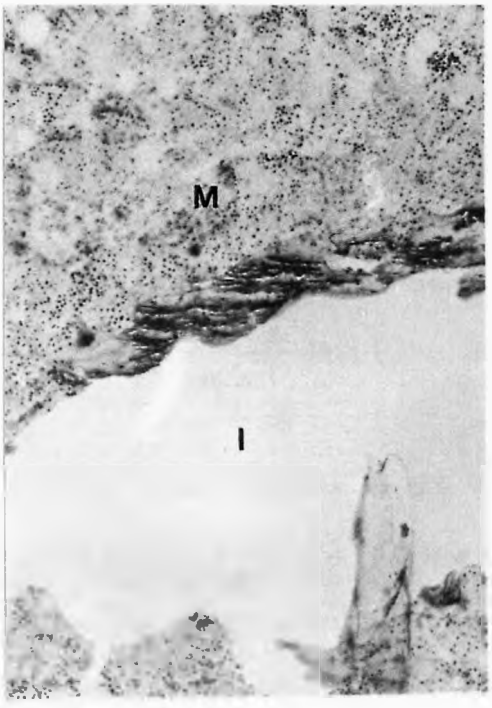

ii) x315

iii) x630

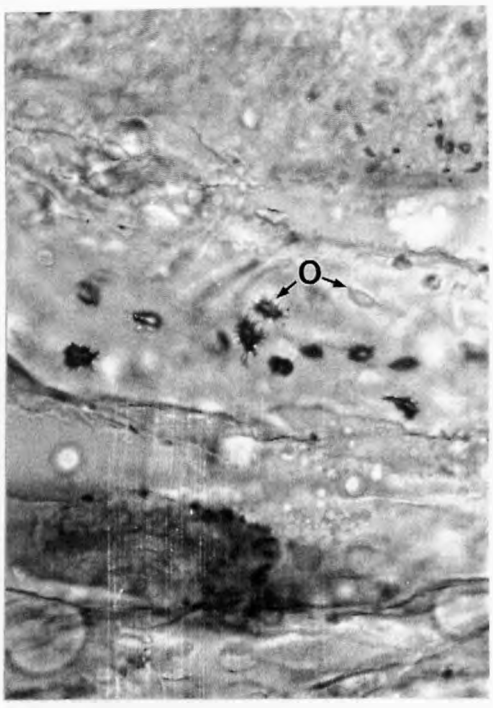

iv) x1000

Figure 5.2d: Intraosseous implantation. Light micrographs showing implantation site of PEEK 3 months post-implantation. Cortical bone (B), marrow tissue (M), implant space (I), osteocyte lacunae (O). Toluidine blue stain.

5.3 Direct contact assay

Typical light micrographs of cells in direct contact with the test and control materials are shown in Figure 5.3a, i-vi. The silastic adhesive used to secure the materials exerts no toxic influence on cells, as can be seen by their healthy appearance when grown in contact with it (Figure 5.3a, vi). The cells adjacent to the test materials had a healthy glistening appearance resembling the control cultures.

Inhibition of cell growth occurred in small areas adjacent to the test materials but not with the negative control (UHMWPE). Only one or two such areas per sample were seen (Figure 5.3b, i-iii). The reason for these random occurrences of inhibition over such a small area of the test disc is not known. A zone of inhibition of cell growth was seen with PVC_{lead}; healthy cells were seen at a distance from the material, whereas cells in its immediate vicinity were rounded up and readily detached upon movement of the plate.

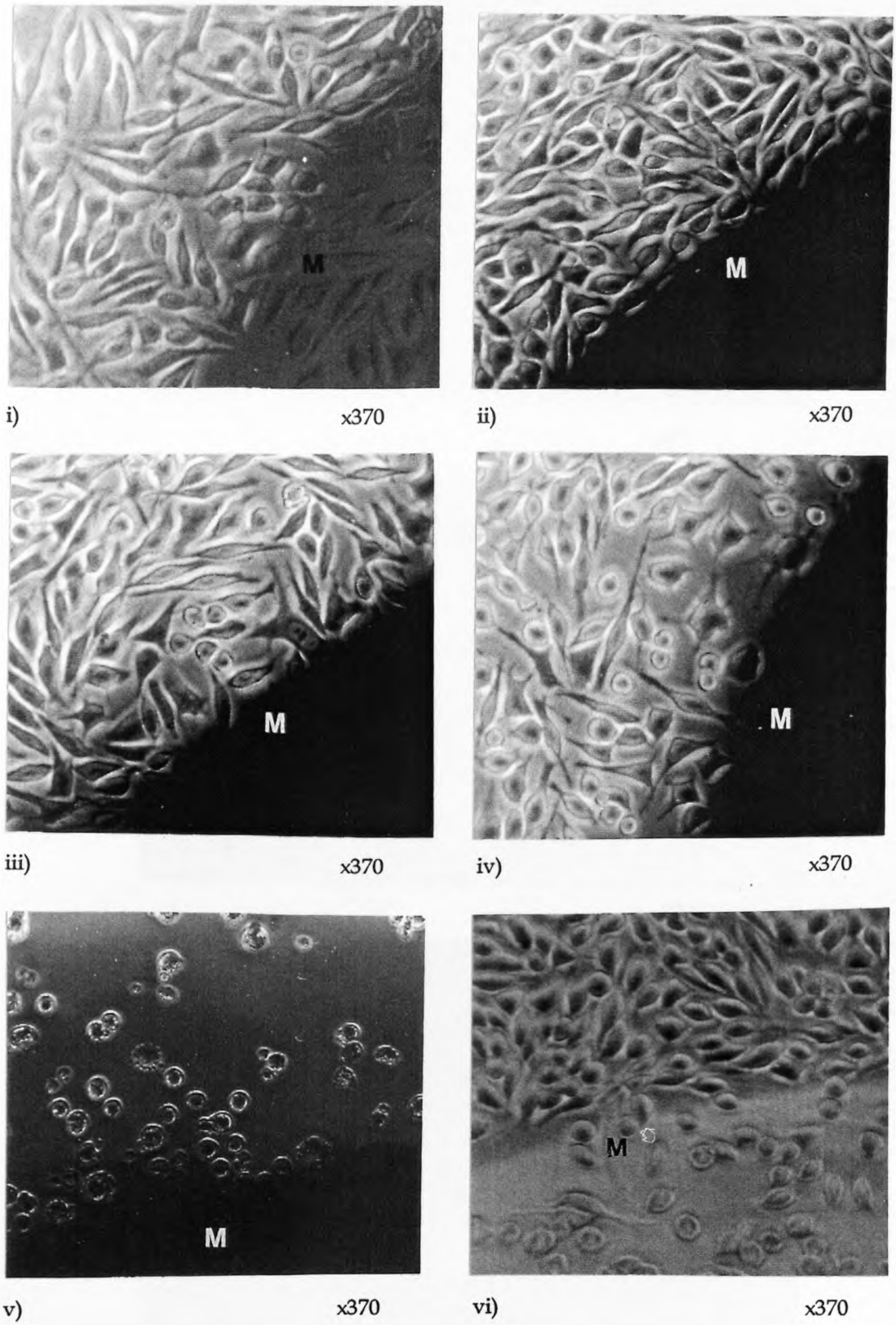

Figure 5.3a: Direct contact test. Light micrographs of M^{c}Coy fibroblast-like cells after 24 hours incubation with UHMWPE (i), PEEK (ii), APC2 (iii), D150CA30 (iv), PVC_{lead}, and silastic adhesive (vi). Material edge (M).

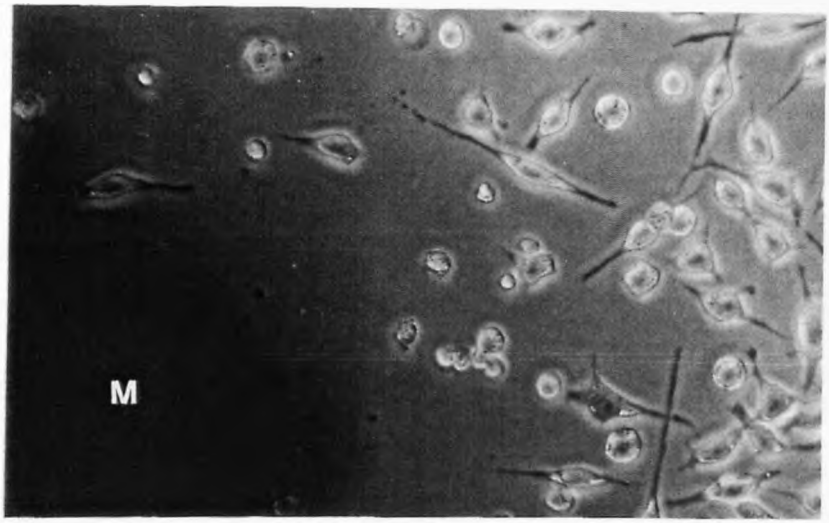

i) x370

ii) x370

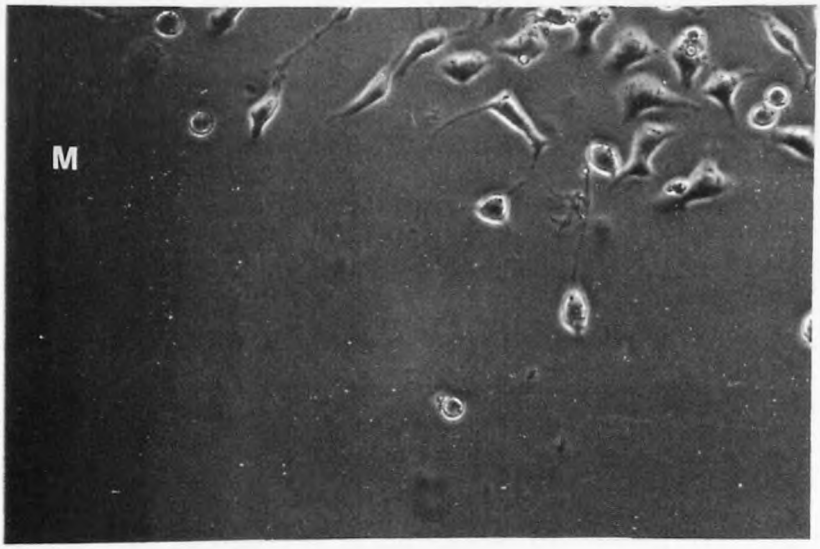

iii) x370

Figure 5.3b: Direct contact test. Light micrographs of M^{c}Coy cells incubated with PEEK (i), APC2 (ii) & D150CA30 (iii) for 24 hours, showing areas of inhibition. Material (M).

5.4 SEM of cells on the material surface

Secondary and primary fibroblast cell lines were seeded onto the surface of 'as moulded' test and control materials. The surface morphology of these materials varied considerably: the PVC_{lead} has a rough surface structure, UHMWPE has an undulating surface, PEEK and the composites all have similar surface roughnesses but exposed fibres were occasionally seen with the composites and surface pores seen with APC2. The material surface morphology can be seen in the micrographs.

Cells adhered to all the materials (except PVC_{lead}) in similar numbers. Different time periods were used (45 minutes, 90 minutes, 24 hours and 48 hours) with cells seen to attach and start to spread after 45 minutes of contact. The morphology of the M^cCoy cells was varied and included rounded, spindle shaped and spread cells, even at the earlier time periods. Figure 5.4a shows SEM micrographs of M^cCoy cells 90 minutes after seeding onto the surface of APC2 (i), PEEK (ii), D150CA30 (iii), UHMWPE (iv), tissue culture plastic (Tc) (v), and PVC_{lead} (vi). The cell morphology was similar on all surfaces. No cells were seen on the PVC_{lead} surface at any time period.

HGF cells seeded onto the surface of PEEK (i & v) and APC2 (iii) for 24 hours are shown in Figure 5.4b. The morphology of the HGF cells was less varied than that of the M^cCoy cells, with the majority adopting a rectangular flattened shape, slightly overlapping one another. This made it hard to distinguish individual cells. The M^cCoy cells did not exhibit this tendency to overlap even after 24 hours incubation, as can be seen in Figure 5.4b, ii (PEEK), iv (D150CA30) & vi (PEEK). Critical point drying of the cells did not always result in optimal preservation of the cell structure; rupture of highly stressed attachment points and incomplete preservation of membrane microvilli was seen.

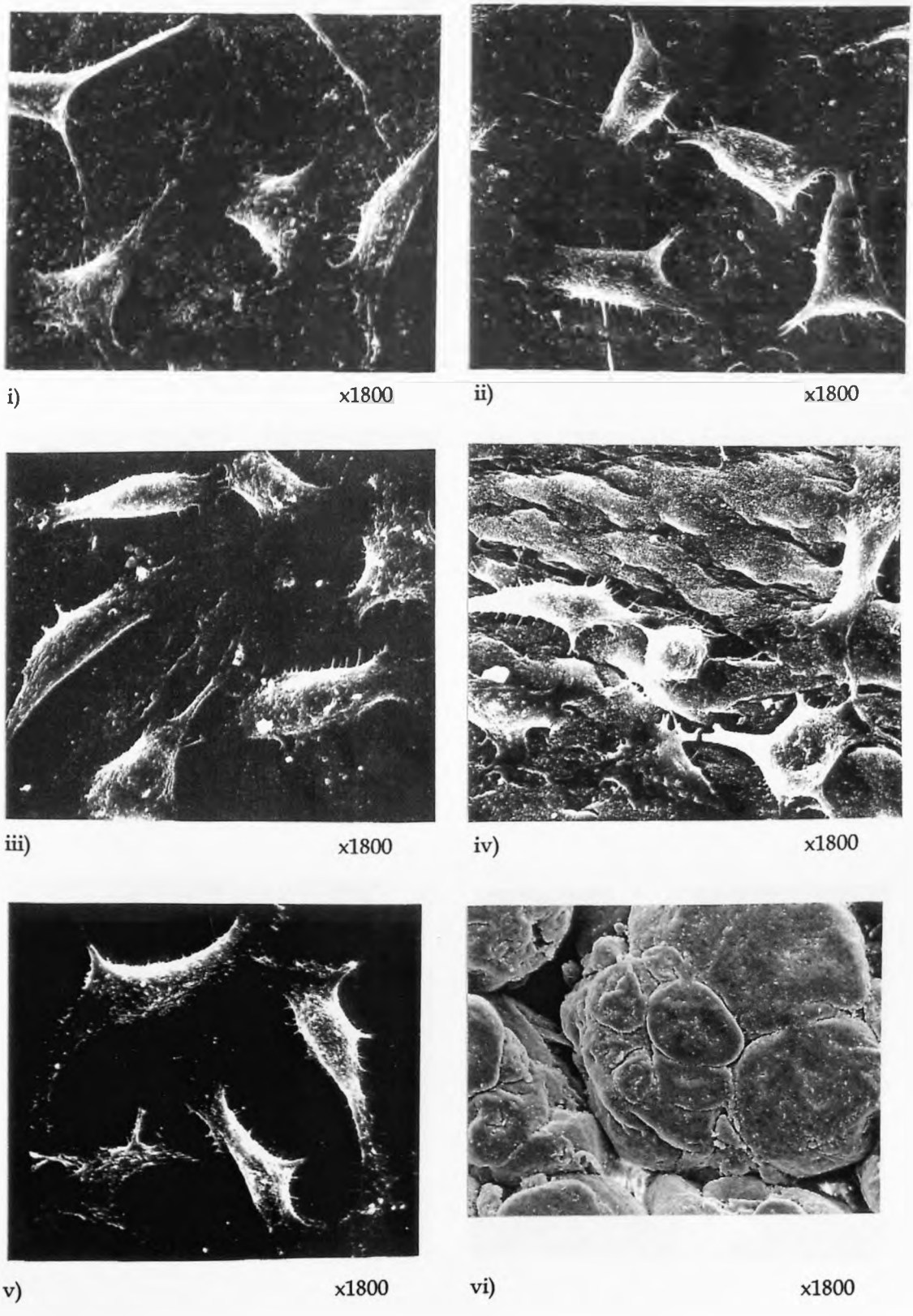

Figure 5.4a: Cell adhesion. SEM micrographs of $M^{C}Coy$ fibroblast-like cells seeded onto APC2 (i), PEEK (ii), D150CA30 (iii), UHMWPE (iv), Tc plastic (v) and PVC_{lead} surfaces for 90 minutes.

i) x520

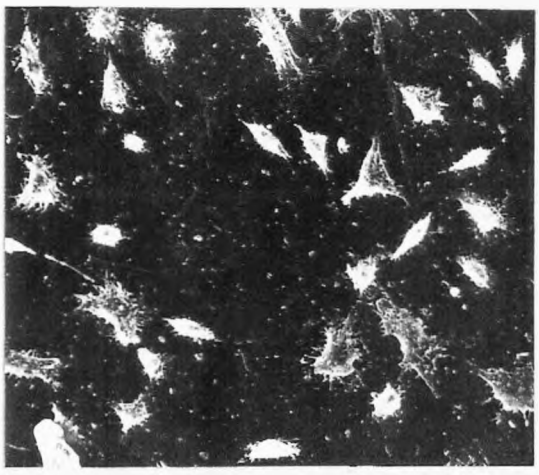

ii) x520

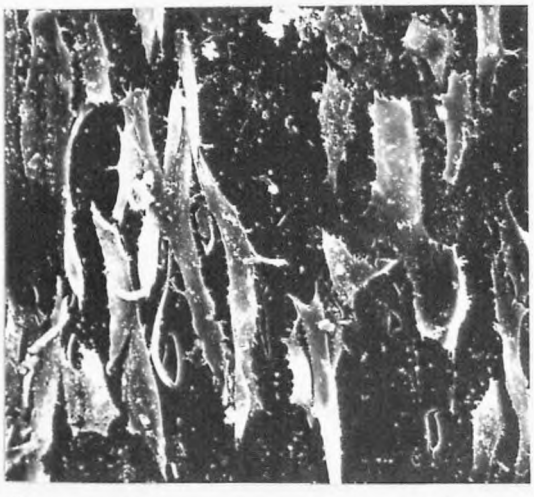

iii) x550

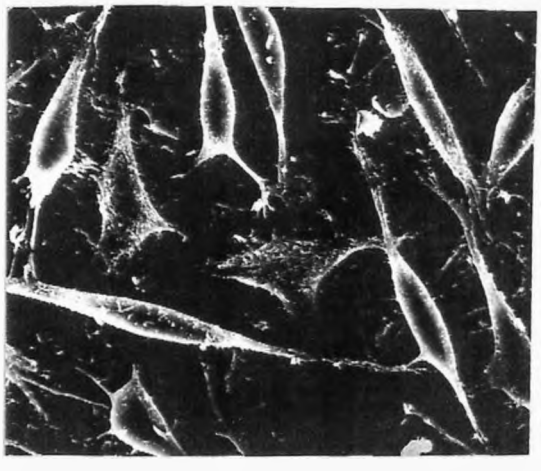

iv) x1100

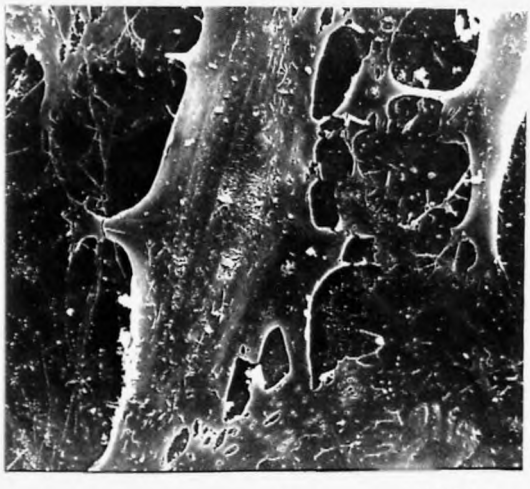

v) x1300

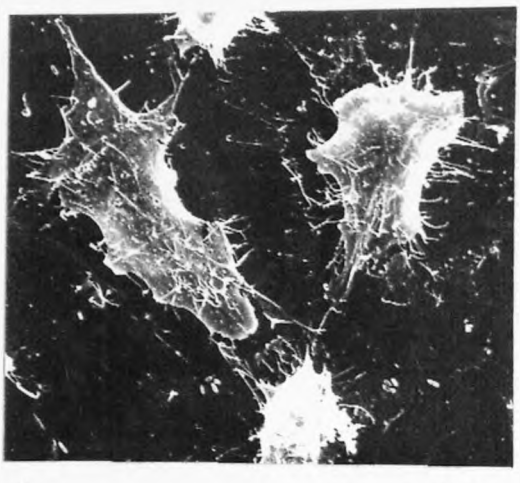

vi) x1700

Figure 5.4b: Cell adhesion. SEM micrographs of HGF fibroblast cells seeded onto PEEK (i & v) and APC2 (iii) for 24 hours; and McCoy fibroblast-like cells seeded onto PEEK (ii & vi) and D150CA30 (iv) for 24 hours.

5.5 Trace element analysis

A full periodic table analysis was done on extracts obtained from materials incubated for 1 month at 80°C using a VG Plasmaquad ICPMS. Table 5.5a gives a list of elements in which ppb were measured in the extracts at more than four times that of the control - double distilled water incubated in the same environment. The accuracy of the results is within a factor of two. The most striking differences were found between the PVC_{lead} extract and the other materials, with very high levels of cadmium, barium and lead being seen. The lead is present in the form of lead stearate and acts as a plasticizer; it is presumed that cadmium and barium also act as stabilizers or plasticizers.

Differences were also seen between the UHMWPE (negative control material in the cytotoxicity tests) and the test materials. Both the PEEK and D150CA30 extracts had double the UHMWPE level of magnesium and all three test materials had more than four times the UHMWPE level of copper. These elements may be contaminants from fabrication of the materials or additives which have leached out. In addition, the D150CA30 extract contained the highest levels of aluminium, magnesium and zinc found. The source of the extremely high level of zinc seen is unknown; the mould release agents used, which may have leached from the material surface, do not contain zinc.

Table 5.5a

Element	Element Concentration / ppb					
	Material Extract					
	DDH_2O	$PVC_{(l)}$	PE	PK	APC	D150
Magnesium	26	180	63	120	81	170
Aluminium	24	5.1	4.4	5.7	3.6	49
Phosphorous	16	90	4.8	5.1	5.6	8.4
Titanium	0.8	5.6	1.3	1.3	0.3	1.0
Magnesium	0.5	11	0.5	1.3	1.5	4.7
Copper	7.1	46	3.8	15	29	21
Zinc	44	110	22	34	33	3500
Strontium	2.3	660	1.5	2.2	2.3	9.2
Cadmium	0.1	23000	0.1	0.3	0.4	0.6
Barium	1.3	29000	0.7	2.3	6.9	7.0
Mercury	0.3	5.0	0.8	2.2	1.7	0.6
Lead	0.4	11000	0.1	0.3	0.2	1.2

Table 5.5a: Materials were incubated in double distilled deionized sterile water at 80°C for 1 month and analysed undiluted using a VG Plasmaquad ICPMS. The analysis was semiquantitative as each extract was internally standardized with 100ppb of indium; the results are accurate to a factor of two.

5.6 Cytotoxicity testing

The linear relationship between cell number and optical density (OD) for the MTT assay is illustrated in Figures 5.6a - c. It can be seen that although the trend is the same, different ODs were recorded for the same cell number measured on different occasions. This was due to variable levels of metabolic activity in the cell population; though the cells were always seeded from sub-confluent populations to ensure cell growth would be in the logarithmic phase when measured.

The relationship between cell number and OD when HGF cells were assayed using the MB assay is shown in Figures 5.6d & e. Again a linear relationship was found. The ODs obtained for different cell numbers were more reproducible than for the MTT assay, reflecting the non-metabolic nature of the assay.

The relationship between population growth, initial cell seeding concentration and OD for M^{c}Coy cells assayed using the MTT assay is shown in Figure 5.6f. For testing the extracts the lower cell number was chosen as: any toxic effect would be increased due to the reduced cell-cell interactions, the cells would be in the logarithmic phase of growth after 72 hours incubation with the extracts, and measurable OD readings were obtained at this time period.

Three extractions of the test and control materials were performed at both 37°C and 80°C, and the extracts obtained tested using both M^{c}Coy and HGF fibroblast cells. Each set of extracts was tested at least twice with each cell line using at least 2 of the cytotoxicity tests. The tests were performed 72 hours after incubation of the extracts with the cells. A complete assessment of material toxicity using the M^{c}Coy cells is shown in Figure 5.6g - i and in Figures 5.6j - l for extracts made on different occasions. Each value is a mean of 5 wells, significant differences as measured using the student's t-test are

indicated on the histograms. The PVC_{lead} extract is the only extract that is repeatably cytotoxic as measured by all three assays. Both sets of results indicate the non-toxicity of the test materials relative to the controls chosen, although the results vary around the UHMWPE control in a different manner for each assay. In Figures 5.6g - i, the differences in response of cells to the test materials in the MTT and ^{3}H-Tdr assays is related to the number of cells present as indicated by the MB assay, rather than stimulation of the cells. Such a clear pattern was not always found (Figures 5.6j - l).

The primary cells did not respond dissimilarly to the secondary cells in the cytotoxic tests apart from a decrease in sensitivity to the PVC_{lead} extract obtained at 37°C (Figures 5.6m & n). This can also be seen in Figure 5.6o which shows the appearance of cells incubated with control and test extracts. The HGF cells have clumped in the presence of the PVC_{lead} extract at both temperatures, but display a more normal morphology at 37°C (5.6o, iv) in contrast to a rounded unhealthy morphology at 80°C (5.6o, vi). The rounded up appearance of M^cCoy cells incubated with PVC_{lead} can be clearly seen (5.6o, v) and was always reproduced after incubation. No difference in appearance between cells incubated with the test and negative control extracts could be discerned (Figure 5.6o, i-iii). Using the M^cCoy cells there was no significant difference in results from extracts obtained at 80°C in comparison to those at 37°C as shown by Tables 5.6a - c.

Tables 5.6d & e, show results from MTT and MB tests performed on the test material surface after 96 hours incubation with M^cCoy cells. Values for cells grown on the tissue culture well surface in equivalent areas are shown for comparison. No significant differences between the test materials and the control were seen. Larger standard deviations were recorded in this set of experiments than with the extracts probably due to surface irregularities.

5.6a

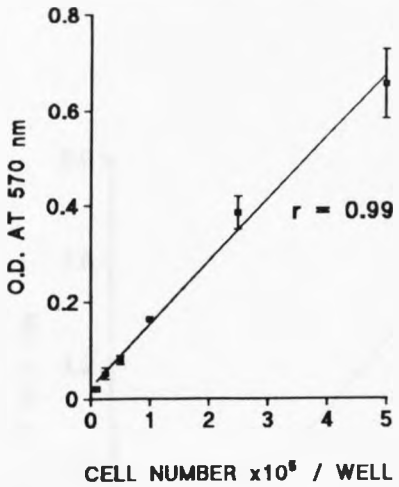

5.6b

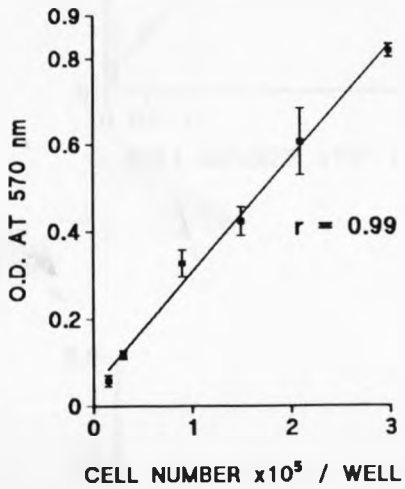

5.6c

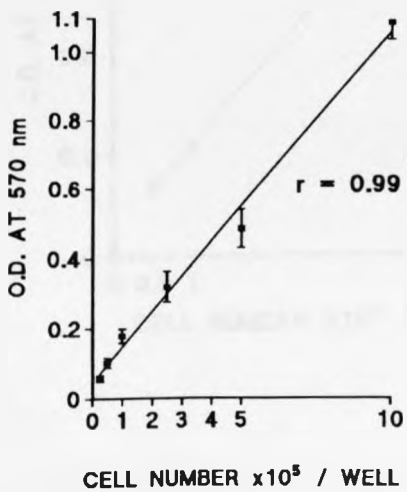

Figures 5.6 a, b & c : MTT assays performed on M^{c}Coy fibroblast-like cells illustrating the linear relationship between cell concentration and OD.

5.6d

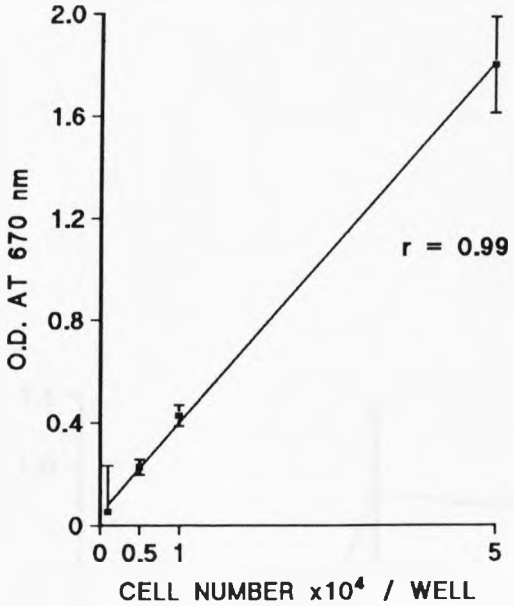

5.6e

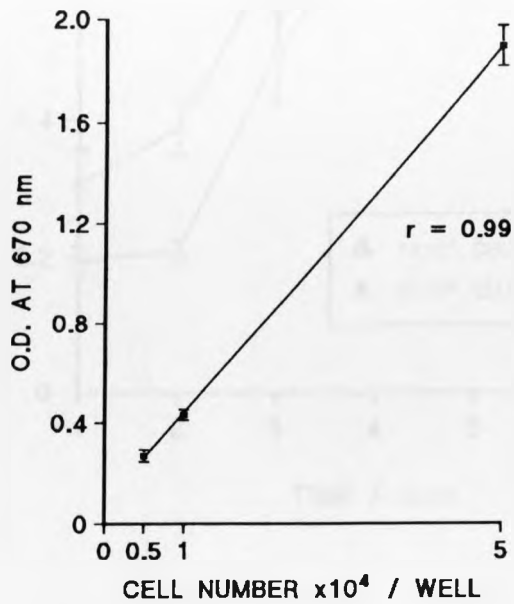

Figures 5.6 d & e : MB assays performed on HGF cells illustrating the linear relationship between cell concentration and OD.

5.6f

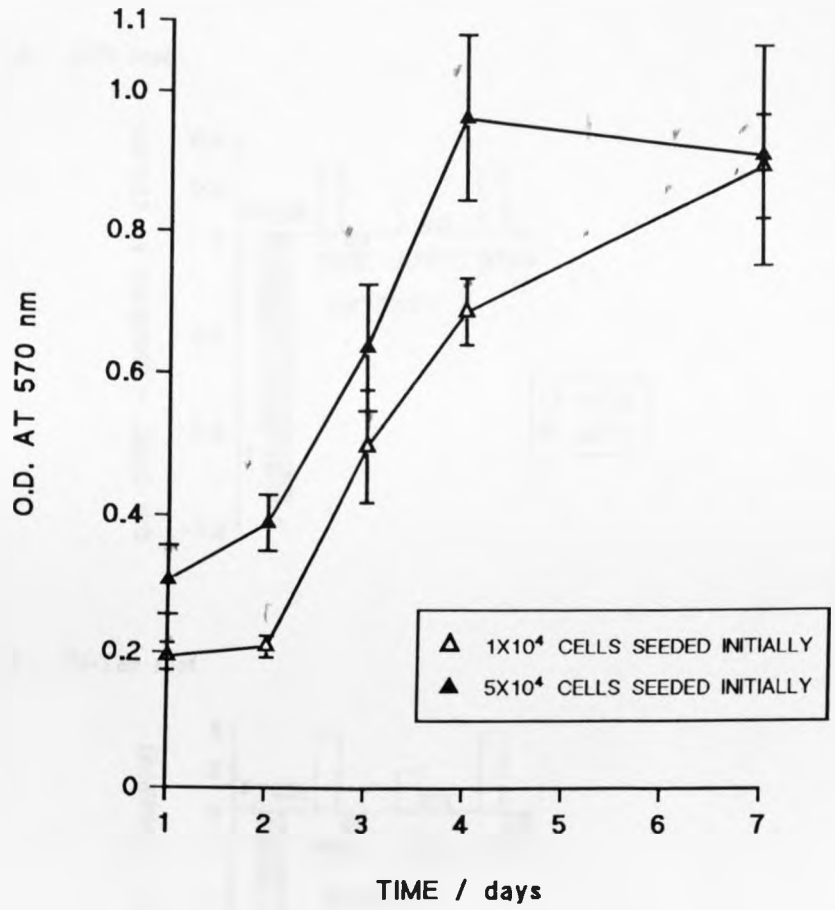

Figure 5.6 f : Growth curves of M^{c}Coy fibroblast-like cells seeded at 2 different initial concentrations and assayed using the MTT test.

5.6g : MTT test

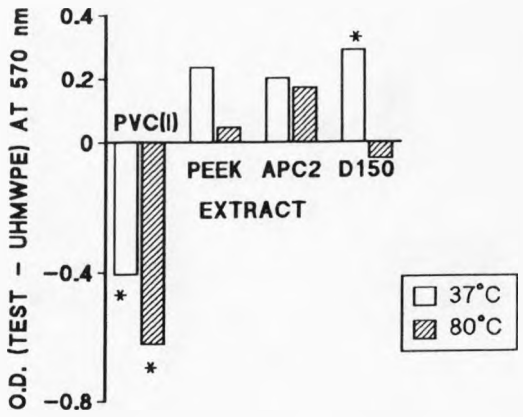

5.6h : MB test

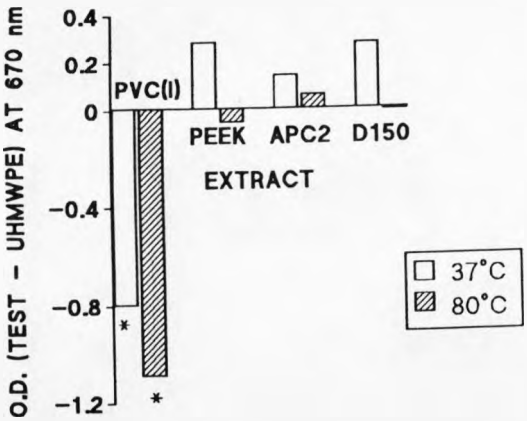

5.6i : ^{3}H-Tdr test

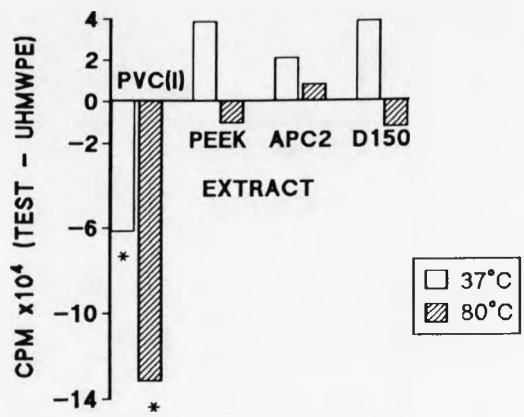

Figures 5.6 g, h & i : Extract cytotoxicity. M^{c}Coy cell behaviour examined after 72 hours incubation with material extracts obtained at 37°C and 80°C. Tests performed simultaneously. Significant differences ($p<0.001$) between the test and UHMWPE extracts are indicated by *.

5.6j : MTT test

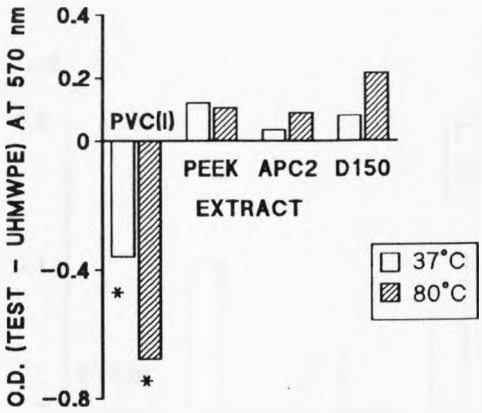

5.6k : MB test

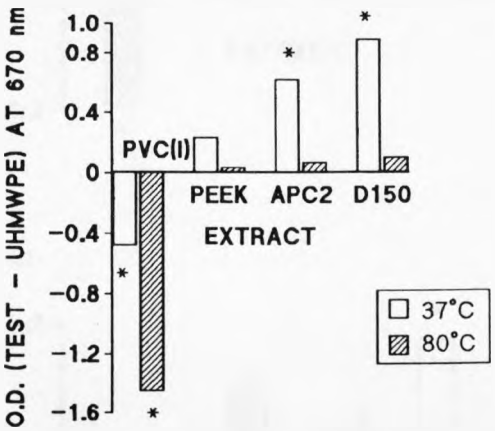

5.6l : ^{3}H-Tdr test

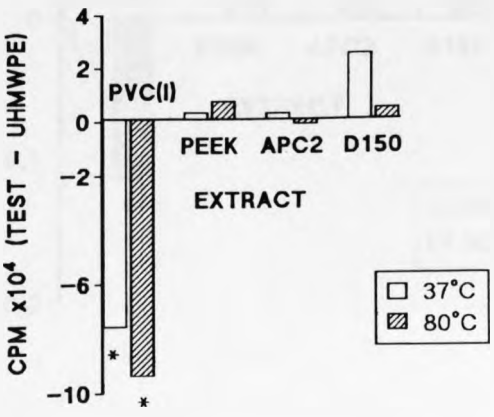

Figures 5.6 j, k & l : Extract cytotoxicity. M^{c}Coy cell behaviour after 72 hours incubation with material extracts obtained at 37°C and 80°C. Tests performed simultaneously. Significant differences ($p<0.001$) between the test and UHMWPE extracts are indicated by *.

5.6m : MTT test

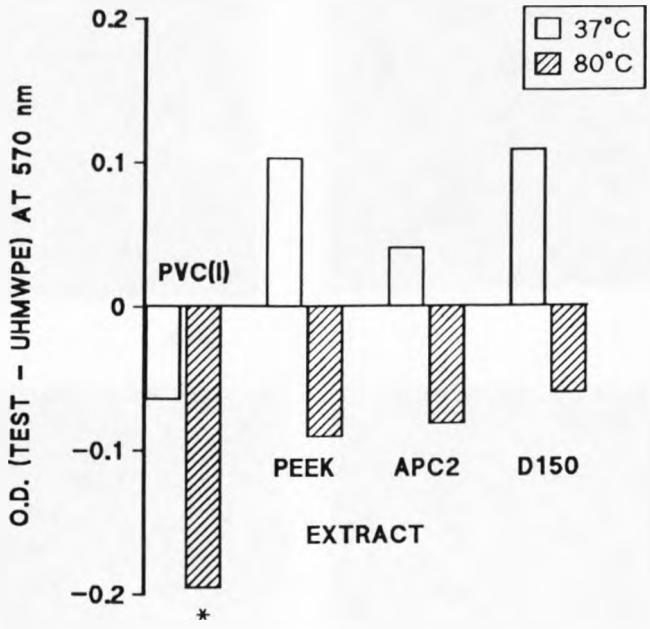

5.6n : MB test

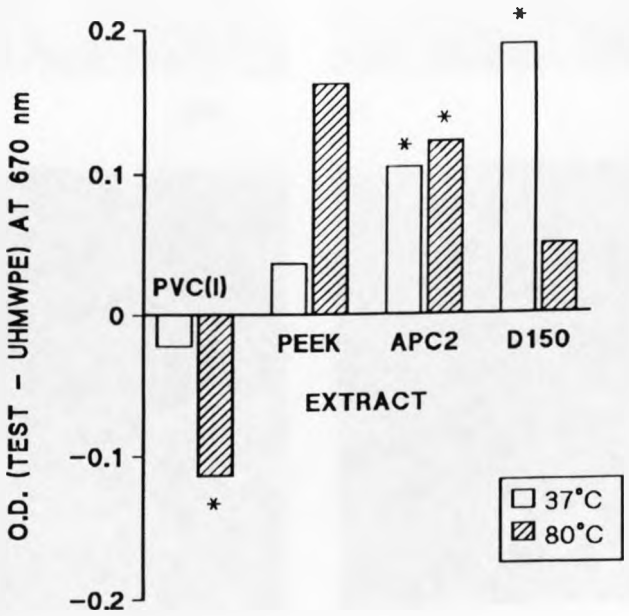

Figures 5.6 m & n : Extract cytotoxicity. HGF cell behaviour after 72 hours incubation with material extracts obtained at 37°C and 80°C. Tests performed simultaneously. Significant differences ($p<0.001$) between the test and UHMWPE extracts are indicated by *.

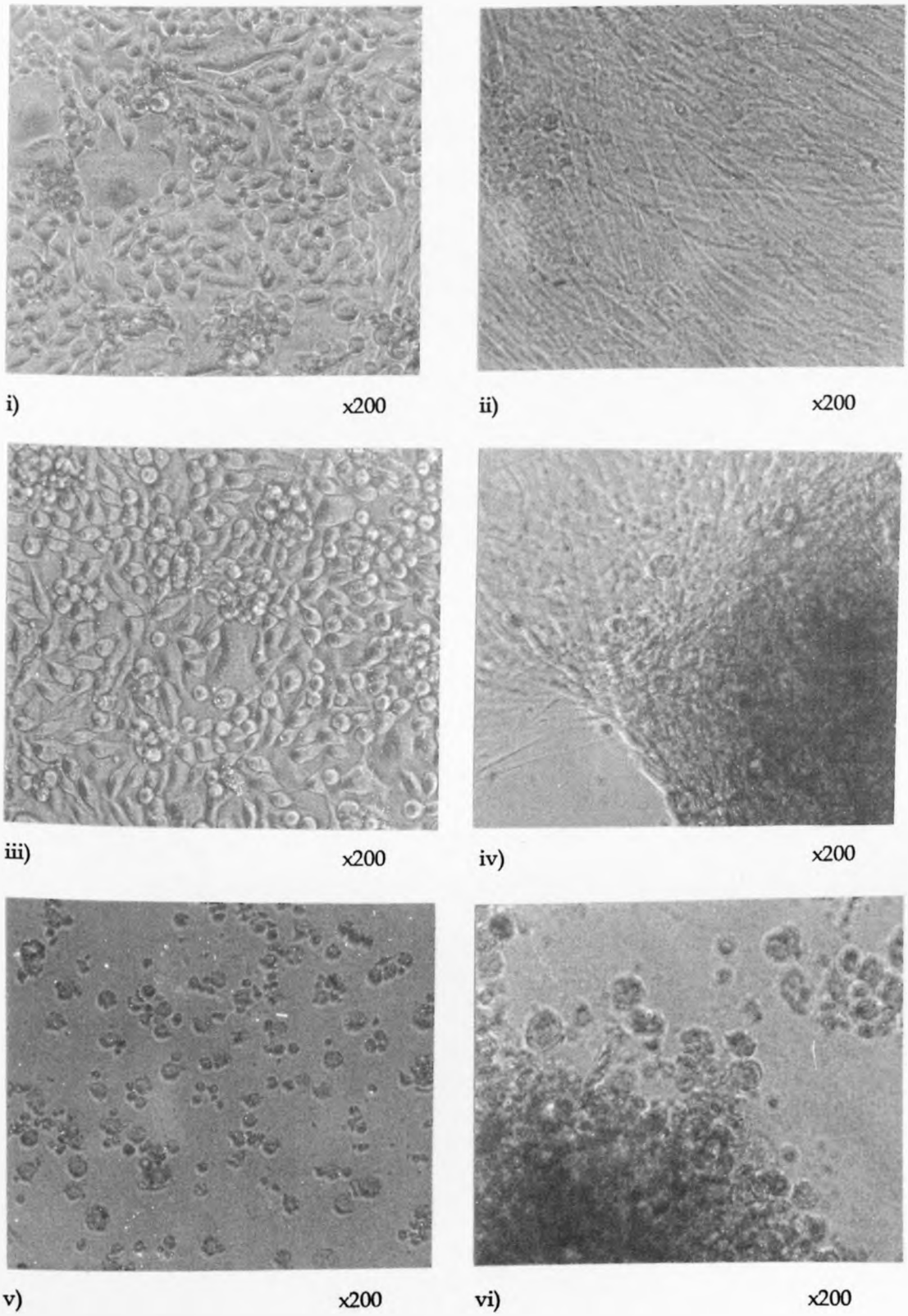

Figure 5.6o: Extract cytotoxicity. Light micrographs of M^{c}Coy fibroblast-like cells incubated with D150CA30 (i), UHMWPE (iii) & PVC_{lead} (v) extracts; and HGF fibroblasts incubated with APC2 (ii) & PVC_{lead} (iv & vi) extracts. All extracts obtained at 80°C except for PVC_{lead} iv - obtained at 37°C. Incubation time was 72 hours.

Table 5.6a: MTT assay

Extract	Mean OD at 570nm ± s.d.	
Temperature	37°C	80°C
PVC(l)	0.01 ± 0.01	0.01 ± 0.01
UHMWPE	0.42 ± 0.10	0.63 ± 0.11
PEEK	0.66 ± 0.08	0.67 ± 0.07
APC2	0.62 ± 0.13	0.80 ± 0.14
D150CA30	0.71 ± 0.08	0.58 ± 0.10

Table 5.6b: MB assay

Extract	Mean OD at 670nm ± s.d.	
Temperature	37°C	80°C
PVC(l)	0 ± 0	0 ± 0
UHMWPE	0.80 ± 0.13	1.09 ± 0.11
PEEK	1.08 ± 0.05	1.04 ± 0.09
APC2	0.94 ± 0.08	1.10 ± 0.14
D150CA30	1.07 ± 0.09	1.07 ± 0.11

Table 5.6c: ^{3}H-Tdr uptake assay

Extract	Mean CPM ± s.d.	
Temperature	37°C	80°C
PVC(l)	27 ± 2269	35 ± 5
UHMWPE	67334 ± 42197	131811 ± 24006
PEEK	106219 ± 13034	121785 ± 29540
APC2	88664 ± 2936	140227 ± 3533
D150CA30	106516 ± 18629	119587 ± 14375

Tables 5.6 a, b & c: Test and control materials were extracted for 1 month at 37°C and 80°C. The resultant extracts were tested simultaneously using the MTT assay, the MB test and the ^{3}H-Tdr uptake assay. Each value is a mean of 5 wells.

Table 5.6d: MTT assay

	Mean OD at 570nm ± s.d.	
	Experiment	
Material	1	2
Tc	0.56 ± 0.12	0.97 ± 0.12
PEEK	0.20 ± 0.10	0.83 ± 0.07
APC2	0.50 0.25	0.87 0.08
D150	0.65 0.13	0.72 0.11

Table 5.6e: MB assay

	Mean OD at 670nm ± s.d.		
	Experiment		
Material	1	2	3
Tc	0.60 ± 0.12	0.47 ± 0.06	0.74 ± 0.04
PEEK	0.43 ± 0.15	0.60 ± 0.08	0.83 ± 0.02
APC2	0.68 ± 0.07	0.73 ± 0.12	N.D.
D150	0.63 ± 0.06	0.64 ± 0.10	0.92 ± 0.02

Tables 5.6 d & e: Test materials incubated with M^{c}Coy fibroblast cells for 96 hours and assayed using the MTT and MB assays. No significant differences between the control tissue culture surface (Tc) and the test materials. Each value is the mean of measurements made on 3 materials.

5.7 Chemiluminescence assay

Results from chemiluminescence studies on PEEK powders are shown in Figure 5.7a. Background readings of 0.5mV obtained with the buffer were subtracted before plotting. Both opsonized and non-opsonized 380P, 150P, PTFE, and PVC_{lead} were examined, but readings above the background level were only found with the PEEK powders. The maximum voltage recorded with the positive control, opsonized zymosan, was 390mV 7 minutes after the reaction was started.

The experiment was repeated twice, but the source of neutrophils and serum was different and no stimulation of cells was seen.

5.7a

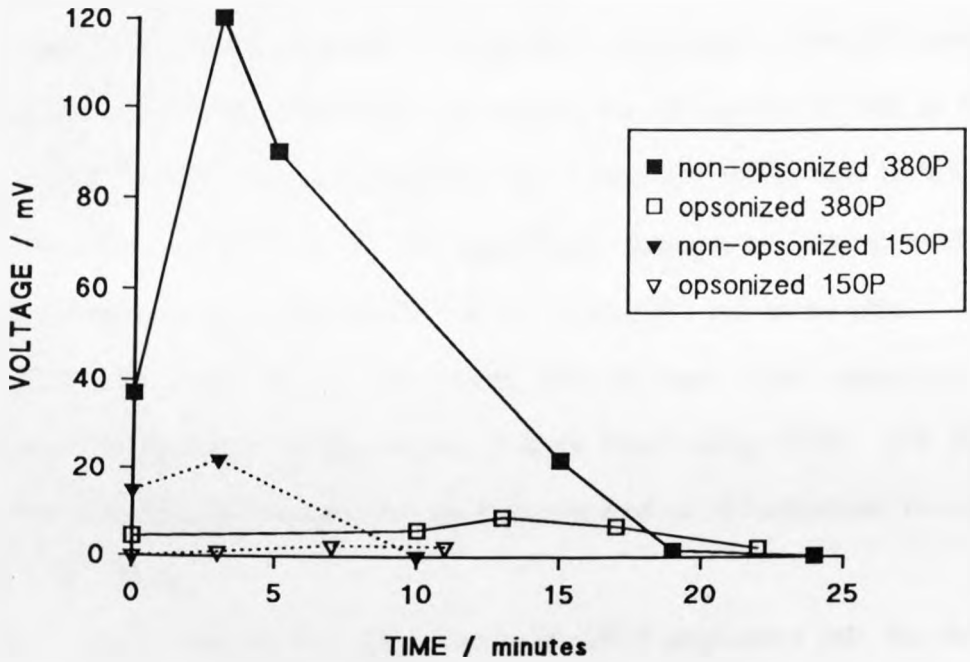

Figure 5.7 a : Chemiluminescent assay. Stimulation of human polymorphonuclear leukocytes by 40µm PEEK powders. The background reading of 0.5mV has been subtracted. No response was seen with PTFE and PVC_{lead} powders assayed at the same time.

5.8 Mechanical testing

Figures 5.8a and b show the change in mechanical properties after ageing in PBS at 37°C and 80°C, and implantation. All the tensile and flexural strength results obtained after ageing are given in Tables 5.8a and b. Microhardness results are given in Figures 5.8c - e. Each value is a mean of 20 measurements made at random on 2 samples. The flexural modulus results performed periodically on test materials aged at 37°C and 80°C are given in Table 5.8c & d.

A significant decrease in tensile strength was seen for APC2 after ageing for 18 months in PBS at 80°C, whilst a significant increase was seen for D150CA30 after ageing in all environments. A significant decrease in flexural strength was seen for APC2 and D150CA30 after ageing for 18 months in PBS at 80°C. A significant decrease in microhardness was found for PEEK and D150CA30 after 16 months in PBS at 80°C. No significant changes in flexural modulus were found for samples aged in PBS at 37°C and 80°C for 16 months.

The fractured ends of the composite flexural bars were examined for evidence of degradation of the matrix / fibre bond using SEM. The fibres were seen to be still fully coated by the polymer and no delamination was seen (Figure 5.8f, i & ii).

Push out tests were performed on rods of APC2 implanted into the femur of male rats. The push out tester used and the location of the rod in bone are shown in Figure 5.8f, iii & iv. Two such tests were performed - on unfixed, fresh tissue. The load-displacement traces obtained were similar in form, although different in terms of peak load recorded, and consisted of an initial peak in load followed by a steady trough and then another peak. The displacement from the start of the trace which corresponded to the thickness of bone was measured to give an estimate of the point on the trace at which

the implant should have been clear of the bone. For both samples, this was before the second peak occurred on the trace; implying that the second peak was due to the resistance of the vacuum sealant used to secure the bone. The first peak recorded was considered to represent the load needed to overcome the strength of attachment of the material to bony tissue.

An estimate of the interface shear strength and interface shear stiffness was made using the maximum area of bone / implant contact as that given by:

$$\text{Area} = \pi \times D \times l$$ where D is the diameter of the test rod and l is the length of the test rod

For sample 1, l = 2.7 mm and D = 2 mm
therefore, Area = 17 mm^2

For sample 2, l = 2.9 mm and D = 2 mm
therefore, Area = 18 mm^2

assuming that the test rod was in contact with bone at all points along its length. The maximum interface shear strength was determined using the first peak load obtained from the load-displacement graph and the area as given above. Interface stiffnesses were obtained from the slope of the straight line portion of the load-displacement graph and were normalized by expressing them in terms of stiffness per unit length (l); this enabled comparison with other published results. The results obtained in this manner are estimates of the *minimum* shear strength and stiffness as the area of bone / implant contact is likely to be less than calculated. The results are given in Table 5.8e.

The implant surface was examined after testing using SEM and compared with a control surface (Figures 5.8f, v & vi). Both surfaces were rough, with carbon fibres exposed on the surface; no adherent tissue could be identified on the implanted surface.

5.8a : Tensile strength

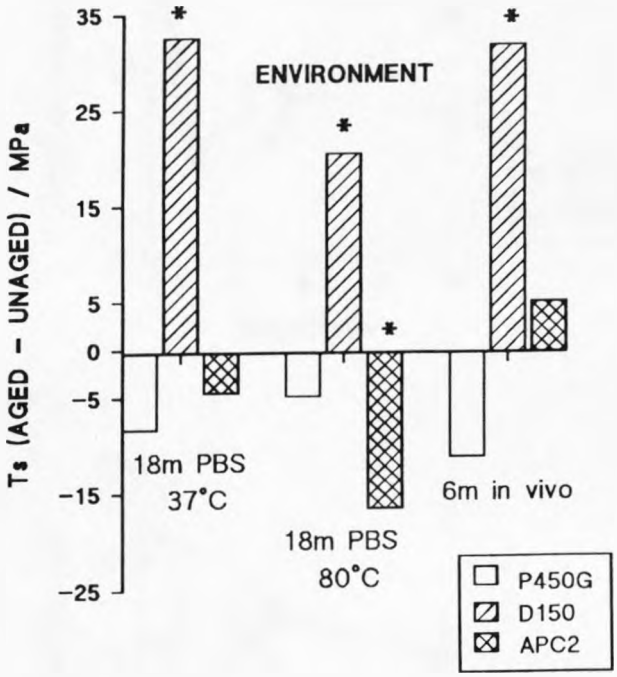

5.8b : Flexural strength

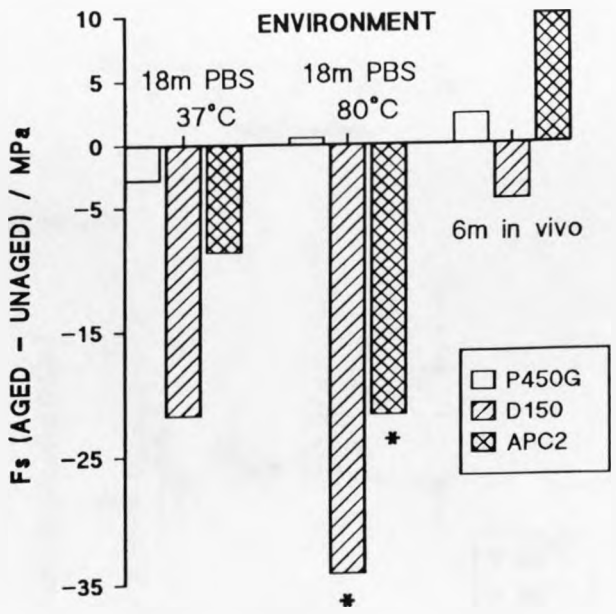

Figures 5.8 a & b : Mechanical strength. Measurments made before and after ageing in different environments. Significant differences, $p<0.001$, are denoted by *; phosphate buffered saline (PBS); months (m).

5.8c : PEEK

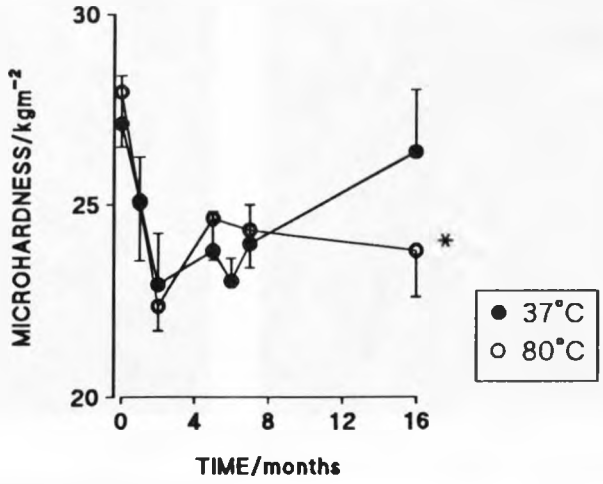

5.8d : APC2

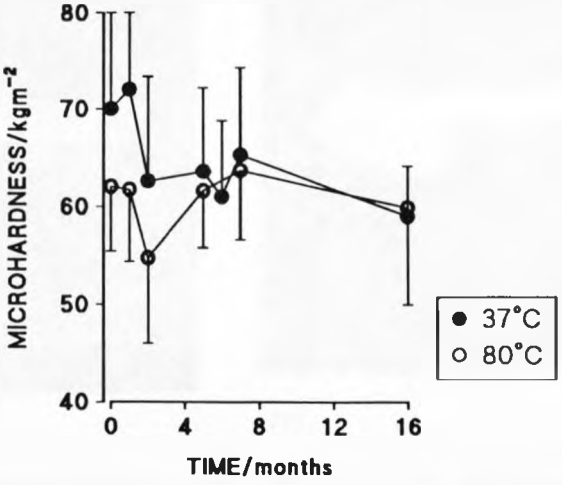

5.8e : D150CA30

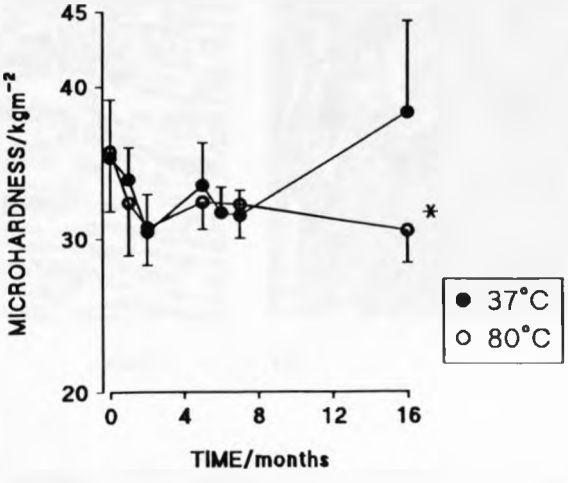

Figures 5.8 c, d & e : Microhardness measurements performed periodically on materials aged in phosphate buffered saline at 37°C and 80°C. Significant differences, $p<0.001$, between measurements at 0 and 16 months are indicated by *.

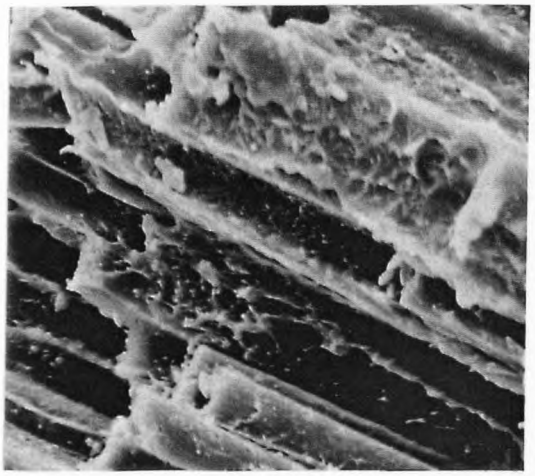

i) x1540

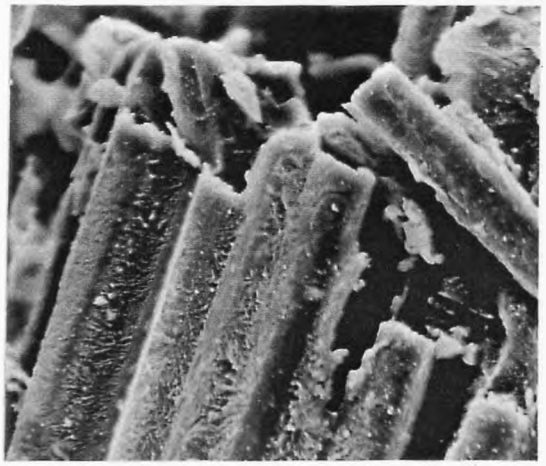

ii) x1540

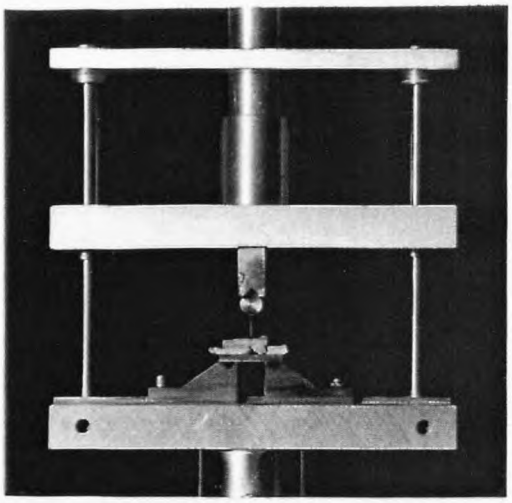

iii)

iv)

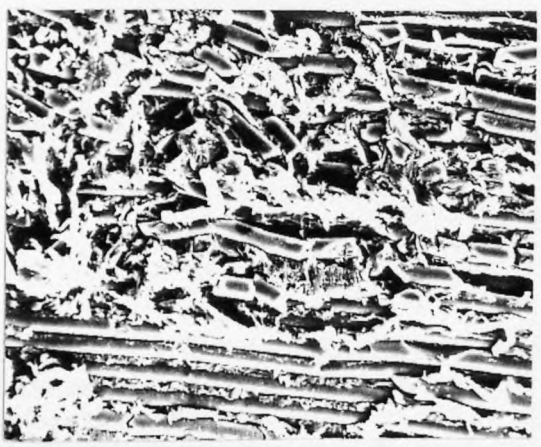

v) x540

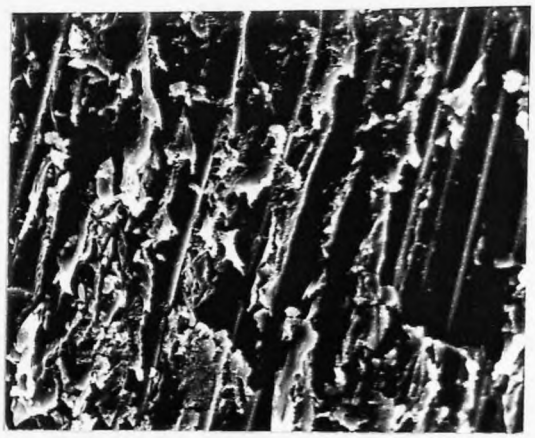

vi) x1140

Figure 5.8f: Mechanical testing. SEM micrographs of APC2 transflex fracture surfaces - unaged control specimen (i) and specimen aged for 18 months in PBS at 80°C (ii). Push-out tester used to examine strength of bone / implant attachment (iii). Rat femur with APC2 test rod in place (iv). SEM micrographs showing surface of APC2 implant before (v) and after (vi) push-out test (6 months intraosseous implantation).

Table 5.8a: Tensile strength

Specimen Orientation		90° to melt flow	90° to fibres	90° to melt flow
Materials:		P450G Ts/MPa	APC2 Ts/MPa	D150 Ts/MPa
Conditions				
Tests performed on JJ				
Unaged	mean	89.7	N.D.	105.9
	s.d.	2.1		16.1
	n	23		10
Autoclaved	mean	91.4	N.D.	108.6
	s.d.	3.8		7.4
	n	24		11
Tests performed on Instron				
Unaged	mean	100.8	72.2	96.2
	s.d.	5.3	9.8	6.8
	n	11	12	12
18 months PBS at 37°C	mean	98.4	67.7	127.8*
	s.d.	2.8	9.5	11.1
	n	11	11	12
18 months PBS at 80°C	mean	101.8	55.6*	115.8*
	s.d.	3.2	8.0	11.6
	n	12	9	12
6 months *in vivo*	mean	95.5	77.1	127.1*
	s.d.	4.7	12.1	8.0
	n	12	12	12

Table 5.8a: Tensile strength tests performed on aged specimens. Significant differences, $p<0.001$, between unaged and aged results are indicated by *. Measurements were made on either a JJ Lloyds M5K using a crosshead speed of 5mm/minute, and a 5kN load cell; or an Instron 1185 using a crosshead speed of 2mm/minute, and a 10kN load cell.

Table 5.8b: Flexural strength

Specimen Orientation		90° to melt flow	90° to fibres	90° to melt flow
Materials:		P450G Fs/MPa	APC2 Fs/MPa	D150 Fs/MPa
Conditions				
Tests performed on Instron				
Unaged	mean	144.0	146.7	176.0
	s.d.	5.4	9.9	18.2
	n	9	19	7
18 months PBS at 37°C	mean	141.2	138.1	154.2*
	s.d.	4.2	13.9	10.4
	n	10	12	9
18 months PBS at 80°C	mean	144.5	124.9*	141.7*
	s.d.	2.7	9.1	18.8
	n	11	11	11
6 months *in vivo*	mean	146.3	156.8	171.5
	s.d.	3.5	7.9	17.2
	n	7	9	9

Table 5.8b: Flexural strength measurements on aged specimens. Significant differences, $p<0.001$, between unaged and aged results are indicated by *. Measurements were made on an Instron 1185 using a crosshead speed of 2mm/minute, and a 10kN load cell.

Table 5.8c: Flexural modulus - samples aged at 37°C

Specimen Orientation		90° to melt flow	90° to fibres	90° to melt flow
Materials:		P450G E_b/GPa	APC2 E_b/GPa	D150 E_b/GPa
Time / months				
0	mean	3.6	8.3	6.1
	s.d.	0.1	0.9	0.6
	n	9	9	9
1	mean	3.6	7.9	6.1
	s.d.	0.1	0.9	0.3
	n	9	9	9
5	mean	3.5	6.8	5.4
	s.d.	0.3	0.8	0.6
	n	9	9	9
6	mean	3.7	7.0	6.3
	s.d.	0.3	0.8	0.3
	n	9	9	9
7	mean	3.7	7.3	6.0
	s.d.	0.1	1.1	0.7
	n	9	9	9
16	mean	3.6	8.1	6.7
	s.d.	0.2	0.9	0.4
	n	9	9	9

Table 5.8c: Samples were aged at 37°C in phosphate buffered saline, PBS, and removed periodically for flexural modulus testing. The modulus measurements were made at a load of 20N - less than 10% of the breaking load for each material - using the Instron 1185.

Table 5.8d: Flexural modulus - samples aged at 80°C

Specimen Orientation		90° to melt flow	90° to fibres	90° to melt flow
	Materials:	P450G E_b/GPa	APC2 E_b/GPa	D150 E_b/GPa
Time / months				
0	mean	3.7	7.3	6.5
	s.d.	0.1	1.1	0.7
	n	9	9	9
1	mean	4.5	8.7	6.8
	s.d.	0.1	1.1	1.0
	n	9	9	9
5	mean	3.8	6.7	6.4
	s.d.	0.1	0.9	0.5
	n	9	9	9
7	mean	3.9	7.0	6.2
	s.d.	0.2	1.2	0.4
	n	9	9	9
16	mean	3.8	7.6	6.5
	s.d.	0.1	0.6	0.6
	n	9	9	9

Table 5.8d: Samples were aged in phosphate buffered saline, PBS, at 80°C, periodically removed and flexural modulus measurements made. Measurements were made at a load of 20N - less than 10% of the breaking load for each material - using the Instron 1185.

Table 5.8e: Push-out tests

SAMPLE	Fmax /N	σ /MPa	Gs /GPa /m
1	146	9	20
2	237	13	19

Table 5.8e: Tests performed on an Instron 1185 tester using a 5kN load cell and a crosshead speed of 1mm/minute. Fmax is the maximum load recorded on the load-deflection curve, σ is the interface shear strength and Gs is the shear stiffness (normalized to take account of the different specimen lengths).

5.9 Differential scanning calorimetry

Heating and cooling scans were made on surface layers of P450G and APC2 aged for 18 months in PBS at 80°C and compared to those of unaged specimens. The results are given in Table 5.9a. No differences were detected between the aged and unaged PEEK polymer samples. The increase in crystallinity in aged APC2 detected in the cooling scan suggests that the aged sample may be marginally better nucleated. A different grade of PEEK is used in the production of APC2 giving rise to the difference in Tp recorded between the P450G and the composite. The Tp values measured were usual for the respective grades of polymer.

Table 5.9a

	Heat Scan		Cool Scan	
Sample	Tp/°C	% X	Tc/°C	% X
P450G unaged	338	32	289	37
P450G aged	338	30	289	39
APC2 unaged	342	35	285	38
APC2 aged	343	35	289	39

Table 5.9a: DSC scans on PEEK and APC2 using a Perkin-Elmer DSC4 with a scan rate of 20°C/minute. The crystallinity of APC2 was calculated assuming a carbon fibre content by weight of 68%. X is crystallinity.

6.1 Intramuscular toxicity assessment

The intramuscular response to the materials was followed from 7 weeks up to a period of 9 months. The host response to the material at all observation times was characterized by a thin, poorly vascularized, fibrous capsule with a few stray inflammatory cells seen on occasion. The longer time periods were chosen so as to reveal any differences in the response to the materials composition which may have been masked by the normal wound healing response. The materials were effectively isolated from the surrounding muscle by the fibrous capsule, and although the inflammatory response may be described as minimal, the materials cannot be thought of as totally unreactive, as the normal repair of muscle tissue with new muscle was disrupted.

The presence of fatty tissue associated with the implant site has been noted before with PEEK (Williams, 1987b). It is thought that such tissue represents degenerative muscle and has accordingly been termed fatty degenerative muscle. The mechanism or reason for muscle to regenerate as fat is unknown. The carbon particles seen in the capsule surrounding the composites were either dislodged from the material surface upon removal or through micromotion at the material / tissue interface during the implantation time. Even if they had been present for a period of time, no inflammatory response was stimulated as they were not associated with macrophages or leucocytes. No migration of particles from the interface into the surrounding tissue was seen.

In general, carbon containing materials have been shown to be highly compatible with minimal tissue response *in vivo*. Woven carbon fibre pads have been successfully used to resurface osteochondral defects in the knee. Animal studies using these pads indicated that carbon fibre debris seen elicited a minimal histiocytic reaction (Muckle, 1990). The biocompatibility of carbon fibre reinforced high density polyethylene (CFRHDP) wear debris has been investigated by Rushton (1984). The debris was injected intra-articularly and the reaction compared with that due to the injection of HDP and carbon fibres. The carbon fibre content was not seen to modify the response. Carbon fibre reinforced thermoplastic plates for fracture fixation have been evaluated (Gillett, 1985). Whilst a moderate inflammatory reaction to particulate debris was occasionally seen, the materials functioned well mechanically.

Removal of the implant led to distortion of the capsule and loss of information on the composition of the material / tissue interface. This did not inhibit assessment of the gross toxicity of the materials, but information as to subtle differences between the carbon fibre reinforced materials and the unfilled PEEK resin may have been lost. Future work on the soft tissue response to the materials would use resin embedding of the tissue block to allow *in situ* sectioning of the materials with the surrounding tissue. Some preliminary investigation into the use of LRGold (Polysciences), a low temperature resin which allows enzyme and immuno- staining of tissue sections, has been undertaken. A satisfactory infiltration and embedding schedule was developed for tissue blocks of the size necessary to examine the tissue response to the material, and the preservation of enzymes demonstrated by testing for alkaline phosphatase and succinic dehydrogenase.

6.2 Intraosseous response to the test materials

The reaction of bone tissue to PEEK and the composites was examined at 6 months and to PEEK alone at 3 months. Only one subcapital fracture of the femur was found (upon sacrifice of the animal), and this was probably iatrogenic. The animals were allowed full weight bearing immediately after operation; any marked changes in local stress caused by the drilling and placement of the material in the femur would have led to immediate fracture. There was no obvious absorption of extracellular fluid causing swelling of the material and leading to an increase in pressure on the bone, as this would also have prompted fracture.

The healing of bone damaged by the drilling procedure follows a recognized pattern, with an initial hæmatoma formed containing inflammatory cells such as neutrophils, lymphocytes and macrophages. This clot, together with damaged bone, will be removed by macrophages and osteoclasts in the first few days post operative. Osteoblasts and osteoprogenitor cells in the endosteum and particularly the periosteum will start to proliferate and osteoblasts migrate to the area of damage. Osteoid tissue will be secreted by osteoblasts forming a callus, which is gradually replaced by fully mineralized bone. During this time, extensive remodelling of newly formed and nearby original bone occurs. Many different local mitogenic and chemotactic factors are involved in this sequence, as well as systemic hormones such as parathyroid hormone (PTH) and vitamin D metabolites. At the time periods examined, no gross inflammatory response or areas of necrotic bone tissue were seen with any of the materials.

The osteoclast, a large multinucleated cell, is thought to be the major cell involved in resorption of bone although its mode of action is still undetermined. It is characterized by a ruffled border associated with the

plasma membrane, which creates a microenvironment where active resorption takes place. The first step in resorption is the dissolution of the mineral phase, possibly by H^+ ions, followed by enzymic degradation of the organic phase. Both neutral collagenases and various lysosomal acid proteases are thought to be involved here. Osteoblasts are thought to act synergistically with osteoclasts in the resorption of bone.

The bone plus implant was sectioned longitudinally, parallel with the long axis of the bone. Transverse sections would have allowed the assessment of the effect of material contact on different bony tissues such as the periosteum, but would not have enabled assessment of the osteoconductive nature of the material.

The presence of an area of lower mineral density, and reversal and arrest cement lines, adjacent to the APC2 implant at 6 months and the PEEK implant at 3 months (identified in the BEI) is indicative of bone remodelling. Reversal lines occur when bone formation follows a period of bone removal or resorption; the irregular edge of this line is due to osteoclast activity. Arrest lines occur when bone formation resumes after an interruption of some sort, and are characterized by a smooth edge. The area probably represents incompletely mineralized osteoid tissue, rather than resorption of calcium (hydroxyapatite crystals) alone, as remodelling is usually a change in total bony tissue mass not just mineral density.

The remodelling seen associated with APC2 at 6 months and PEEK at 3 months may simply be coincidence as the process occurs throughout an animal's life. The implants were placed when the animals were already 7 months old and therefore sexually mature. The excessive remodelling occurring with growth would be expected to have finished at this age. Unfortunately no control femurs were included in the study which would have enabled

comparison with remodelling seen normally. However, areas of lower mineral density were only seen in close association with the material - bone not in contact with the material did not show any such change. The exact stimuli causing remodelling of bone are not known although it is thought to be under hormonal and mechanical control. Normally, bone formation is tightly coupled to bone destruction ensuring a constant mass of bone, but it appears from the BEI micrographs that excessive resorption has occurred in relation to one of the following: the materials' bulk chemistry, surface roughness, or mechanical properties. From the intramuscular and the cytotoxic studies it is unlikely that any substance has leached from the surface of the material which is capable of stimulating the cells. It is more likely that the surface roughness, mechanical properties of the materials, or the closeness of fit upon initial insertion may have affected cell activity.

It is generally agreed that a causal relationship exists between functional activity and bone architecture as described by Wolff's law; if load bearing is reduced, there is a decline in bone mass. The mechanism by which mechanical stimuli influence bone cell behaviour *in vivo* are unknown but may involve electrical signals passed between cells. Deformation of bone has been shown to elicit electrical charges, which may involve piezoelectric phenomena arising from hydroxyapatite crystals or collagen. Recently, Skerry et al (1990) have shown both *in vitro* and *in vivo* that proteoglycan molecules within bone change their orientation upon loading. As proteoglycan molecules are highly charged, their orientation may affect the flow of tissue fluid (which also contains charged particles) through channels in bone tissue, thus perhaps linking electrical and mechanical phenomena.

Remodelling may have occurred due to modification of local stresses by the APC2 implant, perhaps leading to stress shielding and bone resorption, as

discussed in Chapter I. The position of the implant in the bone (perpendicular to the long axis) would mean that any stress shielding occurring would be seen in the bone 'downstream' from the implant. The area of lower mineral density was not localized in this way, but was associated with the area of material/tissue contact. Stress shielding would also be expected to be minimal in a transcortical implant as the materials are not being subjected to physiological loading.

The implants were stabilized by interference fit and, dependent on the tightness of the initial fit, micromotion may have occurred to a greater or lesser extent, leading to a greater amount of remodelling. If this had occurred with the APC2 implant, the imposition of fibrous tissue between the implant and the bone would also be expected. At the 6 month point examined, a fibrous layer was not obvious with the imaging systems used and a very close relationship between bone and implant was seen. Fibrous tissue may have been present at earlier time periods and the remodelling seen could be an extension of the healing period caused by micromotion.

There are two possible reasons why an area of lower mineral density was seen adjacent to the PEEK implant at 3 months but was absent at 6 months. The area may represent a stage of healing which is completed between 3 and 6 months, and which would presumably be seen with the other materials if they had been examined at this earlier time period; or, these areas may have been seen at 6 months if more samples had been examined. The increased numbers of osteocyte lacunae seen in the area of lower mineral density associated with the 3 month PEEK implant indicate that the bone is being laid down as part of wound healing, as osteocytes are derived from osteoblasts involved in organic matrix synthesis.

From the points discussed above it is probable that the remodelling seen

was associated with wound healing in the case of the PEEK implant and with the surface morphology of the APC2 implant. In both cases, initial fit of the implant upon insertion may have played a part. An area of remodelling was also seen at the periosteal edge of the bone containing the APC2 implant, this probably corresponds to periosteal thickening; a mechanism of increasing the mass of bone in response to functional needs.

Some blocks were excluded from the SEM study because their surface was pitted due to air bubbles introduced when embedding, however these were sectioned for light microscopy as were the 'SEM blocks'. On all the sections examined a thin spur of bone was seen to surround the implant perimeter to a greater or lesser extent. This indicates that the materials may be osteoconductive as the bone was formed from an existing ossified front, cortical bone, into the marrow tissue. This thin layer of bony tissue was also seen using BEI and with toluidine blue stained thin sections of the 3 month PEEK implant. The black appearance of some lacunae and canaliculi in sections examined using light microscopy may have been caused by a processing artefact resulting in differential staining of non-viable osteocytes. However, further investigation is required to explain this staining.

Very close apposition of bone tissue to all the implant materials was seen on all specimens. A small gap between the implant surface and bone was seen using high magnification, although the nature of any material in the gap could not be ascertained. Further studies using TEM are necessary to establish the nature of the tissue contact at the surface.

Despite the small number of specimens examined, it is obvious that the test material surface is very attractive to bone. Further studies should use larger sample sizes and extend the periods of observation to include the stage of wound healing. It is also important that the cellular response to all of the

test materials at a variety of time periods be assessed by examining sections which are thin enough to be stained and examined under light microscopy.

Any effect the mechanical properties of the materials may have on the bone tissue with respect to remodelling, stress shielding, or porosity have only been touched on in this study; obviously as the materials are potential orthopædic materials this is an important area for future work. As low modulus materials, bone loss due to stress shielding should be reduced compared to high modulus materials such as cobalt-chromium alloys. This could be evaluated by observing the amount of disuse osteoporosis associated with the use of external fixation plates fabricated from the test materials. Studies have shown that the greatest loss in bone mass occurs under the plate (Schatzker, 1978), and that it may also be related to the contact pressure between the plate and the bone which can lead to ischemia and osteonecrosis. Backscattered electron imaging (BEI) was shown to differentiate areas of differing mineral density and could therefore be used to assess any change in mineral density associated with the formation of spongy, porous bone that is seen with osteoporosis.

Backscattered electron imaging was shown to give interesting and useful results in this study but there are few other reports describing its use in examination of the implant / bone interface (Holmes, 1987). The causes of the areas of lower mineral density adjacent to the implant could be established by several studies. Samples of all test materials should be examined 3 months and earlier after implantation to see if similar areas are seen and can be more closely associated with wound healing. It may be possible to injection mould samples of PEEK and D150CA30 which would have a smooth finish; these could then be compared with machined samples as used in this study. APC2 samples could not be fabricated in this way, but larger samples could be held against a polishing cloth and smoothed - entailing a larger animal model.

6.3 Cytotoxicity testing

The study was designed to assess different aspects of cell behaviour after exposure to the test materials in a variety of forms. Assessments of cell morphology, adhesion, metabolism and proliferation were made in comparison to positive (PVC_{lead}) and negative (UHMWPE) control materials.

All 3 test material surfaces were shown to support secondary and primary fibroblast adhesion and spreading. The surface was "as moulded" and was not specially prepared. No difference in morphology between cells on the UHMWPE and the test materials was seen. Proliferation of the cells on the surfaces could not be determined directly from these experiments, but the presence of a mixed population of round and spread cells after 24 and 48 hours indicates that the cells may have rounded up as part of mitosis. The level of attachment was quantified and shown to be comparable to that on tissue culture plastic using the MTT and MB assay.

The effect of short term leaching (24 hours) of the materials in the presence of cells was assessed in the direct contact assay. Cells adjacent to the material had a healthy appearance and were morphologically indistinguishable from the controls. Small areas of cell inhibition were occasionally seen with the test materials but not with the negative control. Over such a short time period, these areas are more likely to represent leaching of surface inhomogeneities than leaching from the bulk of the material. Also, such a local effect is unlikely to result from the diffusion of toxic plasticizers or additives from the bulk of the material as these would diffuse more evenly. The common factor between the test materials is the presence of PEEK; these areas may therefore represent inhomogeneities in the PEEK rich surface layer. Occurrence of the patches could not be correlated with material edge roughness and no local discoloration of medium was seen which would indicate a change in pH. The

significance of these small areas of inhibition with respect to normal cell metabolism cannot be deduced from this experiment and highlight the drawbacks associated with qualitative assessment of materials in this fashion.

Extended extraction of the materials was performed under physiological and stressed conditions and the extracts tested on primary and secondary fibroblast cells using 3 different tests of cell behaviour. No evidence of toxic activity of the extracts was found. Cells adhered (MB assay), proliferated (^{3}H-Tdr uptake assay) and respired (MTT assay) at the same levels as the controls. Extracting the materials at the higher temperature of 80°C did not produce any differences in cell behaviour; this is consistent with the chemical stability of PEEK materials as discussed in Chapter II. Extraction of the materials in a non aqueous medium, eg. cottonseed oil, may have led to the extraction of toxic additives, although this is unlikely on examination of the data on environmental resistance of the materials (see Chapter II).

A criticism of short term toxicity tests such as the direct contact assay is that cells subject to toxic influences may only show a response several days later, and so examination of the effect of the extracts was performed after 72 hours incubation to allow time for any subtle toxic effect to be exerted. However, the tests only revealed cells which were incapacitated in some way at the time of assay; survival tests, where the test substance is removed and culture continued are a way of measuring the long term effect of exposure. If any significant differences had been seen between the test and control material response, survival tests would have been performed.

It has been suggested that primary cells are more sensitive to the environment and toxic challenge than established cell lines (Feigal, 1985). This was not found with the HGF cells; in contrast, these cells were more robust than the M^{c}Coys in the presence of the PVC_{lead} extract. PVC_{lead} was repeatably

toxic in all of the cytotoxicity assays performed using M^{c}Coy cells: no cells were ever seen adhering using the SEM, no cells were ever seen adjacent to the material in the direct contact assay, and there was reduced adhesion and a change in morphology of cells upon incubation with the extracts. The mechanism of toxicity of the PVC_{lead} could not be deduced from any of the experiments. Trace element analysis of the extracts showed the presence of lead, barium and cadmium, all at less than 30ppm. Cadmium and lead have been shown to affect enzyme activity *in vitro* (Vallee, 1972). Although slight differences were seen in the levels of elements present in the other extracts when examined using ICPMS, most notably the presence of zinc in the D150CA30 extract, no modification of the cell response was seen.

Until recently, the MTT assay had not been described for use in biomaterial assessment; one of the aims of the study was to evaluate its use as a quantitative means of appraising biomaterials. It was found to yield similar results to those of the MB and thymidine uptake assays with the advantages of yielding data on the metabolism of the cell, rather than just cell attachment as in the MB assay, and of being safer to use than radiolabelled thymidine. It was also possible to quantify the cell behaviour on the test material surface using the MTT (and MB) assay, although on other materials examined (UHMWPE and Biomer) the formazan could not be fully released from the surface even though a variety of solvents was tried. The MTT assay is therefore not universally applicable to all material surfaces. It is not suggested that other *in vitro* tests should be abandoned in favour of the MTT assay, but rather that the MTT assay be used as an easy first screening test whose results should be confirmed with further *in vitro* tests.

The MTT assay was used in these experiments purely as a viability test and not as a means of examining cell activation by the materials. However, it has

been shown that activated T-cells, identified using an immunofluorescent stain for the Il-2 receptor, exhibit MTT staining (Schauer, 1989). It has been suggested that MTT used in this way can be used clinically, to characterize activated T-cell subsets. It is possible therefore, that MTT may be used in a similar fashion to examine cell activation by biomaterials.

Results from the chemiluminescence assay indicated that the PEEK powders may be capable of stimulating human neutrophils. Neutrophils will be present during the early phase of the inflammatory reaction and are normally not found after a few days. Stimulation releases superoxide anions and highly reactive oxygen radicals which may degrade the polymers, and which will certainly cause tissue damage in the surrounding locale. If constantly stimulated by the continuing presence of a powder, macrophages and neutrophils would proliferate in the area and a chronic inflammatory response may ensue. A very small response was seen with opsonized powders and no response was seen with PTFE and PVC_{lead} powders. That no response was seen with the PVC_{lead} is surprising as it was shown to be toxic to fibroblasts in both extracted and solid form.

It is doubtful that the results seen with non opsonized powders would be mimicked *in vivo* as the powders would become covered with a protein coating in the first few seconds in place. This, as was seen with the results from opsonized powders, would mask the potentially activating surface of the material and reduce any stimulatory effect. Stimulation of neutrophils was only seen on one occasion; this does not invalidate the experiment where results were seen, but highlights the problems of using human primary cells in *in vitro* assays. The repeated experiments were not controlled with respect to the source of neutrophils and serum used, and as is shown by hypersensitivity experiments, human neutrophils respond differently to the

same stimuli eg. nickel. The results are therefore inconclusive and must be repeated in a properly controlled manner maintaining a constant source of neutrophils and serum. It may also be advantageous to use an animal cell such as the peritoneal macrophage derived from either the rat or the mouse; this is likely to be less variable in response and easier to obtain. Macrophages would be a pertinent cell to study the effect of the PEEK powders on, as they would be the major cell type involved in an inflammatory reaction to any wear particles.

Fibroblasts are an important component of the wound healing process as they secrete collagen and are involved in wound contraction; however, they can only be termed a general biocompatibility screening tool in this study as the test materials are putative orthopædic materials and will be interacting with bone cells. Kirkpatrick (1990) has suggested that *in vitro* biocompatibility testing should consist of two stages; a first general screening stage and a second more specific stage where pertinent cell lines are used. In this way *in vivo* conditions are simulated as closely as possible. The interaction of osteoblasts and the material surface is of paramount importance to successful incorporation of an intraosseous implant and should be examined in future *in vitro* studies.

6.4 Physiological ageing of the materials

Simple mechanical tests were used to assess the integrity of the material structure after ageing in essentially aqueous environments at 37°C and 80°C. Apart from a decrease in microhardness at 80°C, little change in mechanical properties was seen with the resin PEEK. The gradual decrease in microhardness of PEEK over the time period of observation may have been due to gradual absorption of water which would act as a plasticizer, decreasing the toughness and hardness of the material. No other significant changes were seen with PEEK, and the DSC results showed no difference in the crystallinity of aged and unaged PEEK.

Testing of the composites was performed in the weakest direction ie. at 90° to the melt flow or fibre direction so that any effect of water absorption or degradation of the fibre matrix bond would be enhanced. A decrease in flexural strength was seen with both the composite materials after ageing in phosphate buffered saline (PBS) for 18 months; at 80°C, the change was significant. A decrease in microhardness of D150CA30 was also seen after ageing at 80°C. Results from both these tests will be dominated by the skin or surface of the specimen rather than the bulk. Any absorption of water might therefore be expected to have a noticeable effect as a gradient will probably exist with water concentration decreasing from the surface towards the bulk. No degradation of the fibre-matrix bond could be seen on electron microscopic examination of fractured ends of the tensile and flexural specimens, with the pulled out fibres still seen to be covered by resin. The mechanical failure was therefore presumed to be primarily due to matrix failure.

Consistent with the decrease in transverse flexural strength of the APC2 samples aged at 80°C there was a significant decrease in tensile strength at this temperature after ageing. The reason for the increased detrimental effect of the

elevated temperature on the mechanical properties of APC2 is unknown. Although the higher temperature is nearer the Tg of the resin (143°C), it is unlikely that the crystallinity of the matrix is being affected as no differences between the matrix of aged and unaged APC2 samples were detected using DSC. It may be that some additive or sizing agent present in the composite is more soluble at this temperature. Over an 18 month period, these chemicals may leach out and weaken the fibre / matrix bond, thus reducing the mechanical strength.

The tensile test results for D150CA30 are inconsistent with the flexural strength results and the microhardness results in that the strength seems to increase after ageing rather than decrease. The increase may be due to physical ageing of the specimen, although as this is related to the polymer, the other materials would be expected to behave in the same way. The somewhat erratic changes in mechanical properties of D150CA30 seen after ageing may be due to batch differences between aged and unaged specimens. That inter-specimen variation might account for the differences seen is reinforced by the flexural modulus results where little change was seen over a 16 month period with repeated measurements on the same samples. Anisotropy of the fibres within the moulding will also contribute more to anisotropy in the strength characteristics of the test specimens than to that of the APC2 specimens. In the injection moulding the majority of fibres in the skin will be aligned in the direction of flow but those in the core will be more randomly orientated (Bozarth, 1987). Flexural test results depend largely on the outer skin characteristics of the specimen; in this case the aligned carbon fibres. Tensile test results are not so dependent on skin characteristics and the randomly orientated carbon fibres in the mid-section of the specimen will have more of an effect, resulting in strength anisotropy.

An orthopædic appliance must have reliable mechanical properties; the results of the mechanical testing show that under physiological conditions little significant change in mechanical properties of the PEEK materials was seen. The design of the tests ensured that the samples were tested in a highly stressed direction after ageing in order to simulate hostile conditions *in vivo*.

The minimum shear strength and stiffness at the bone / APC2 implant site were calculated from the push-out tests by estimating the maximum area of bone / implant contact which could occur; this was presumed to be the length of the implant rod. Exact measurements would require a precise knowledge of the area of bone / implant contact. The interface shear strength was found to vary from 9 to 13 MPa; this compares favourably with 6 month results reported by Tanner (1989) where a rabbit model was used: polyethylene - 1.6 MPa, polyhydroxybutyrate (PHB) - 8.6 MPa, 40% hydroxyapatite reinforced PHB - 6.6 MPa, and a hydroxyapatite reinforced glass - 19.3 MPa. Clemow (1981) reported the interface shear strengths of porous coated titanium implants implanted in dogs for 6 months to vary from 3.5 to 8.6 MPa, depending on the experimental conditions. Using a canine model, Thomas (1987) found the interface shear strength of uncoated and hydroxyapatite coated titanium rods to be 10 MPa and 14 MPa respectively. The interface shear stiffnesses determined for the two APC2 implants were found to be similar - 19.5 ± 0.5 GPa /m - when expressed in terms of unit length. This figure is higher than that found by Clemow for the porous coated titanium implants (1981) - 2 to 9 MPa /m, but less than that for uncoated (37.9 GPa /m) and hydroxyapatite coated (69.7 GPa /m) titanium implants at 10 weeks postimplantation (Thomas, 1987). As hydroxyapatite and titanium are both materials which have shown direct bony tissue apposition, higher interface stiffness might be expected than for APC2. It must also be remembered that the values quoted for APC2 are

minimum values, as the area of contact is likely to be overestimated. Only rough comparisons can be made between different experiments as the materials, animal models, push-out testers and method of determining the interfacial area were different. A recent exchange of letters in the Journal of Biomedical Materials Research (de Groot, 1989) highlighted the problems occurring when comparing the results of different groups which use different methods (even if the materials are similar), especially as it seems that methods are not always fully reported in original publications.

Transcortical implant push-out tests are useful for demonstrating differences in interfacial attachment strength for different materials and surface treatments but they do have limitations. The stress measured at the interface is not purely shear stress but includes tensile and compressive components (Soltesz, 1989) and the implants are not in a physiological load bearing situation (as already discussed in section 6.2 with respect to the toxicity assessment of the materials in bone). They do however represent models for the healing process associated with devices, such as porous coated hip joint replacements, which are implanted and protected prior to actual load bearing function. They are also simple to perform and so widely used that they have been accepted as a standard test of the strength of interface attachment (Black, 1989).

Further mechanical evaluation of the materials would include push-out tests of the other test materials to enable the effect of the carbon fibre reinforcement. on the interface mechanics to be assessed. Rabbit femurs are less angular than the rat femur and their use would help to overcome the problem with alignment of the loading pin and the implant. A better means of securing the alignment would be to pot the ends of the bone in a quick setting resin.

In the physiological environment, the materials will be under a cyclical stress and will be subjected to relative motion at the soft tissue interface for a fixation

plate, as well as any micromotion that might occur at the implant / bone interface. Cyclical loading of materials leads to fatigue failure where materials fail at levels below the normal yield stress. Fatigue of composite materials varies with fibre direction in a similar manner to other mechanical properties (see Chapter II). For multilayer composites, as might perhaps be fabricated in the design of an isoelastic hip prosthesis, fatigue stress cycling would be expected to produce gradual reduction in the modulus of elasticity due to fibre breakage and matrix cracking, with ultimate failure occurring in compression due to buckling of the fibres.

Relative motion between two surfaces can lead to the production of wear particles which in the physiological environment could lead to inflammation, either locally or systemically, as for example already discussed with respect to PMMA (Chapter I). In the case of fibre reinforced composites such as APC2 or D150CA30, any fibre fracture created by abrasion at the surface would be expected to decrease strength; stress concentration sites may be created which would also lead to a reduction in strength. A complicating factor is the possibility of exposure and subsequent deterioration of the fibre-matrix interface in the environment. It is important therefore that the fatigue resistance and tribological properties of the materials be assessed under physiological conditions in any further examination of the material mechanical properties.

6.5 Summary

The biocompatibility testing performed indicates that the materials show promise as orthopædic materials; the materials were stable both in terms of the host or cell response and mechanical properties, and the intraosseous results indicate close apposition of bone at the material surface.

7.1 Introduction

Material surfaces which encourage the direct apposition of bone, providing biological rather than purely mechanical attachment are being investigated as a means of attaining a stable host/implant interface. Ideally such an interface would withstand long-term duress without weakening, unlike present methods of fixation (Chapter I). The successful attachment of a prosthesis to bone tissue will depend on the elaboration of bone tissue at the surface, necessitating cell attachment and proliferation. Cell proliferation has been shown to follow cell spreading (Ben-Ze'ev, 1980); although cell spreading on material surfaces does not necessarily follow cell attachment. The cellular response to a material surface is known to be influenced by characteristics such as surface chemistry (particularly surface energy and charge) and topography (roughness and porosity), although the relative importance of these variables is debatable.

7.2 Cell attachment

In vivo, cell attachment is mediated via proteins and components of the extracellular matrix. Early experiments, correlating the extent of cell adhesion and spreading with the adsorption of various proteins from mammalian sera used in cell culture, identified fibronectin as a mediator of cell - substratum interactions (Klebe, 1974). Fibronectin is a dimeric glycoprotein of which there are two major forms; plasma fibronectin found in blood, and cellular fibronectin found in extracellular matrices and secreted locally onto cell surfaces. The two monomers of fibronectin (fn) are joined by a disulphide bond to form the dimer with a molecular weight of approximately 500kDa. Fibronectin forms

an extensive extracellular matrix in cultures of many types of cells although the main source of fibronectin *in vivo* is probably fibroblast cells (Kleinman, 1981).

Vitronectin or serum spreading factor, a single chain polypeptide, is another plasma glycoprotein which mediates the attachment and spreading of cultured cells (Hayman, 1982). Vitronectin interceded spreading occurs independently of that via fibronectin. Both fibronectin and vitronectin have binding regions for collagens and glycosaminoglycans as well as cells.

The cell binding site of fibronectin contains the tetrapeptide sequence arginine-glycine-aspartic acid-serine (RGDS) (Pierschbacher 1984), and that of vitronectin the tripeptide sequence arginine-glycine-aspartic acid (RGD) (Pytela, 1985). Synthetic peptides containing the RGDS sequence can block the adhesion of cells to fibronectin, inhibit binding of soluble fibronectin to cells, and, under certain conditions, promote the adhesion of cells (Yamada, 1987). A second site within the fibronectin cell binding domain has also been identified as necessary for efficient adhesion and cytoskeletal organisation (Obara, 1988).

In contrast to the early studies on cell adhesion which identified fibronectin as the major attachment factor involved, there is evidence that vitronectin or serum spreading factor is the more effective extracellular matrix molecule for cell adhesion and spreading. It has been found (Underwood, 1989) that under normal tissue culture conditions using serum supplemented medium, only vitronectin can be adsorbed onto the substratum in concentrations high enough to mediate cell adhesion, spreading and growth. Fibronectin, in the presence of other serum proteins shows very little adsorption onto the substratum.

Plasma membrane receptors which interact with the cell binding domain of fibronectin and vitronectin have been isolated from mammalian and avian cells and tissues (Pytela, 1985). These receptor systems belong to a large family of

related glycoprotein complexes called 'integrins' and are composed of alpha and beta subunits of about 140kDa and 120kDa respectively (Buck, 1987). Integrins possess extracellular, transmembrane and cytoplasmic domains (Argraves, 1986) and provide the link between extracellular molecules and cytoskeletal components such as actin filaments.

The collagens, a large family of multimeric structural glycoproteins, are also involved in cell adhesion, both directly via specific receptors, and indirectly by the binding of other glycoproteins such as fibronectin which then bind to the cell surface. The integrins that bind collagen have recently been identified by the use of monoclonal antibodies which specifically inhibit cell-adhesive functions (Wayner, 1987).

Integrin mediated binding provides the major mechanism for cell attachment to a surface, however proteoglycans (proteins with glycosaminoglycan side chains) present at the cell surface can bind to the glycosaminoglycan part of a glycoprotein such as fibronectin and reinforce cell attachment. Syndecan, a membrane intercalated proteoglycan carrying both heparan sulfate and chondroitin sulfate chains acts in this way, binding to collagen and fibronectin via its heparan sulfate chains (Couchman, 1983). In contrast, soluble proteoglycans or those bound to extracellular matrix can inhibit cell adhesion; by either binding to the glycosaminoglycan binding site on the glycoprotein and thereby making it inaccessible to the cell surface proteoglycan or by preventing the binding of an integrin to the cell attachment site by steric hindrance (Saunders, 1986).

Several cell substratum interaction sites have been described using techniques such as transmission electron microscopy and interference reflection microscopy (Izzard, 1976). Focal contacts with a cell-substratum distance of 10 - 20 nm are often observed at the edges of cells and cell junctions and are integrin

mediated cell adhesion sites (Chen, 1982). Although they occupy only a small part of the total interface they provide the strongest adhesion site. Close contacts with gaps of 30 - 50 nm often surround focal adhesions (Hynes, 1981), and extracellular matrix contacts represent cell substratum distances larger than 100nm (18).

7.3 Material characteristics influencing cell attachment

7.3.1 Surface energy

Atoms in the surface of a material will experience a net attraction force tending to pull such atoms into the bulk of the material, placing the surface under tension. The surface energy is the work required to create unit area of surface against the surface tension. A correlation between the surface energy of a substrate and the substratum cell adhesiveness has been described by many workers, (Lydon, 1985; Schakenraad, 1986; van der Walk, 1983). A hypothetical zone of substratum free energy starting at about 40 erg/cm^2 where materials are biocompatible has been described by Baier (1975). At 20-30 erg/cm^2 a bioadhesive minimum is described where no adhesion occurs. Schakenraad (1986) demonstrated that materials with high surface free energy (more hydrophilic) encourage cell spreading whereas those with low surface free energy (more hydrophobic) do not, even in the presence of serum proteins. However, cell growth was not found to differ significantly on substrates with different energies in the presence of serum proteins. An *in vivo* culture model has been developed by the same group (1987), where tubular porous grafts filled with cultured rat smooth muscle cells are implanted intraperitoneally. Cell adhesion and spreading was shown to be increased on the grafts of higher surface energy - confirming their *in vitro* studies.

In contrast to the above work, which emphasizes the ability of more

wettable, hydrophilic substrates to support cell attachment and spreading, several researchers have demonstrated the opposite. Cell attachment has been found to improve as the hydrophilic hydrogel, hydroxyethylmethacrylate has been copolymerized with hydrophobic polymers (Horbett, 1988; Lydon, 1985). Research into the attachment and growth of fibroblasts on polypeptides of different wettabilities has also found an increase in cell attachment and growth rate on more hydrophobic polypeptide substrates (Kang, 1989). Klebe et al (1981) found that hydrophobic substrates bound more fibronectin than hydrophilic surfaces and were more active in promoting cell attachment and growth.

It is clear that the wettability of materials cannot solely account for cell attachment. Indeed, the terms hydrophobicity and hydrophilicity have been criticised for only describing the macroscopic wetting behaviour of such materials by water in air (Hoffman, 1986). Studies made on block copolymers of hydrophilic and hydrophobic monomers have stressed the influence of the microheterophase structure of such copolymers on cell attachment and growth (Minoura, 1989).

Factors such as the mobility of the polymer molecular chain, and the excluded volume of a polymer have been proposed as more important than surface energy. The excluded volume of a polymer is related to its ability to undergo chain rotation and swelling in a solvent. In poor solvents the volume decreases because polymer chains would prefer each other and tend toward maximal packing eg. a hydrophobic polymer in a physiological environment. Polymers with increasing hydrophilicity would show more tendency towards solvation thus creating a larger excluded volume by virtue of decreasing chain-chain interactions for chain-water interaction. Cells also have an exclusion volume due to glycopolymers on the cell membrane. The cell-substrate surface

characteristics will combine to yield a net exclusion volume. Maroudas (1975a) has postulated that cells attempt to overcome the exclusion barrier by concentrating their glycopolymers at the site of adhesion. This will reduce the mobility of the substrate polymer chains and so decrease the exclusion volume. On highly hydrophilic substrates (100%pHEMA) the cells cannot compensate for the large exclusion volumes in this way and adhesion fails. Both chain mobility, and excluded volume were considered to explain results obtained by Lentz et al (1985) on the adhesion of macrophages to polymer surfaces. Adhesion was maximal on polymers with rigid structures and small excluded volumes.

7.3.2 Surface charge

The nature and density of charged groups at the material surface have also been implicated as important determinants of cell attachment and spreading. Cell membranes carry a net negative charge attributed mainly to components of glycoproteins and glycolipids, however, there are also domains of positive charge arising from amino groups of amino acids. Cells approaching charged materials will therefore experience varying electrostatic forces depending on the particular surface groups in contact with the charged substrate. They must overcome this electrostatic barrier in order to adhere. It has been proposed that ionic groups can influence cell adhesion by restructuring the aqueous solvation sheath at the material surface (Schakenraad, 1987; Curtis, 1986a), thereby lowering the electrostatic barrier to adhesion, and also influencing the ionic and organic adsorbents in the interphase between the cell and the surface.

Bergethon (1989) investigated the attachment of cells to polyHEMA modified by the addition of copolymers containing both positive (-NH_3) and negative (-COOH) ionizable groups. It was found that the hydrogel supported cell attachment with either of these modifications, but needed further addition of collagen to allow cellular proliferation. Positive and negative charges have been shown to affect the morphology of attached osteoblasts (Shelton, 1988). On positively charged surfaces the cells adopted a more flattened morphology with the ventral cell membrane indistinguishable using TEM. The charge density of the substratum was found to affect the distance between the negatively charged substrate and the cell ventral membrane. The charge density was also found to be important in the spreading of BHK fibroblasts on a charged surface, with Maroudas suggesting it was more important than the charge sign (1975b). Curtis et al (1986a) found that cellular adhesion to hydroxylated polystyrene was inhibited by very high charge densities. An optimal density was described for BHK cells as being at about 0.5nmol/cm^2.

Curtis et al (1983) demonstrated that the incorporation of hydroxyl groups into polystyrene after sulphuric acid treatment rendered the material adhesive for cells. In contrast, polyHEMA, containing hydroxyl groups, can be rendered adhesive by the incorporation of COOH groups using a sulphuric acid treatment (McAuslan, 1987). The importance of carboxyl groups has also been shown by experiments investigating short term cell attachment (Vogler, 1987). Initial rates of attachment were related to the presence of carboxyl groups whereas equilibrium rates of adherence were controlled by the formation of receptor-ligand complexes and interfacial energies. Recent work by Brandley (1987) found that short term adhesion was most strongly mediated by hydroxyl groups whereas long term growth was greatest in the presence of carboxyl moieties, suggesting different requirements for attaching and spreading cells.

7.3.3 Attachment of bone cells

The incorporation of materials into bony tissue without the imposition of a fibrous layer has been described as osseointegration, and is thought to be associated with the surface chemistry of the material. Materials which act in this way have been termed osteophilic and include titanium, titanium alloys such as Tivanium, bioactive glasses and calcium phosphate ceramics such as hydroxyapatite.

Synthetic ceramics such as hydroxyapatite (HA) resemble the mineral phase of bone and appear to be recognized as such by forming bone, resulting in the deposition of natural calcium hydroxyapatite on the implant surface. Hydroxyapatite is a brittle material and is therefore unsuitable as a bulk orthopædic material, but it has been applied as an osteophilic coating on more mechanically suitable materials such as titanium. Such coatings have been shown to improve the interface shear strength and promote earlier bone growth compared to uncoated titanium controls (de Groot, 1987). Seballe et al (1990) found a hydroxyapatite coating to diminish the negative influence of a noninterference fit on initial implantation. This was thought to be due to the early formation of a layer of bone on the HA surface leading to two ossification fronts rather than just one from the existing bone.

Bioglasses consist of Si, Ca, P and Na in various proportions. In an aqueous environment, *in vivo*, a silica-Ca/P rich gel layer is formed on the surface which can be mineralized. For this to occur, osteoblasts must proliferate at the material surface, secreting extracellular matrix which is then mineralized. Several interfacial bonding mechanisms have been suggested, including an electrostatic attraction between the negatively charged oxygen rich surface and positively charged amine groups present in the cell membrane, (Hench, 1971). Osteoblasts have been shown to colonize bioactive glass with the production

of abundant extracellular matrix and in some cases interdigitation of collagen with the bioglass surface (Matsuda, 1987).

The reasons for the osteophilic behaviour of titanium are unknown. When implanted in bone, it has been shown to be directly incorporated into the tissue without the interposition of fibrous tissue and with very little inflammatory reaction. Using TEM, bone has been observed up to 3nm (limit of detection) from the implant surface and cellular processes were separated from the surface by a 20 - 30nm proteoglycan layer. Other metals were separated by a layer 50 to 500nm thick, whereas the layer associated with PMMA was observed to be 2000nm (Branemark, 1983). As a proteoglycan layer up to 20 nm thick may be seen between individual collagen filaments or at cell - collagen interfaces, it has been argued that the titanium surface is unique amongst examined materials in displaying bonding on this level. Electrostatic forces between the bone and the surface and the physical characteristics of the titanium oxide layer are thought to be responsible.

Recent studies have suggested however, that the osseointegration of titanium is not an exclusive reaction to the implant material, but is the expression of a nonspecific and basic healing potential in bone. Linder (1989) found that given identical healing conditions, materials having different surface chemistries (titanium alloy, cobalt-chrome alloy and stainless steel) were all accepted by bone in the same way as pure titanium. It has also been emphasized by Albrektsson (1987) that it is important to obtain an interference fit with surrounding bone to prevent implant movement and avoid the interposition of a fibrous tissue layer between implant and bone.

7.3.4 Surface Topography

Surface roughness may be measured at the protein level (nm) or cellular level (μm). Roughness may be induced using chemical etching, ion beam sputtering, sand/grit blasting or mechanical means.

The influence of substrate topography on cell orientation was first described by Weiss (1941) who demonstrated the phenomenon of contact guidance. On a grooved substratum cultured fibroblasts will become orientated so that the cell long axis is parallel to the grooves. Typically, fibroblasts will move along the grooves rather than cross them. Where a percutaneous or dental device penetrates the epithelium, epithelial cells will often migrate in such a manner so as to isolate the device from connective tissue (marsupialization) leading to device failure. Surface grooves have been used in an attempt to direct the migration of these cells in such a way that their downgrowth is impeded on percutaneous devices (Chehroudi, 1988). The geometrical configuration of implant surfaces has also been proposed to influence whether a capsule or an orientated fibrous attachment is developed in relation to implants *in vivo* (Inoue, 1987). It was found that smooth surfaces bearing circumferential grooves favoured the development of capsule like structures; *in vivo* this could favour the development of a contiguous fibrous capsule which would not provide attachment to the host. This effect was not seen with porous surfaced materials implying that *in vivo*, better attachment would be seen with this type of surface.

Research into vascular materials has shown that thrombogenicity may be reduced by using textured grafts which lead to the early formation of a confluent luminal surface of endothelium (Taylor, 1983). Exudates recovered from implanted textured grafts show greater growth and attachment promoting activity (Korman, 1984) than nontextured when applied to cells *in vitro*. In

contrast, Lindblad (1987) found no consistent differences with various expanded PTFE grafts when examining cell attachment and spreading *in vitro*.

Different proportions of cells have been observed in association with rough and smooth PE and PSF particles *in vivo*, with more foreign body giant cells (fused macrophages) observed on rough particles (Behling, 1986). However, in their work on charged beads, Shelton et al (1988) did not note any effect of bead roughness on protein or cell adsorption *in vitro*. A study investigating the effect of varying surface texture on a wide range of orthopaedic materials found that roughened implants displayed direct bone apposition whereas smooth implants exhibited various degrees of fibrous tissue encapsulation (Thomas, 1985). The implant surface chemistry ranged from metal (titanium) to polymer (PMMA) and ceramic (aluminium oxide) and did not significantly affect the interface response.

7.4 Techniques used to modify the test surfaces

The surface characteristics of the test materials were altered with respect to wettability and roughness, using a plasma technique to achieve both conversions. The plasma processes affect only the top few molecular layers (1-10μm) and do not change properties of the bulk material such as the mechanical strength.

A plasma can be generated by passing an electric field through a gas, creating a partially ionized mixture of ions, electrons, free radicals and atoms; any of which may react with a material surface if present in the plasma reactor. This technique is also known as glow discharge polymerization.

If the energy of the energetic species is more than the bond energy of groups in the material surface, bonds will be broken by scissioning, reducing the length of polymer chains and creating active sites and unsaturated bonds on the surface. Groups such as amines or halogens may attach by covalent bonds to the unsaturated sites. The shorter chains may further react with each other producing stable crosslinks or branches, with other free radicals which will scission the chain further, or with other components of the plasma gas to form new chemical species in the surface. Any volatile species formed will be removed by the vacuum system. The shorter the chains produced, the lower their molecular weight and therefore the higher their mobility. They will have a greater tendency to migrate inwards towards the bulk of the polymer leading to a gradual change in the surface energy and chemistry. This ageing effect is increased with more reactive plasmas such as oxygen which not only produce a lot of low molecular weight species, but also functionalize the surface with groups such as -C=O, -OOH and -OH. The longer the plasma is in contact with the surface, the more the surface is physically rather than chemically changed. Amorphous polymer is removed faster than crystalline

polymer leading to the introduction of a surface topography. This process is a form of dry microetching. In summary, the principal changes brought about by exposure of a polymer to a plasma are in molecular weight and chemical composition. The properties of a plasma treated surface are governed by the monomer gas, substrate, sample placement, reaction chamber geometry, and reaction conditions such as the power, pressure, flowrate, and treatment time.

In the biomedical field plasma treatments have been used to modify materials which have the desired bulk properties but whose surface does not exhibit the appropriate biological interactions, and to design surfaces to meet specific needs. Plasma treatments have been used to improve the blood compatibility of vascular grafts, for example, by the attachment of amines which are then used as 'hooks' for the localization of heparin; though there is debate as to whether surface bound heparin retains its anticoagulant properties after such treatment. In an effort to permit better attachment and growth of endothelial cells, Tran & Walt (1989) used an ammonia plasma to reduce the hydrophobicity of PTFE grafts and enable covalent attachment of collagen. An ammonia plasma has also been used by Sipehia (1990) to enhance attachment and growth of endothelial cells onto polystyrene and PTFE. Various fluoroethane plasma polymers have been deposited on silicone rubber and expanded PTFE grafts, producing amorphous surfaces which were demonstrated to reduce platelet attachment *in vivo*, (Yeh, 1988). They have also been used to change the hydrophilicity of contact lenses (Ho, 1988), stop the leaching of low molecular weight toxins from material surfaces, control the release rate of drugs and to provide protective coatings on medical devices (Yasuda & Gazicki, 1982). It is generally assumed that plasma polymers have good adhesion to inorganic substrates, although this is not the case in the preparation of hydrophilic polymer surfaces due to penetration of the film by

water molecules. Recent work by Marchant et al (1990), has described the deposition of a hydrophilic plasma polymerized film composite onto a range of inorganic surfaces including glass and aluminium foil. The surface was achieved by copolymerization of a previously deposited hexane film with N-vinyl-2-pyrrolidone, thus providing good adhesion between the inorganic support and the outer hydrophilic surface.

The plasmas used in the present study were generated in oxygen (O_2), argon (Ar), ammonia (NH_3), hexafluoropropane (HFP) and hexafluorobenzene (HFB); these were chosen so as to impart a range of wettabilities to the test materials. Although the gross effect desired was a change in the surface hydrophilicity / hydrophobicity, each plasma reacts with the material in a distinctive way, introducing different functional species to the test surface.

Argon will tend to crosslink the surface leading to an increase in molecular weight of the test material and also an increase in wettability. With HFP/HFB, a thin film of the plasma polymer of HFP/HFB will be formed on the surface leading to a decrease in the surface wettability. Oxygen will scission the chains leading to a decrease in molecular weight. The incorporation of oxy-functional groups will lead to an increase in wettability. A decrease in molecular weight and increase in wettability will occur with the ammonia plasma. The surface produced by the oxygen plasma will be the least stable as the most low molecular weight species will be produced. Etching of the APC2 surface was produced by increasing the time of treatment with the oxygen plasma resulting in preferential etching of the resin matrix, PEEK, leaving the carbon fibres exposed. The wettability of the surface was also increased.

7.5 Techniques used to characterize the modified surfaces

The surface energy of the plasma treated materials was assessed using the contact angle technique. The contact angle is the angle a drop of liquid makes with a surface; it varies with the nature of the liquid and that of the surface, and is described by Young's equation,

$$g_{LV}\cos\theta + g_{SL} = g_{SV}$$

where θ is the contact angle, g_{LV} is the surface energy of the liquid in equilibrium with its vapour, g_{SL} is the solid-liquid interfacial energy and g_{SV} is the surface energy of the solid in equilibrium with the vapour of the liquid.

It can be seen that the angle θ is indirectly related to the surface energy of the solid. The higher the surface energy of the material, the lower the contact angle. Thermodynamically, the equation represents the energy needed to create a unit area of the interface where none existed before.

The surface chemistry of the materials was assessed using X-ray photoelectron spectroscopy or XPS. The samples are irradiated by a beam of low energy X-rays, ejecting photoelectrons from the sample surface which are analysed according to their binding or kinetic energy. The energy peaks obtained are characteristic of the elements present. Small shifts in these energy peaks arise from changes in chemical state and provide structural information. The sampling depth is from 1-5nm depending on the particular photoelectron studied and the spatial resolution is in the range of a few mm.

7.6 Analysis of the effect of surface modifications

The effect of the modified surfaces on the cellular response to the materials was assessed both *in vitro* and *in vivo*. Fibroblast cells were seeded onto the surfaces and their attachment, spreading and morphology assessed by fixing the cells at different time points after initial seeding. Experiments were performed under physiological (serum supplemented) and non-physiological (serum free) conditions in an effort to enhance the effect of the modified surface; previous reports have shown that greater differences are seen on cells on modified surfaces in the absence of serum than in the presence of serum (Schakenraad, 1986). SEM micrographs were taken of the fixed cells on the material surface; these were analysed using a computerized image analysis system to enable quantification of the results and reduce observer bias.

As a preliminary study into the metabolism of cells on the treated surfaces, the MTT assay was performed on the surface of O_2 plasma etched APC2 and compared to that on controls. MTT is a tetrazolium salt which is reduced to formazan by mitochondrial enzymes as discussed in Chapter III. Its use enabled a comparison of cell respiratory activity to be made between the controls and the etched samples.

Treated material discs were implanted intramuscularly in rats and retrieved after 1, 2, 7 and 14 days. To enable staining of specific cell types using immuno-histochemical stains, the tissue had to be frozen to preserve the enzyme and antigenic sites. Unfortunately this entailed removal of the specimens as they could not be sectioned on the cryostat. The immunohistochemical stains used relied on the indirect labelling of surface antigens on rat leukocytes using a primary monoclonal antibody directed against the desired antigen and a secondary biotinylated polyclonal antibody directed against the primary antibody. Biotin is a vitamin which has been

shown to bind with great affinity to avidin, an egg white glycoprotein, in the ratio 4:1. As a great number of biotin molecules are conjugated to the second antibody, more than one avidin molecule can bind. The avidin used was complexed to biotinylated enzyme (horseradish peroxidase) and so for every one biotinylated antibody, avidin bound three biotinylated enzyme molecules; in this way amplifying the original labelling. The substrate, horseradish peroxide, was linked to the chromagen diaminobenzidine which becomes brown on oxidation. Immunohistochemical techniques were used to identify macrophages, T-cells, B-cells and activated T-cells.

A Joyce Loebl Mini Magiscan image analysis system was used to analyse the SEM micrographs and slides. A video image of each photograph or slide was captured via a Hitachi KP140 solid state camera, thus converting the analogue information into digital information. The system has a 6-bit processor and so recognizes 64 levels of contrast or grey levels in each image. The images were then called sequentially into task routines written using a Genias25 software package. Each task routine calibrated the system from previous measurements using the magnification bar on the SEM micrographs and a stage graticule for the slides.

The SEM micrographs were analysed in terms of object number, circularity (4π x area / perimeter^2), perimeter, length and area. From observations on tissue culture plastic, circularity might be expected to decrease with time as cells started to spread and adopt a spindle shaped morphology, and then increase as they flattened further; over a period of 24 hours, cell division would occur (if conditions were favourable) and these cells would be rounded in appearance. The object area would only increase as the cells flattened and spread; again as cells rounded up for cell division the area might decrease. Spindle shaped, elongated cells would have greater object lengths than rounded

cells; surfaces where these cells predominated would therefore have a higher mean object length. Object perimeter is an alternative measurement reflecting the size or area of the cell.

For analysis of the sections, the number of objects stained was counted using a specific task routine.

8.1 Materials used

Plaques of polyetheretherketone (PEEK) and APC2 were used as before. Areas of the plaque were machined down from an initial thickness of 3mm to 1mm. Discs of diameter 1 cm (early experiments) or 5 mm were then punched from these plaques. The machined surface was marked to enable easy identification throughout the treatment and experiments. Prior to treatment the samples were cleaned in 1% Lipsol detergent by sonication and then rinsed extensively in sterile, double distilled, deionized water before drying. They were then stored until required in a desiccator under vacuum.

8.2 Surface Modification

Plasma treatments were performed using an RF parallel plate PMI Plasma Reactor. The samples were secured to a glass slide (as moulded face up) using double sided sticky tape. This slide was then placed on the down turned lid of a plastic petri dish in the middle of the chamber.

The plasmas used were oxygen (O_2), argon (Ar), ammonia (NH_3), hexafluoropropane (HFP) and hexafluorobenzene (HFB). Due to a change in the COSHH regulations regarding the safety of HFP, it was replaced with HFB. Generally, both HFP and HFB would be expected to give the same surface hydrophobicity with fluorine incorporated. The conditions used to generate each plasma were determined empirically by previous workers in the laboratory and were as shown in the table below. The system was flushed out between reactions to remove any residual active species from the chamber.

Table 8.2a: Conditions used in plasma treatments

	Plasma					
Conditions	Ar	NH_3	HFP	HFB	O_2	O_2 etch
Time/minutes	2	10	0.3	0.3	2	60
Power/watts	100	100	100	100	100	100
Pressure/torr	0.25	0.05	0.25	0.25	0.25	0.25
Flow rate/sccm*	100	50	40	-	100	100

* sccm is standard cubic centimetres

8.3 Surface characterization

8.3.1 Surface wettability

After treatment, the wettability of the material surface was assessed by measuring the contact angle using the sessile drop technique. Samples were positioned on the stage of a goniometer and a drop of double distilled water placed carefully on the surface using a Hamilton syringe. The contact angle was obtained from measuring the angle created by the tangent at the edge of the drop of water. A mean of five measurements was made on each surface.

8.3.2 Surface chemistry

The surface chemistry of the modified materials was characterized using a VG SCI ESCALAB with a magnesium source. As it was not possible to examine the materials immediately after treatment they were stored under vacuum as soon as possible and until analysis could be done.

8.3.3 Surface roughness

The roughness of the surface was assessed using a Tencor Alpha Step 200 Surface Profiler. The average roughness was recorded over a scan area of 400μm and using a scan speed of 8 seconds. Three scans were made for each material.

8.4 Cell adhesion and spreading *in vitro*

The same cell lines were used as in the biocompatibility studies; an established fibroblast like line, the M^cCoys and a primary fibroblast line established from human gingival fibroblasts, HGFs. Each cell line was maintained in the manner described previously (see Chapter IV).

The 1 cm diameter materials were placed in 12 well plates (Linbro) and 1 x 10^5 cells seeded on top in 2 ml of medium. The 5 mm diameter materials were placed in the bottom of a microtitre well (Falcon) and cells seeded on top at 2.0 x 10^4 cells/well in 150µl of the required medium. Control wells with cells and no material were always seeded so the course of cell spreading could be followed during the experiment using phase contrast light microscopy. To examine the effects of serum upon cell spreading, the cells were washed in serum free medium before seeding, thereby removing any associated protein. With the first experiments performed in serum free medium, only one washing step was used; this was later increased to 3 washes. Both short (minutes) and long (hours) time periods were used enabling a range of cell morphologies to be observed. Time periods used included 0.5, 1, 3, 4, 6, 24 and 48 hours.

After each time period the supernatant from the relevant wells was removed and the material surfaces were washed with excess 0.1M phosphate buffer to remove unattached cells. The samples were then processed for SEM examination as described previously (Chapter IV). Specimens were examined using a JEOL JSM 35-C scanning electron microscope and a beam energy of 15kV.

For each sample, the entire surface was scanned before representative areas were chosen and photographed at low power (x300). Usually two photographs were taken, but if the cell coverage on the surface was very low, more areas were selected. Negatives were printed using the same enlargement and

contrast, enabling pictures to be processed using image analysis without constant recalibration of the system. Each micrograph was analysed in terms of object number, circularity, area, length and perimeter using a Joyce Loebl Mini Magiscan image analysis system in conjunction with the Genias25 software package.

MTT assays were performed on the surface of the O_2 plasma etched APC2 samples and control APC2 samples using the method detailed in Chapter IV. The surfaces were seeded with M^{c}Coy fibroblasts for 96 hours prior to assay.

8.5 The *in vivo* response to the modified materials

Test and control material discs were implanted into the dorsolumbar musculature of Liverpool black and white rats for periods of 1, 2, 7 and 14 days, according to the procedure described in Chapter IV. The O_2 plasma etched materials were implanted for a maximum of 7 days. Care was taken to ensure that the samples were placed treated side down, actually on the muscle bed. Immediately after sacrifice, muscle was excised and the samples carefully removed and processed for SEM (see Chapter IV). The tissue was frozen in an isopentane-cardice mixture and stored at -70°C until required for sectioning. The materials were fixed in formol buffered saline (10%) for 24 hours and then processed for SEM. The frozen tissue blocks were sectioned at 7μm as described previously (Chapter IV).

The sections were stained using a haematoxylin and eosin stain to locate the implant site. When this was found specific stains were used to identify macrophages and lymphocytes on the 7 day (O_2 plasma etched APC2 and 14 day (plasma treated PEEK) samples. The macrophages and lymphocytes were identified using murine monoclonal antibodies (Serotec) raised against cell specific antigens as shown in Table 8.5a.

Table 8.5a

Monoclonal antibody	Specificity	Dilution
ED2	macrophage	1:100
MRC OX-8	T-suppressor/cytotoxic cell	1:40
MRC OX-39	Il-2 receptor (activated T-cell)	1:100
MRC OX-19	T-cells and thymocytes	neat
MRC OX-33	B-cells	neat

The sections were fixed in acetone for 10 minutes, air dried and incubated for 20 minutes in 0.6% hydrogen peroxide/methanol to destroy any endogenous hydrogen peroxidase activity. They were then washed in distilled water followed by PBS (Gibco) for 10 minutes, and dried. Non specific binding sites were blocked by incubating for 25 minutes in rabbit serum (Serotec) diluted 1:5 with PBS. Sections were stained with the desired monoclonal antibody for 90 minutes, rinsed in PBS for 5 minutes and dried. Rabbit anti-mouse polyclonal antibody (Dako) was diluted 1:100 in PBS and approximately 200µl of rat serum added to block any cross reactive antibodies. This was then applied to slides for 40 minutes, followed by a 30 minute incubation in peroxidase conjugated avidin-biotin complex (Dako). The slides were washed in PBS for 5 minutes after each step. Sites of peroxidase activity were visualized by incubating for 15 minutes in diaminobenzidine (DAB) at a dilution of 0.67 mg/ml DAB in PBS containing 15µl/ml 3% H_2O_2. The slides were rinsed in distilled water for 2 minutes before dehydrating through alcohol and mounting. All steps were carried out at room temperature.

Object numbers on each slide were determined using the Joyce Loebl Mini Magiscan image analysis system in conjunction with Genias25 software. 20 images from each slide were captured at x200 magnification giving a total analysed area of 2.06×10^6 μm^2.

9.1 Surface wettability

Contact angle measurements were made on samples of PEEK and APC2 before and after treatment with various plasmas. Table 9.1a gives results from measurements made on samples subsequently used to obtain results given in Table 9.4a and Figure 9.4p.

The variability associated with contact angle measurements is shown by measurements made on different samples of untreated PEEK at various times (Table 9.1b).

9.2 Surface chemistry

XPS was used to characterize the surface chemistry of treated and control PEEK materials. Table 9.2a gives results obtained from samples examined 3 days after treatment - the shortest lag time. The peak binding energies obtained were corrected for charging using a binding energy reference of 285.0 eV for the C1s peak (Briggs & Seah, 1983), representing carbon bound either to itself or to hydrogen. Charging occurs because of the insulating nature of the polymers. The most striking differences were seen between the HFB treated surface and the control, with a large fluorine peak seen giving a F/C ratio of 3.1. The O/C ratio was increased after all surface treatments. A small nitrogen peak was seen after ammonia treatment.

These same samples were kept under vacuum and examined again after 4 months (Table 9.2b). On all the samples a higher O/C ratio was seen than previously. The counts recorded were much higher due to recalibration of the system between measurements. The F/C ratio was decreased to 1.1 from 3.1.

This set of treatments was repeated and samples analyzed in the same manner, however the lag time was 1 month (Table 9.2c). Apart from a fluorine peak found with the HFB sample, none of the other effects were repeated. The fluorine peak found was much smaller than that seen previously; the F/C ratio was 0.75.

Ammonia treated samples were examined on two other occasions and the results are given in Table 9.2d. Nitrogen was incorporated into the surface with a N/C ratio of 0.72 for sample 1 and 0.56 for sample 2.

On several occasions silicon contamination from the mould release agent was found on the surface of the materials.

9.3 Surface roughness

Results from examination of the surface roughness are given in Table 9.3a. The smooth 'as moulded' surface was the one examined in each case. It can be seen from the figures that the PEEK surface was the smoothest and the APC2 etched, the roughest. The difference between the mean Ra (average roughness) of the etched and non-etched APC2 surfaces is small; although the morphology is completely different, as is clearly shown by SEM micrographs in section 9.5. This small difference is due to the irregular roughness of the non-etched APC2, which has many surface pores and cracks.

	Contact Angle	
Treatment	PEEK	APC2
Control	65 ± 5	72 ± 2
NH_3	42 ± 2	
O_2	17 ± 2	
Ar	35 ± 2	
HFB	>90	
O_2 etch		20 ± 22

Table 9.1a: Contact angle measurements made on materials after plasma treatments. Each value is a mean of at least 5 measurements.

Experiment	Contact Angle
1	79 ± 2
2	72 ± 7
3	65 ± 5

Table 9.1b: Contact angles measured on untreated PEEK surfaces on different occasions.

	C peak		O peak		*N / #F peak	
Treatment	BE/eV	Cts/s	BE/eV	Cts/s	BE/eV	Cts/s
Control	285.0	896	532.2	528		
Argon	285.0	632	532.6	552		
Oxygen	285.0	752	533.0	664		
Ammonia	285.0	840	532.6	680	*398.6	336
HFB	285.0	492	532.6	452	#688.2	1504

Table 9.2a: XPS studies on PEEK surfaces 3 days after plasma treatment. BE is binding energy and Cts is counts per second.

	C peak		O peak		F peak	
Treatment	BE/eV	Cts/s	BE/eV	Cts/s	BE/eV	Cts/s
Control	285.0	1856	533.4	1408		
Argon	285.0	2032	533.4	2160		
Oxygen	285.0	1472	533.4	1488		
Ammonia	285.0	1664	531.8	2096		
HFB	285.0	1824	533.4	2080	688.6	2000

Table 9.2b: XPS studies on PEEK surfaces 4 months after plasma treatment. Same samples as for Table 9.2a. BE is binding energy and Cts is counts per second.

	O / C ratio	
	Period between treatment and analysis	
Treatment	3 days	4 months
Control	0.6	0.8
Argon	0.9	1.1
Oxygen	0.9	1.0
Ammonia	0.8	1.3
HFB	0.9	1.1

Table 9.2c: Ratio of Cts for O1s / C1s. Samples as in Tables 9.2a & b.

	C peak		O peak		N peak	
Sample	BE/eV	Cts/s	BE/eV	Cts/s	BE/eV	Cts/s
1	285.0	784	534	1072	402	568
2	285.0	800	534	1280	402	448

Table 9.2b: XPS studies on PEEK surfaces, 1 month (sample 1) and 2 months (sample 2) after treatment. BE is binding energy and Cts is counts per second.

Mean Ra / kÅ		
PEEK	APC2	etched APC2
2 ± 0.4	6 ± 1	8 ± 3

Table 9.3a: Surface roughness measurements performed using a stylus load of 9mg and a scan area of 400μm over a period of 8 seconds.

9.4 The effect of surface chemistry modifications *in vitro*

Figures 9.4a - j show results obtained from plasma treated PEEK materials (1 cm diameter samples) seeded with M^{c}Coy fibroblast-like cells in the presence and absence of serum and observed at 0.5, 1, and 4 hours after seeding. One sample was examined at each time point. The lag time between treatment of the surfaces and cell seeding was 16 days.

The most striking differences were seen with cell number on the HFP surfaces in the presence and absence of serum. In the presence of serum, the cell number was greatly reduced in comparison to the other surfaces examined, (Ar, O_2 and the control), whereas in the absence of serum the reverse was seen (Figures 9.4a & b). The argon treated surface was seen to support the most cell attachment in the presence of serum. The cell number tended to decrease slightly with time for all of the surfaces. Typical micrographs of the surfaces 0.5 hours after seeding are shown in Figures 9.4k, i-vi.

No significant variation was seen with any of the other object parameters measured; although the numbers of cells seen on the surfaces differed, their morphology did not differ greatly. In the presence of serum, the cells gradually spread from the initial rounded shape adopting a more flattened morphology after 4 hours (Figure 9.4l, i-vi). A predominance of elongated spindle shaped cells was seen on the HFP treated surface. In the absence of serum fewer spindle shaped cells were seen. Under all conditions, 'spiky' cells were seen; this appearance was due to the numerous microvilli expressed on the cell surface. The spindle shaped cells were not as spiky as the round cells.

APC2 surfaces (1 cm diameter samples) treated at the same time in the same manner as the PEEK surfaces were tested simultaneously. Typical micrographs of the surfaces are shown in Figures 9.4m, i-vi. Figure 9.4m, iv shows the morphology of the faint spread cells seen on the HFP treated surface in the

absence of serum. The response of the cells to the treated surfaces was different to that on PEEK. Generally, fewer cells were observed on the surfaces and no striking differences were seen. Fewer cells were observed adhering in the presence of rather than the absence of serum. The variation in cell number observed in serum supplemented and serum free medium is shown in Figures 9.4n & o. No pattern in cell number at different time periods could be discerned. The greater variation seen in these results may be due to the influence of surface morphology. Surface cracks and pores were seen on all the samples and made it difficult for accurate analysis of the micrographs as the software could not distinguish on some occasions between a cell and a pore.

Further plasma treated PEEK samples (5 mm diameter samples) were examined with a shorter lag time of 2 days between treatment and testing. The range of treatments was expanded to include ammonia gas, and 6 time periods were examined - 0.5, 1, 3, 6, 24 and 48 hours. Table 9.4a shows results of image analysis performed on photographs of M^cCoy cells seeded onto test samples for 3 hours in the presence of serum. Again, the most striking difference was with the number of cells adhering to the surfaces. No cells were seen at any time on the HFB surface and fewer cells were seen on the NH_3 and control surfaces than the O_2 and Ar surfaces. The cell coverage on the NH_3 treated surface was similar to that on the control surface. At the initial observation point, 30 minutes after seeding, cells were not seen on any surface. At 1 hour, the argon surface alone supported cell attachment; the cells seen were similar in morphology to those shown in Figures 9.4k, i-vi. The different experimental arrangement used in these experiments, 5mm diameter samples in a microtitre well as opposed to 1 cm diameter disc in a 12 well dish, may explain the decreased adherence of cells at the early time periods.

The course of cell spreading was similar to that described above where the initial cell shape was rounded, becoming more spindle shaped with time. Over the longer period of observation the cells flattened considerably, with the nucleus difficult to distinguish on most flattened cells. Microvilli were rarely seen on the flattened cells but numerous filopodia could be seen attaching the cells to the substratum. After 3 hours of incubation, the cells seeded on the control, O_2 and Ar treated surfaces became too flattened to be distinguished against the background by the image analysis system (Figures 9.4p, i-iii).

A similar experiment was performed on plasma treated PEEK materials (5 mm diameter samples) in the absence of serum. The lag period between surface treatment and observation of cells was again 2 days. The cells were rounded up with no spread cells seen and tended to form clumps making accurate quantitative analysis using the image analysis system difficult. Cells were not observed adhering on any surface until 24 hours after initial seeding; qualitatively, little difference in cell number or cell morphology could be seen at this time. However, at 48 hours, more cells were definitely seen to adhere to the HFB surface with the NH_3 surface next most popular (Figures 9.4p iv-vi). No difference in cell morphology could be seen. Again, the difference in the number of cells adhering to the test surfaces may be due to the different sample size used or to more extensive washing of the cells in serum free medium before seeding.

9.4a

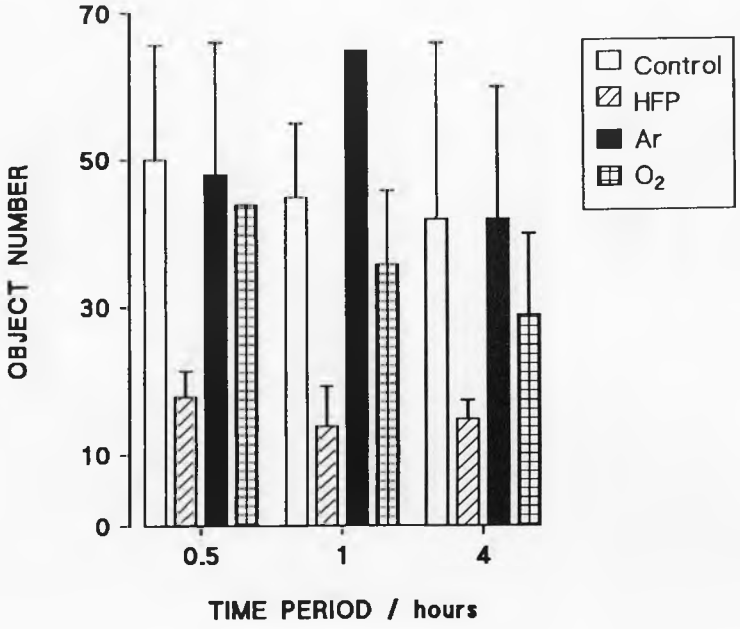

9.4b

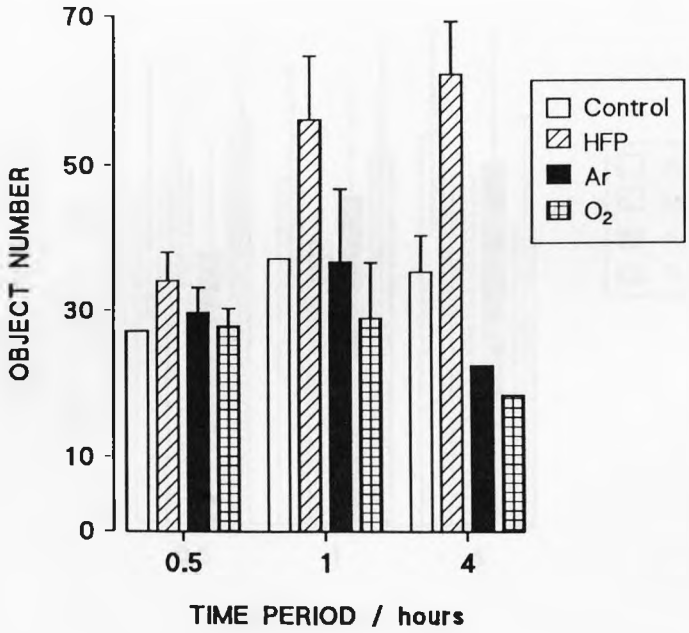

Figures 9.4 a & b : ***Object number*** measured on plasma treated PEEK surfaces seeded with M^{c}Coy fibroblast-like cells in the presence (a) and absence (b) of serum.

9.4c

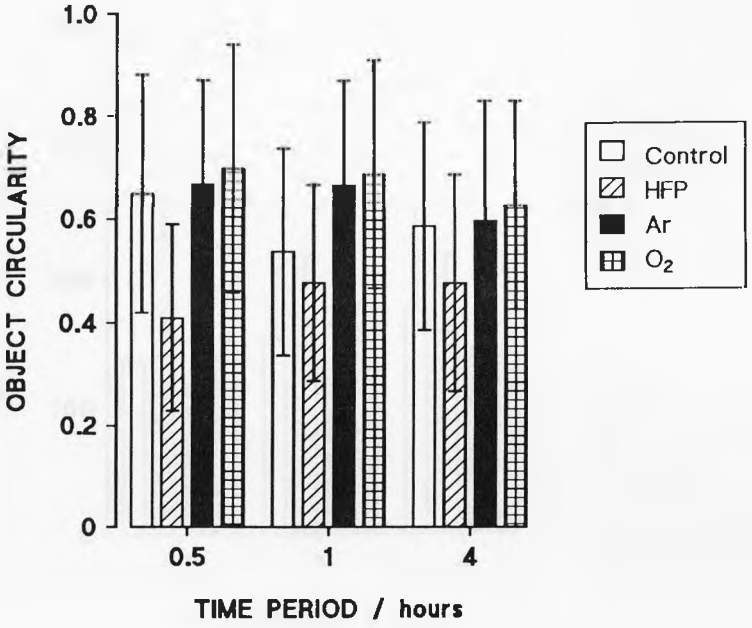

9.4d

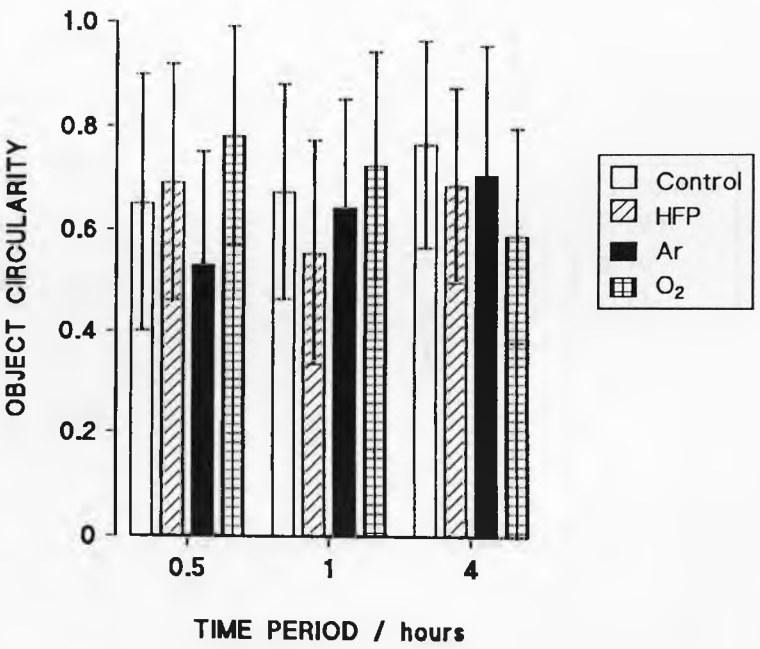

Figures 9.4 c & d : Object circularity measured on plasma treated PEEK surfaces seeded with M^{c}Coy fibroblast-like cells in the presence (c) and the absence (d) of serum.

9.4e

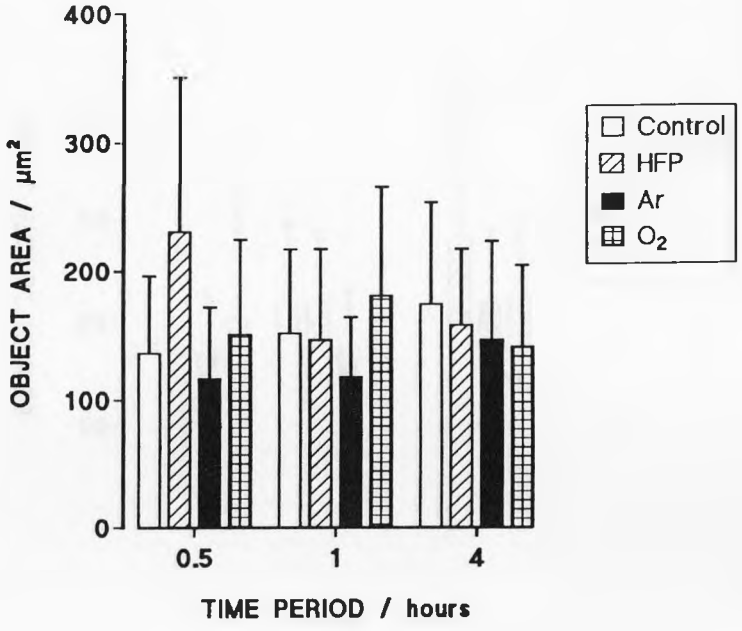

9.4f

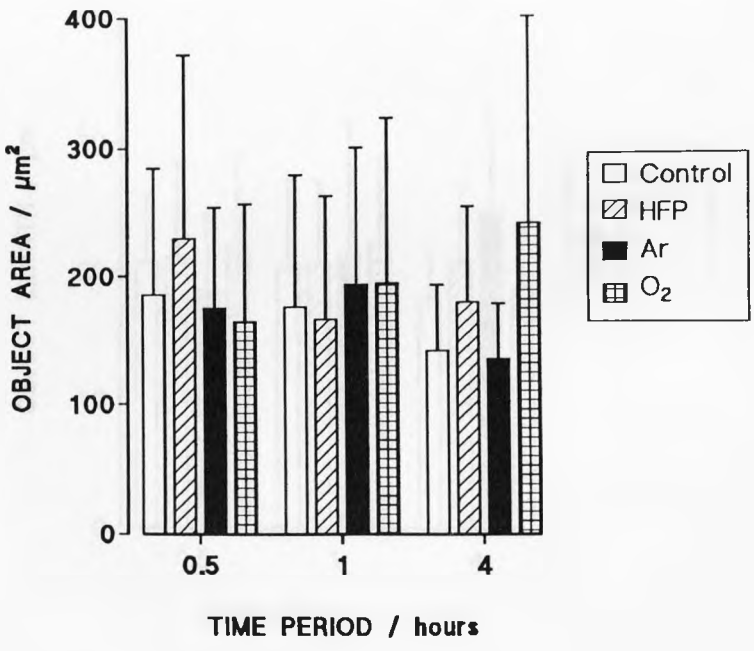

Figures 9.4 e & f : Object area measured on plasma treated PEEK surfaces seeded with M^{c}Coy fibroblast-like cells in the presence (e) and absence (f) of serum.

9.4g

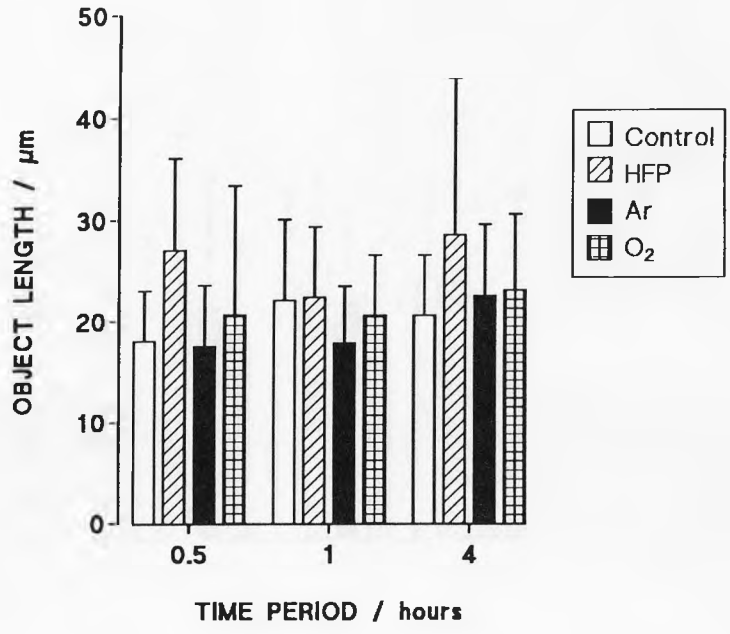

9.4h

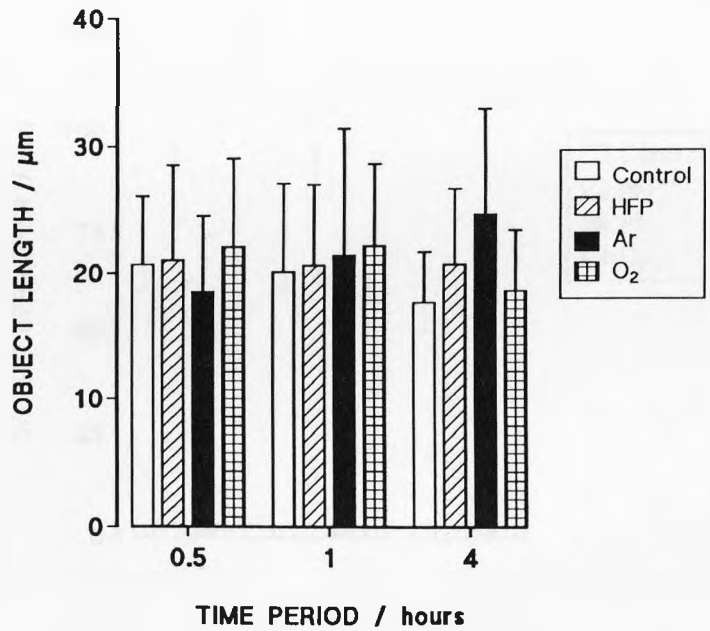

Figures 9.4 g & h : Object length measured on plasma treated PEEK surfaces seeded with M^{c}Coy fibroblast-like cells in the presence (g) and absence (h) of serum.

9.4i

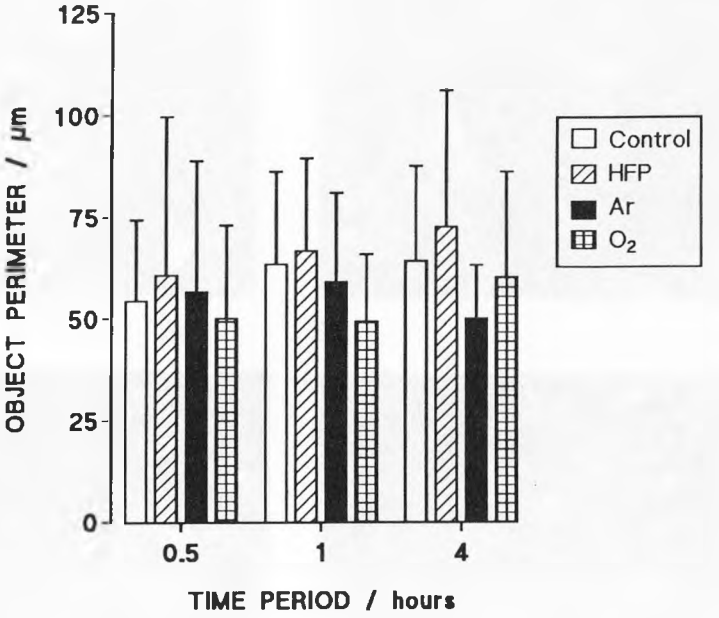

9.4j

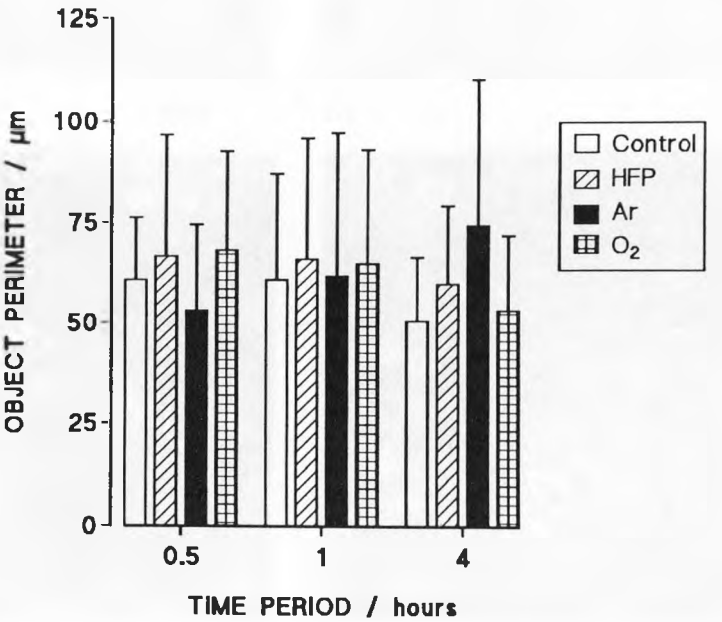

Figures 9.4 i & j : Object perimeter measured on plasma treated PEEK surfaces seeded with M^{C}Coy fibroblast-like cells in the presence (i) and absence (j) of serum.

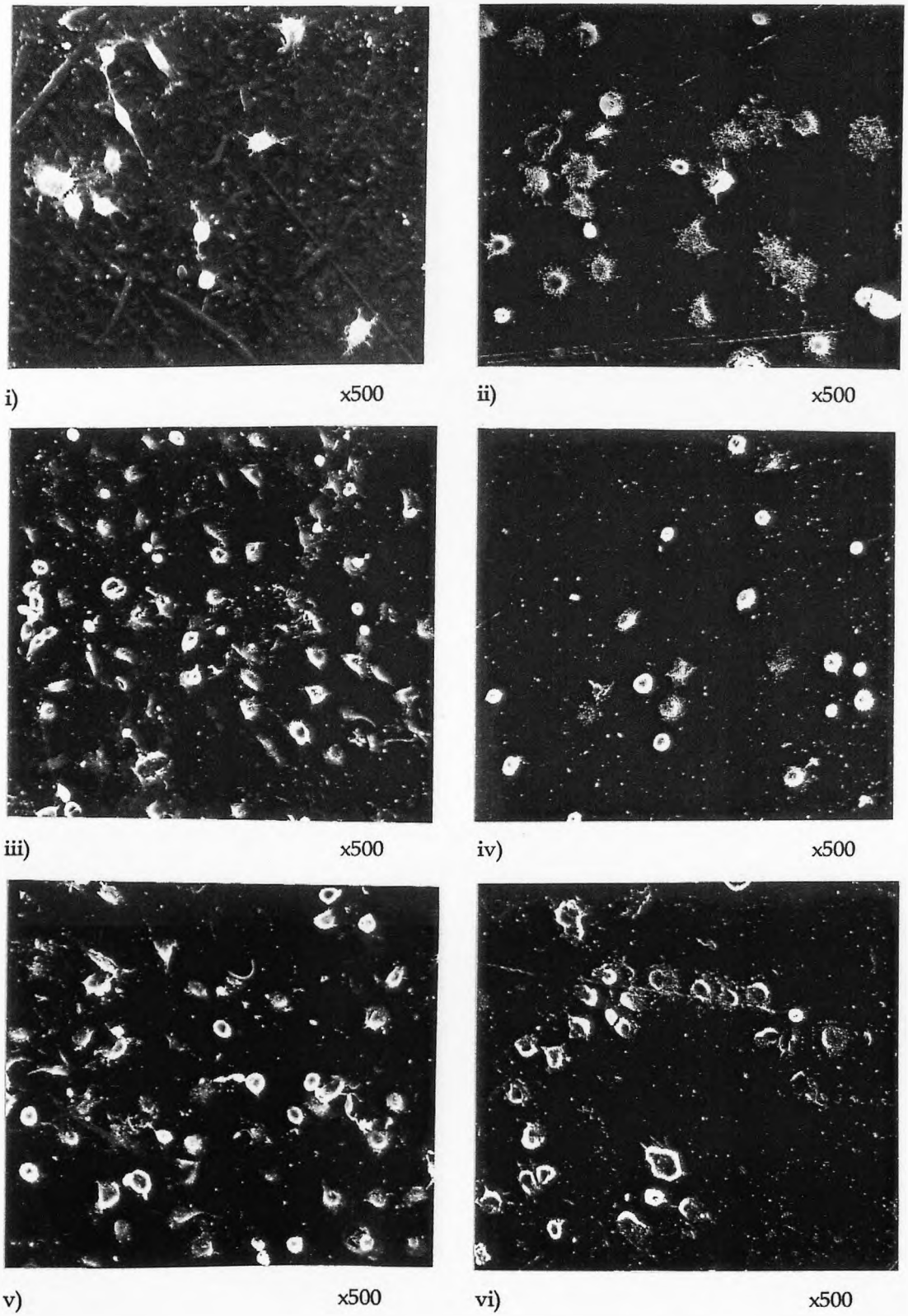

Figure 9.4k: Surface wettability. SEM micrographs of M^{c}Coy fibroblast-like cells seeded on HFP (i & ii) and Ar (iii & iv) plasma treated PEEK surfaces; and untreated PEEK (v & vi). Experiments were conducted in the presence (i, iii & v) and absence (ii, iv & vi) of serum. The incubation time was 30 minutes.

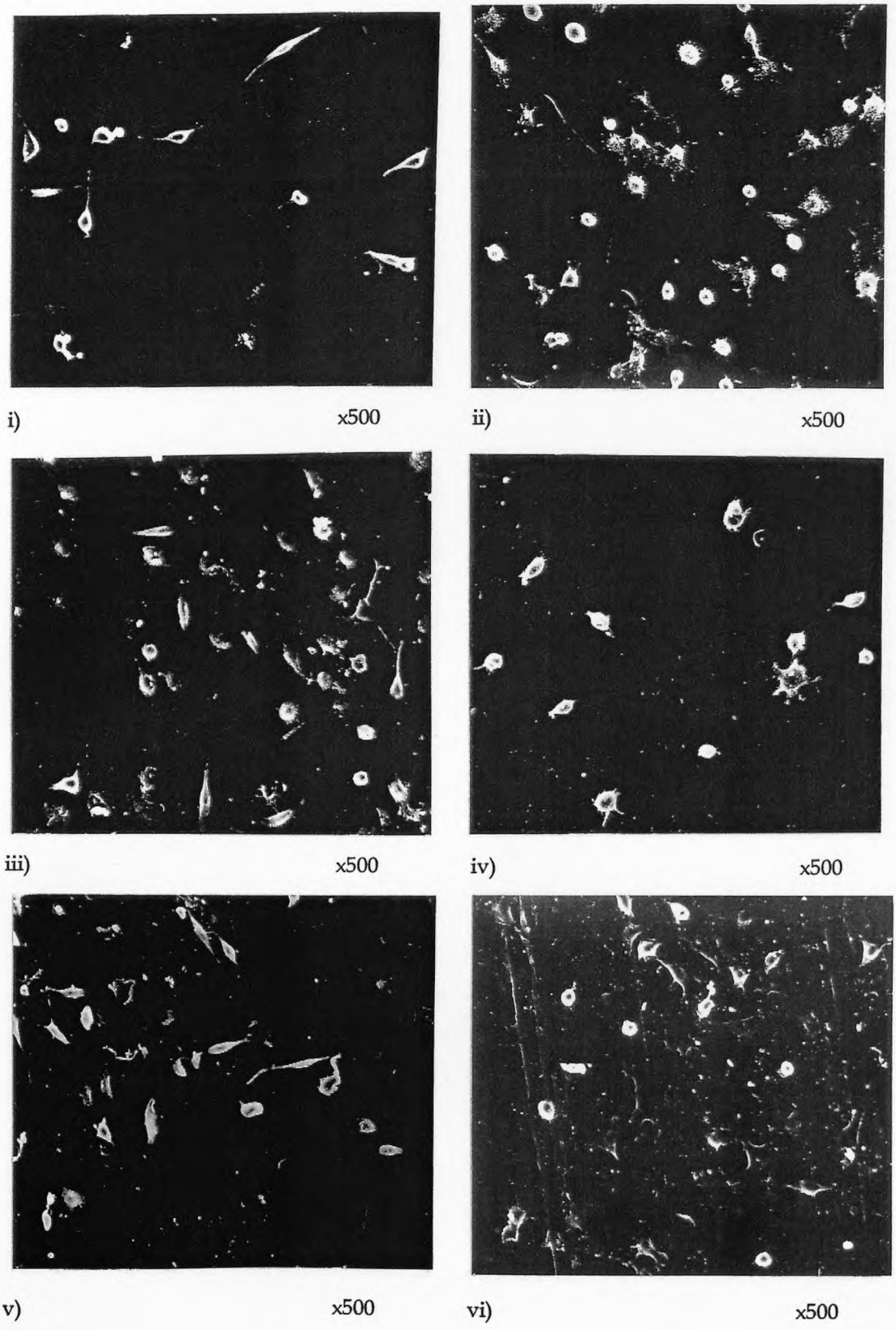

Figure 9.41: Surface wettability. SEM micrographs of M^cCoy fibroblast-like cells seeded on HFP (i & ii), Ar (iii & iv) and O_2 (v & vi) plasma treated PEEK surfaces. Experiments were conducted in the presence (i, iii & v) and absence (ii, iv & vi) of serum. The incubation time was 4 hours.

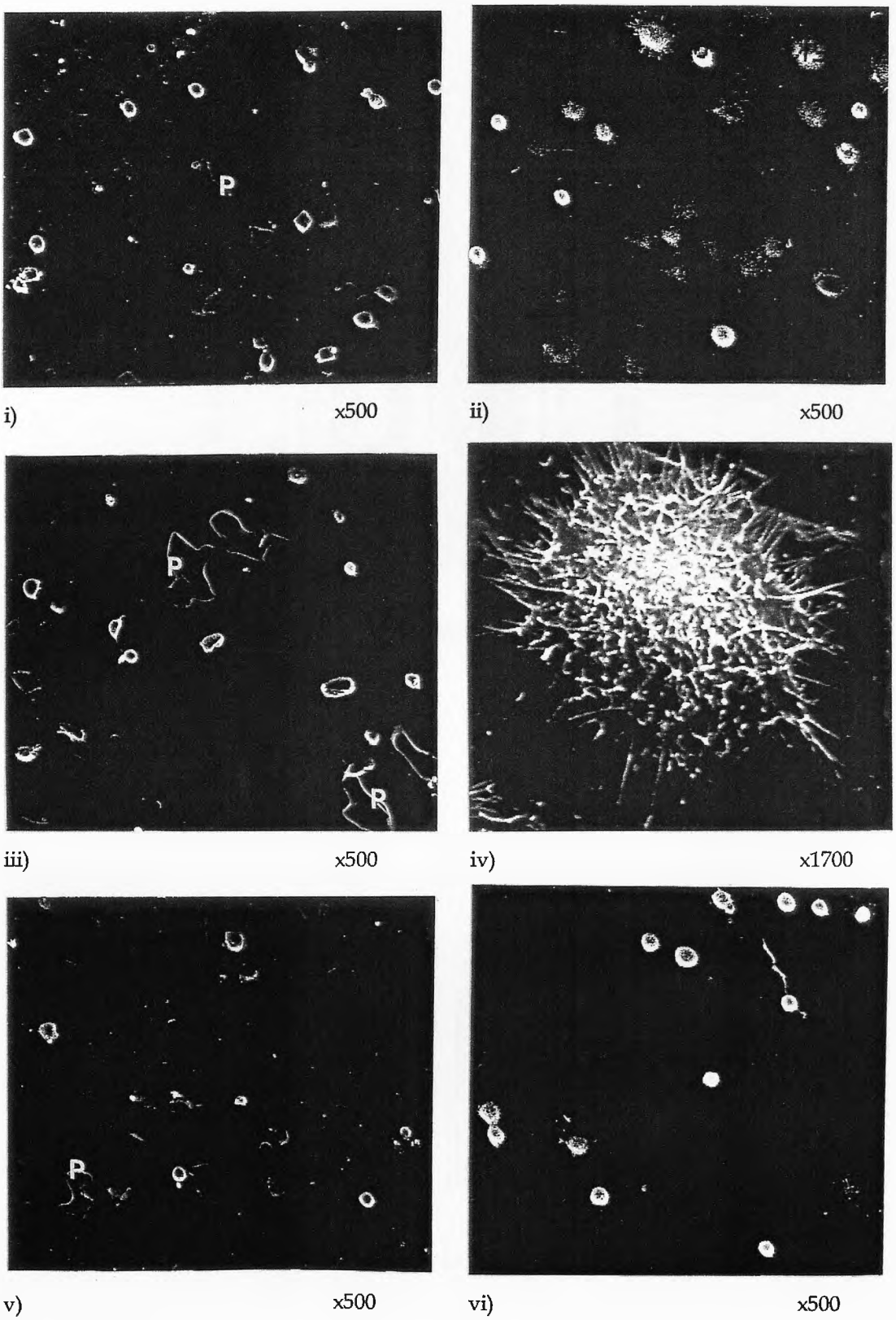

Figure 9.4m: Surface wettability. SEM micrographs of M^{c}Coy fibroblast-like cells seeded on HFP (i, ii & iv) and Ar (v & vi) plasma treated APC2 surfaces; and the control surface (iii). Experiments were conducted in the presence (i, iii & v) and absence (ii, iv & vi) of serum. The incubation time was 30 minutes. Surface pores (P).

9.4n

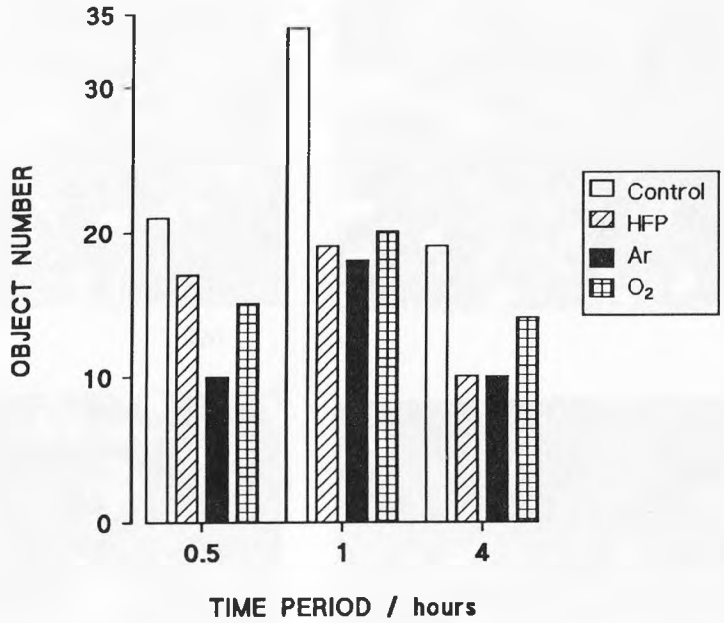

9.4o

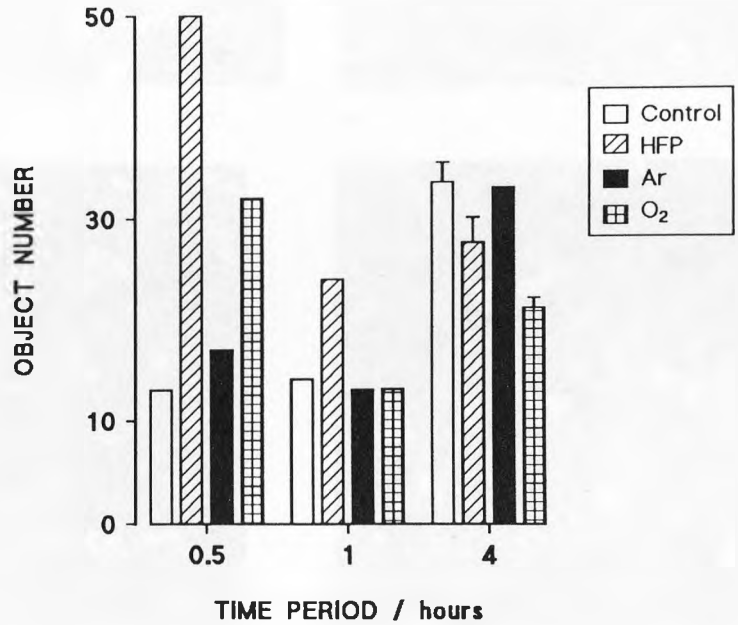

Figures 9.4 n & o : Object number measured on plasma treated APC2 surfaces seeded with M^{c}Coy fibroblast-like cells in the presence (n) and absence (o) of serum.

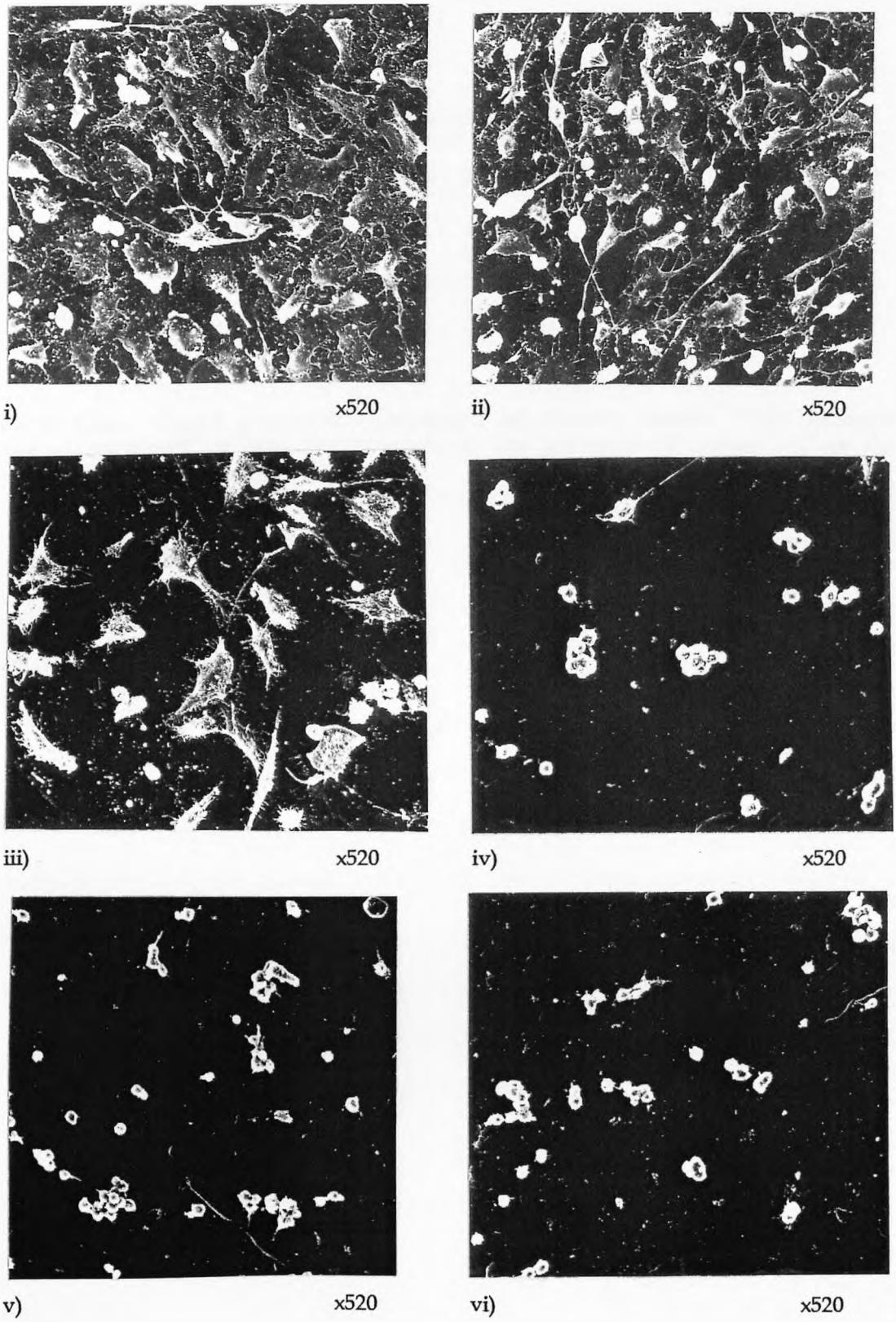

Figure 9.4p: Surface wettability. SEM micrographs of M^{c}Coy fibroblast-like cells seeded on O_2 (i), Ar (ii & iv), NH_3 (iii & v) and HFB (vi) plasma treated PEEK surfaces. Experiments were conducted in the presence (i, ii & iii) and absence (iv, v & vi) of serum. The incubation time was 48 hours.

	Plasma treatment				
Object parameter	C	Ar	O_2	NH_3	HFB
Number	11	72	48	4	0
Circularity	0.5	0.5	0.6	0.4	0
Area / μm^2	178	294	398	322	0
Length / μm	22	27	30	26	0
Perimeter / μm	63	87	96	97	0

Table 9.4a: Object parameters measured on plasma treated PEEK samples seeded with M^{c}Coy cells for 3 hours in the presence of serum. C is the control, untreated surface.

9.5 The effect of changes in surface roughness *in vitro*

The polymer rich surface of APC2 samples (5 mm diameter) was preferentially etched using an oxygen plasma for 60 minutes, exposing carbon fibres at the surface. The carbon fibres were irregularly roughened by the treatment. The samples were not always etched, this may have been due to variation in the height of support of the samples above the ground electrode. The nearer the samples to the ground electrode the more virulent the reaction seemed to be, on some occasions the layer of carbon fibres may have been completely removed leaving a smooth layer of PEEK. Also, the samples were not cut from the same batch of APC2 and therefore may have had different surface thicknesses of polymer.

The presence of carbon fibres in the image impeded the isolation and measurement of objects in the field and so the task routine used to analyse the objects on the surface chemistry modified materials was adapted. Uniformly aligned carbon fibres were removed using a linear filter in the same direction as the fibres. Unfortunately, any cells draped over the fibres (Figure 9.5c, iii and 9.5d, iv) or lying alongside were also removed. Together with the errors introduced because of the presence of pores and cracks in the surface, this made image analysis unsuitable for these surfaces.

Qualitatively, the most noticeable difference seen was with cell number. No cells were seen to adhere at the observation point of 30 minutes on the control samples, whilst cells were seen on the etched surface at this time (Figure 9.5a, i & ii). After 1 hour, cells were seen to be spread on the etched surface in comparison to the control; at the 3 hour observation point, spread cells were seen on the control surface (Figure 9.5a, iii-vi). From this time period onwards, no difference between the control and etched surfaces as regards cell number or spreading could be discerned (Figure 9.5b, i-iv). Figures 9.5a, i-vi and 9.5b,

i-vi are typical of the SEM micrographs obtained. The majority of cells on the etched surfaces are attached to fibres; this attachment is probably providential rather than preferential. The cells will gravitate towards the surface after seeding and will 'hit ' and attach to the fibres before the matrix as these are raised from the surface.

Higher magnification micrographs (Figures 9.5c, i-v) show the morphology of cells adhering to fibres. In Figure 9.5c, v the cell is bridging 2 carbon fibres and supporting its central mass with a broad spread of cytoplasm rather than numerous filopodia. The alignment of a spindle shaped cell with carbon fibres can be seen in Figure 9.5c, iii. The mass of the cell is not quite fully on the carbon fibre and attachment fibres can be seen connecting the unsupported edge of the cell to the polymer matrix. Blebs can be seen on the cell surface. Artefact due to shrinkage of the cells during critical point drying is especially noticeable in Figure 9.5c, v and ii, where the cytoplasm has fractured. The ventral space and humped appearance of the cell in Figure 9.5c, ii would lead to tension at the attachment points putting the cytoplasm under great stress, even with minor shrinkage.

The experiment was repeated with HGF cells instead of M^{c}Coys extending the period of observation to 48 hours. The HGF cells displayed a greater tendency to align themselves in the direction of the carbon fibres and to overlap each other, making image analysis even more unsuitable for quantification of the morphology of the cells. The most striking difference between the etched and control surface was the lack of cells on the control surface 30 minutes after seeding, and the alignment of spread cells with the fibres.

Figures 9.5d, i-iii are high magnification micrographs illustrating the intense membrane activity seen on cells adhering to fibres (i & ii) after 30 minutes, and

the morphology of clumped cells seen on the control surfaces (iii) after 1 hour. In the micrographs shown, only membrane blebs can be seen on the cells on the fibres. Figure 9.5d, iv illustrates the preferential spreading of cells in the fibre direction after 48 hours, in contrast to the rounded morphology seen after 30 minutes (i & ii). Figures 9.5d, v & vi are micrographs taken 24 hours after initial seeding and illustrate the difficulties described above in analysing the images.

Table 9.5a gives results for MTT and MB assays performed on the surface of the etched and control materials.

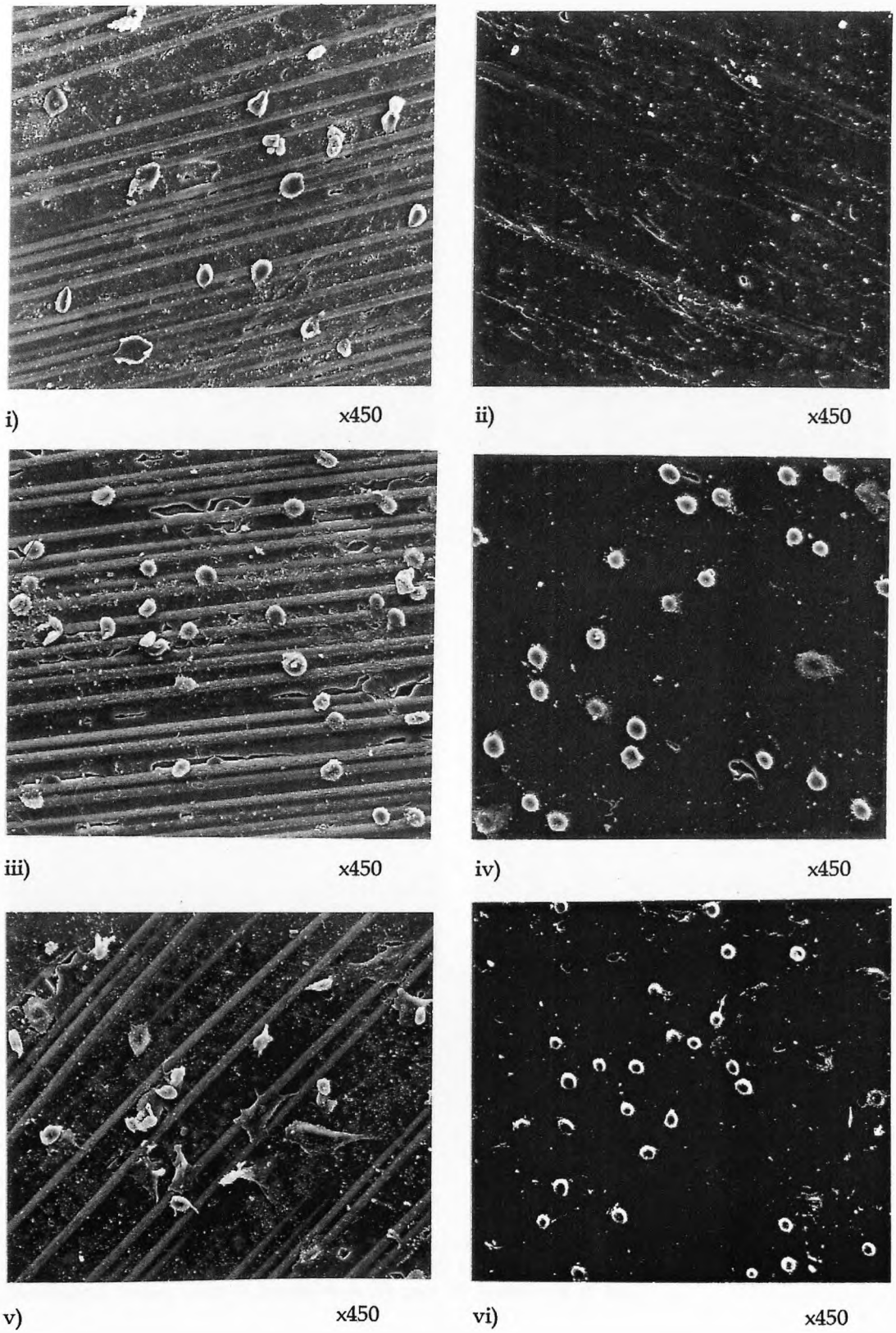

Figure 9.5a: Surface roughness. SEM micrographs of M^{c}Coy fibroblast-like cells seeded on O_2 plasma etched (i, iii & v) and control (ii, iv & vi) APC2 surfaces in the presence of serum. Incubation times were 30 minutes (i & ii), 1 hour (iii & iv), and 3 hours (v & vi).

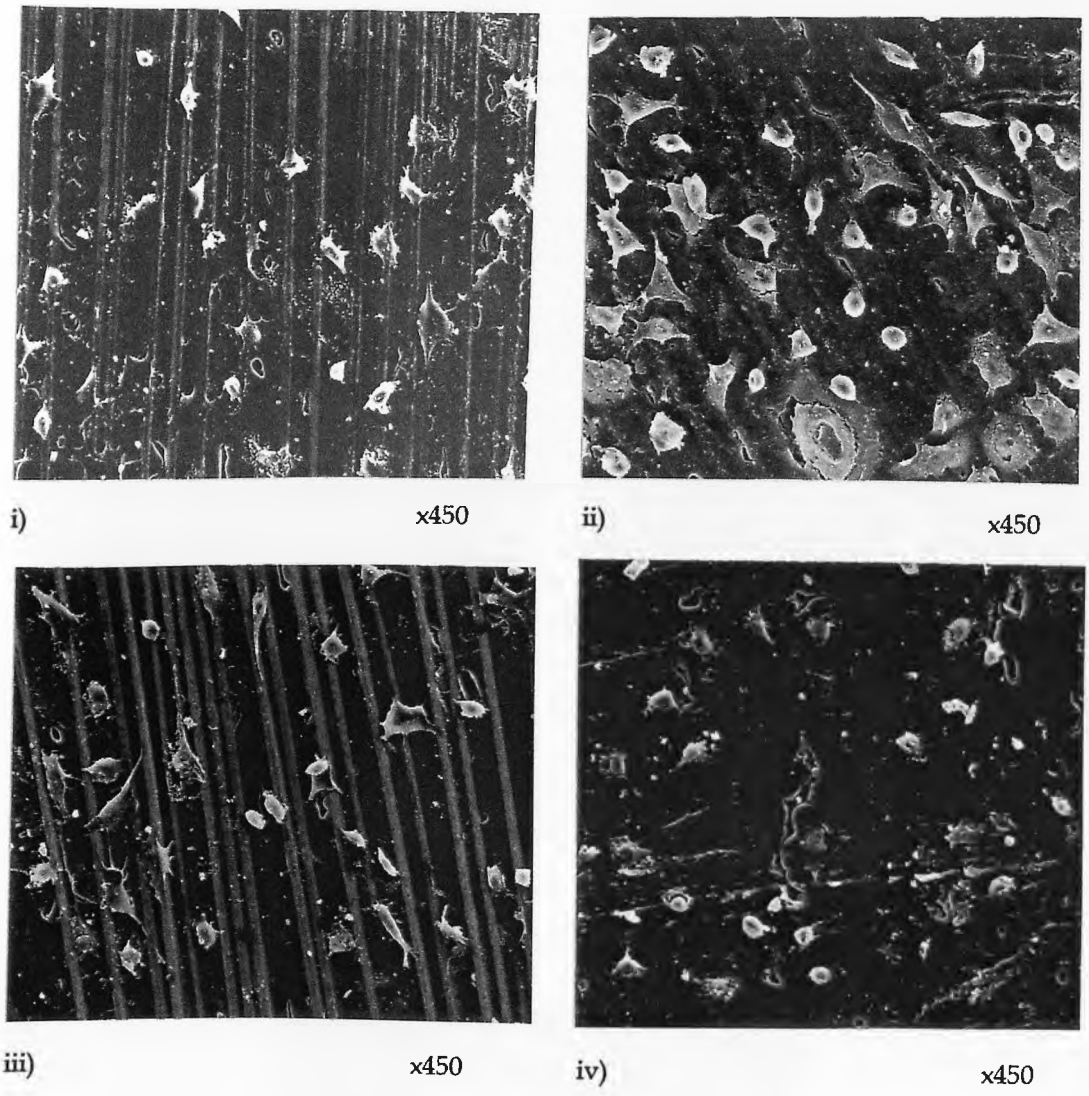

Figure 9.5b: Surface roughness. SEM micrographs of M^{c}Coy fibroblast-like cells seeded on O_2 plasma etched (i & iii) and control (ii & iv) APC2 surfaces in the presence of serum. Incubation times were 6 hours (i & ii) and 12 hours (iii & iv).

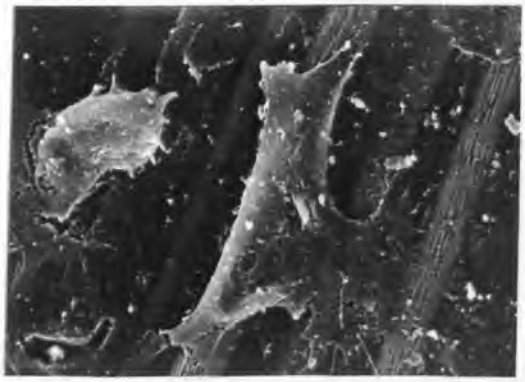

i) x2200

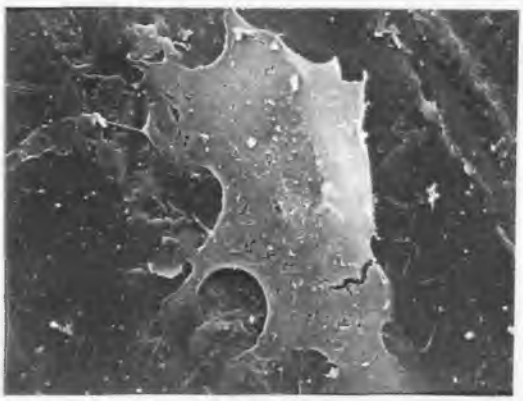

ii) x2000

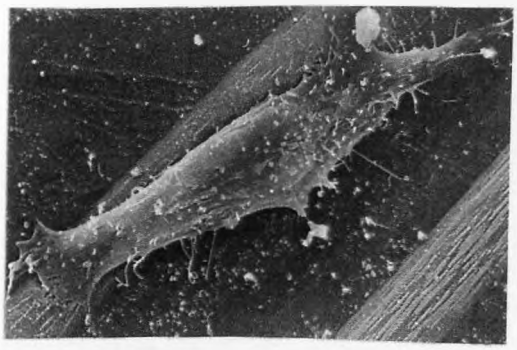

iii) x3000

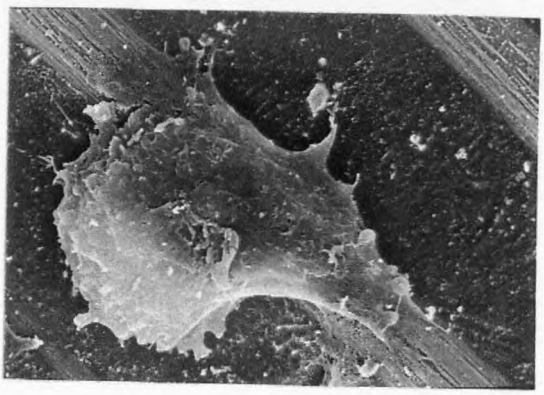

iv) x3000

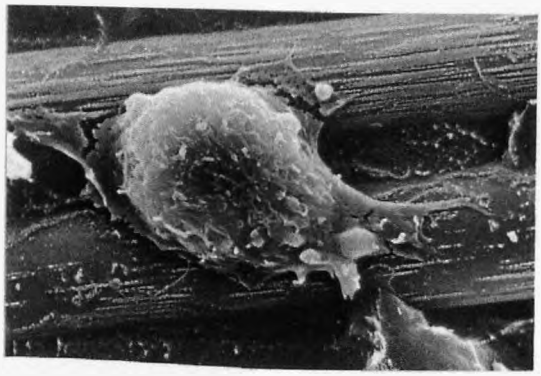

v) x4400

Figure 9.5c: Surface roughness. SEM micrographs of M^{c}Coy fibroblast-like cells seeded on O_2 plasma etched (i, iii, iv & v) and control (ii) APC2 surfaces in the presence of serum. Incubation times were 6 hours (i & ii), 3 hours (iii & iv) and 1 hour (v).

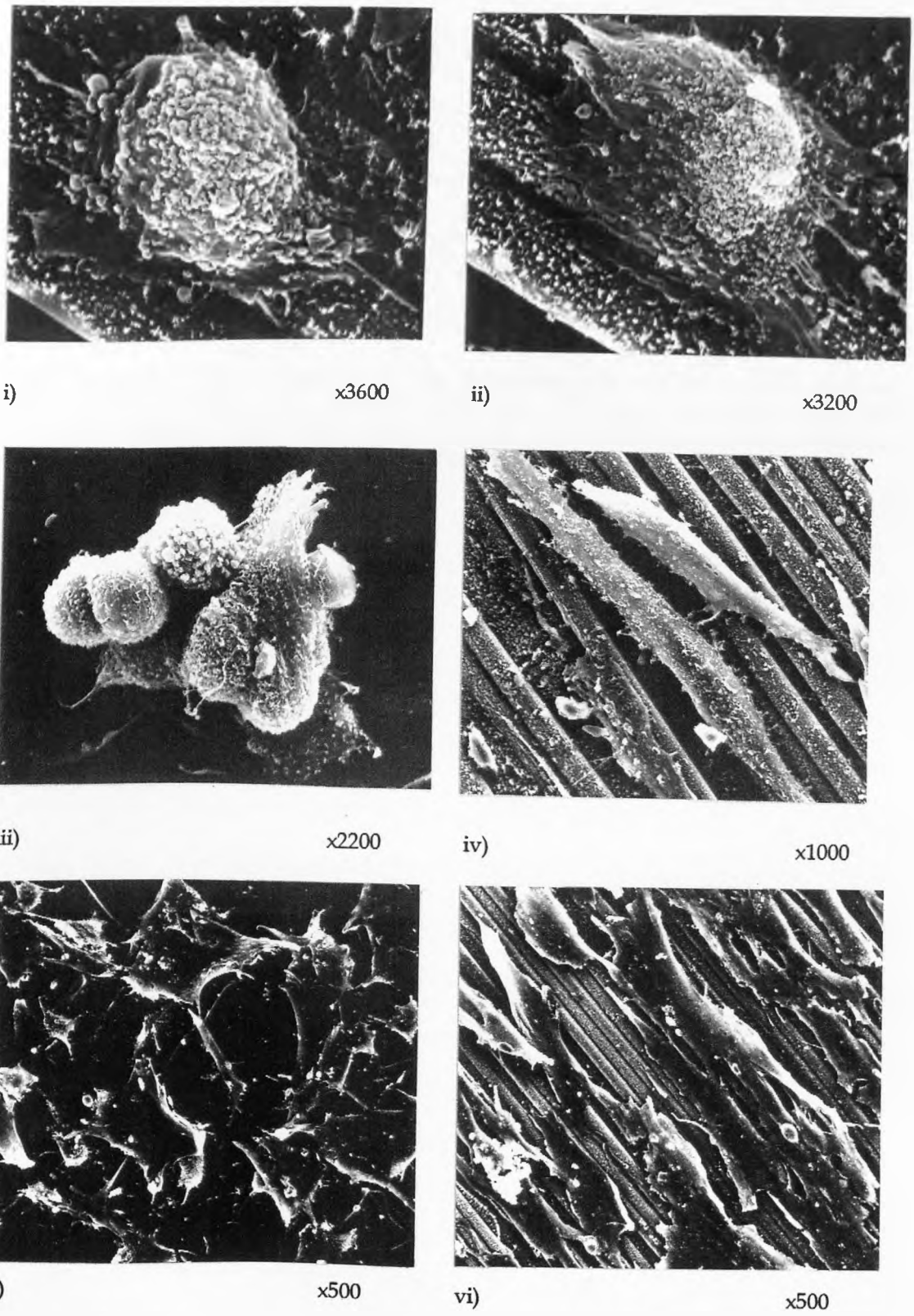

Figure 9.5d: Surface roughness. SEM micrographs of HGF fibroblasts seeded on O_2 plasma etched (i, ii, iv & vi) and control (iii & v) APC2 surfaces in the presence of serum. Incubation times were 30 minutes (i & ii), 1 hour (iii), 24 hours (v & vi), and 48 hours (iv).

	Assay	
APC2 surface	MTT	MB
Control	0.49 ± 0.26	0.68 ± 0.07
Etched	0.77 ± 0.05	0.88 ± 0.10

Table 9.5a: $M^{c}Coys$ cells seeded onto the surface of control and O_2 plasma etched APC2 surfaces and assayed using the MTT and MB assays after 96 hours incubation. For each assay, n = 3. The differences seen are not significant as calculated using the Student's t-test.

9.6 The effects of surface modifications *in vivo*

Plasma treated PEEK and APC2 discs (5 mm diameter) were implanted intramuscularly into rats and retrieved after 1, 2, 7 and 14 days (PEEK samples only). Distortion of the implant site eradicated the information required for evaluation of the tissue reaction to the surface treatments. However, the H & E stain allowed a general appraisal of the early wound healing response to PEEK materials. Granulation tissue was present at all time periods and consisted of macrophages, neutrophils, lymphocytes, and dead muscle and other cells (Figure 9.6a, i & ii). This tissue is common to the inflammatory stage of all wound healing and represents an earlier, more cellular stage of fibrocollagenous tissue, which was seen at the later observation periods used in the biocompatibility study (Chapter V). In contrast to the implant site at the later time periods, fatty tissue was not evident in any of the sections.

The implant site of the 14 day PEEK and 7 day APC2 samples were the most intact and were therefore evaluated using immunohistochemical stains specific for macrophages, B - cells and resting and activated T - cells. A few lymphocytes were seen, mainly in association with sutures; macrophages were seen in higher numbers and were associated with the implant site. Image analysis was used to quantify the number of macrophages present in one section from each block. Table 9.6a gives the objects associated with the implant area in each section. A slightly higher number of macrophages was seen at the 7 day observation period. Figure 9.6a, iii shows an H & E stained area associated with untreated PEEK, in comparison figure 9.6a, iv shows the same area on a subsequent section stained for macrophages. Analysis of the surface of the retrieved implants using SEM revealed patches of adherent tissue and blood cells; no other cells were seen.

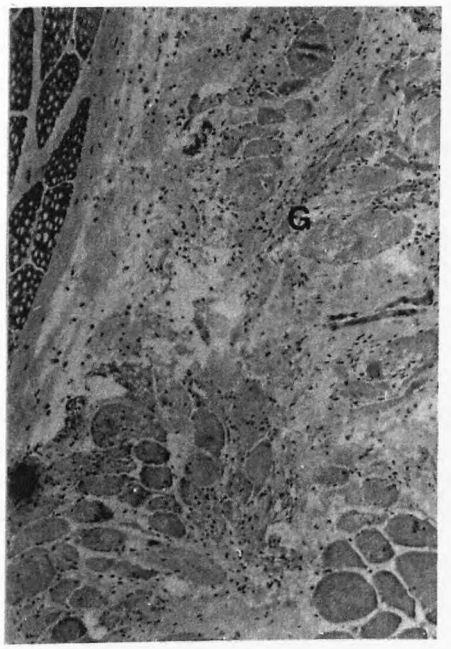

i) x120

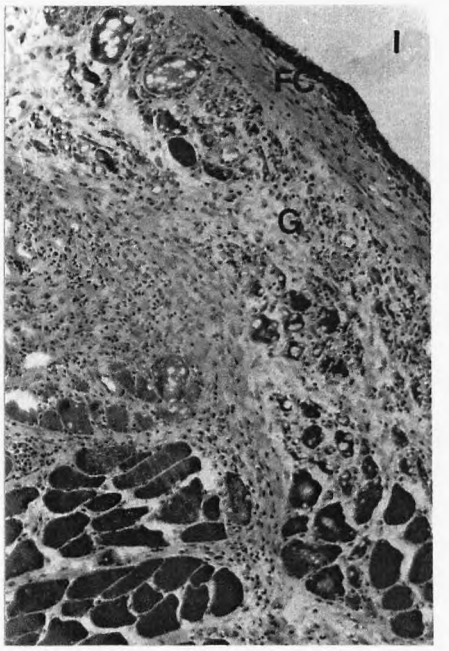

ii) x120

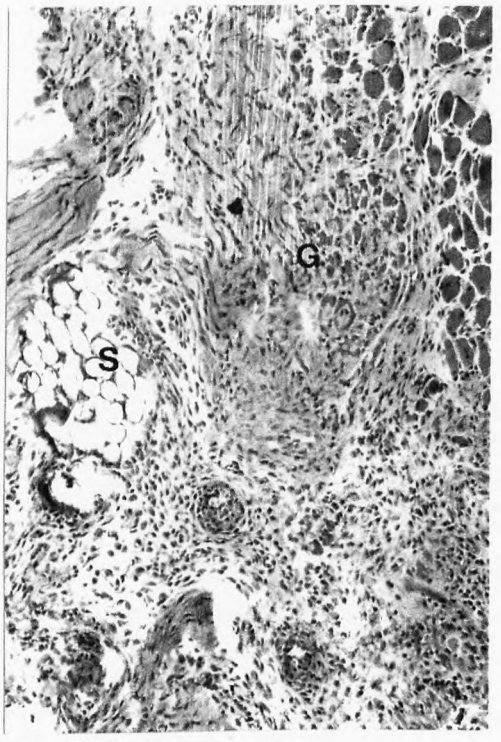

iii) x320

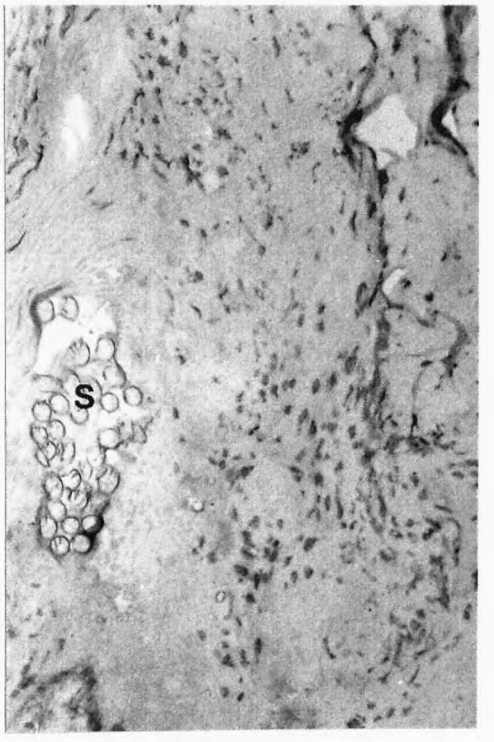

iv) x320

Figure 9.6a: Intramuscular implantation. Light micrographs showing implantation site of: HFB plasma treated PEEK 2 days post-implantation (i), untreated PEEK 7 days post-implantation (ii), and untreated PEEK 14 days post-implantation (iii & iv). Haematoxylin & eosin stain i - iii. Macrophage specific immunohistochemical stain - iv. Micrographs iii & iv are taken from sequential sections. Fibrous capsule (FC), granulation tissue (G), implant site (I), sutures (S).

Object number				
Plasma treatments				
PEEK			APC2	
C	O_2	HFB	C	etched
475	335	318	587	483

Table 9.6a: Number of macrophages counted in equivalent areas (2.06×10^6 μm^2) of muscle associated with the implant site of plasma treated PEEK specimens removed after 14 days and plasma etched APC2 specimens removed after 7 days implantation. C is the control untreated material.

10.1 Surface wettability and roughness

Plasma treatment of biomaterials to provide surfaces of specific functionality whilst maintaining bulk chemistry has been described mainly for hæmocompatible materials. Little has been reported on the use of plasma treatments to modify materials for hard tissue replacement or augmentation; although plasma related techniques such as sputtering or spraying have been used to deposit thin layers onto prostheses. Mainly hydroxyapatite (de Groot, 1987) and titanium have been used. In the present study, plasma treatments were used with a view to improving hard tissue implant attachment by influencing the cellular response at the surface of the test materials.

PEEK and APC2 surfaces were plasma treated to induce a change in surface wettability and morphology whilst keeping the bulk polymer unchanged. Only the top few molecular layers were affected, up to a depth of approximately 10nm. A range of surface wettability was produced as measured by contact angle,

$$O_2 < Ar < NH_3 < \text{Control} < HFB/HFP$$

hydrophilic ----------> hydrophobic

with the most hydrophilic surface being the oxygen treated and the most hydrophobic being the HFP/HFB treated. The increase in wettability of the surfaces indicates the incorporation of polar groups which are able to form hydrogen bonds with water, allowing a droplet to spread on the surface thus leading to a lower contact angle.

The nature of any polar groups incorporated into the surface after treatment could not be readily seen from the XPS data as low resolution scans over a

broad range of binding energies were made rather than high resolution scans over a narrow (10 eV) range. Marked changes in surface chemistry occurred after treatment with HFB and NH_3 where fluorine and nitrogen were detected in the surface. The increase in surface oxygen content seen after ammonia and argon treatment is probably due to further reactions of free radicals at the polymer surface on exposure to the environment.

Ageing, or the rearrangement of surface molecules is a feature of polymer surfaces, which are more mobile than ceramic or metallic surfaces. Unless the polymer surface produced after modification is highly crosslinked, the molecules at the surface will rearrange themselves in response to the environment, until the interfacial free energy is minimized. Although contact angle measurements were not made immediately before the samples were used, a qualitative assessment of the surface wettability was made to ensure that differences were still present. The time elapsing between surface modification and seeding with cells varied from 3 to 16 days. At both these extremes, cells were seen to react to the surfaces implying that little ageing of the surfaces occurred within this time period. Material surfaces examined by XPS 3 days and then 4 months after treatment showed a reduction in the F / C ratio on the HFB treated surface to approximately a third of that recorded originally, whilst no nitrogen peak was seen on the NH_3 treated surface after 4 months. Similar results were found with another set of samples examined one month after modification; a smaller F / C ratio was seen compared to other samples examined after 3 days treatment, and no N peak was found on the NH_3 treated surface. These findings suggest that over this time period some ageing might have taken place.

The reorientation of polymer side chains and segments may depend on the nature of the adjacent phase. If unstable moieties are still present on the

modified polymer surfaces when they are seeded with cells in aqueous medium, or implanted *in vivo*, rearrangement may occur giving a thermodynamically stable conformation which is different to that found in air. Any ageing might result in a less attractive surface being presented to the cell population. If this occurred over a period of time coincident with wound healing, optimal stabilization of the implant might never occur. Further investigation into the ageing of the plasma treated surfaces in relation to the physiological environment is therefore necessary.

The only change in surface texture observed after treatment was that on APC2 after O_2 plasma etching. It has been shown that a decrease in contact angle occurs on etched surfaces (Andrade, 1985), but the increase in wettability seen here may also be due to residual oxygen species in the surface of the polymer creating a more polar surface.

10.2 The cellular response to surface modifications *in vitro*

As an initial *in vitro* investigation into the effect of the modified surfaces, cell attachment and morphology were observed using SEM. Image analysis was used in an attempt to reduce the observer bias encountered in trying to perceive cells as being different from each other in respect to shape and size. However, such analysis was found to be limited in its usefulness and required careful control of the conditions of the experiment with respect to the number of cells seeded, the time period of observation and the texture of the surface being examined. At high cell concentrations individual cells could not be resolved by the system and cell aggregates rather than single cells were counted. Identification of very spread cells was also a problem as the contrast between the background and the cells was too small for the analysis system to resolve; this was especially noticeable at the 3 hour and longer time periods.

The presence of surface flaws which were similar in size to cells was a further source of error, particularly on the APC2 surfaces, as these could not be filtered out of the image without also removing cells. Polishing of the surfaces would in future reduce this error, although some deep surface cracks may not be removable. A similar problem was found with the etched surfaces in that the cells tended to align themselves alongside and over the fibres and were therefore removed from the image when the fibres were filtered out, meaning that image analysis could not be used on these surfaces.

The HFP treated surface was the most hydrophobic of the surfaces as shown by the contact angle measurements, and supported the least cell attachment in the presence of serum. Cells are thought to adhere to surfaces via the specific interaction of cell surface receptors (integrins) with pre-adsorbed proteins. Proteins in solution contain hydrophilic, charged and hydrophobic regions, surrounded by a hydration shell. The conformation of the protein usually leads to most of the hydrophobic regions being in the interior of the molecule. Proteins may adhere to a surface via electrostatic attraction, hydrophobic bonding, or hydrogen bonding; at a hydrophobic surface such as presented by the HFP / HFB treated PEEK, hydrophobic bonding of the serum proteins will occur. In this way the interfacial free energy, which is high due to the ordering of water dipoles at the apolar interface, will be reduced. In order to present its' hydrophobic regions to the material surface, the protein will have to change its conformation. In the case of the fluorinated PEEK, it seems that there is either less reliance on protein mediated adhesion, or a change in the conformation of the adherent proteins making them unattractive to cells. As proteins have been shown to adhere preferentially to hydrophobic surfaces (Klebe, 1981), it seems that in the case of fluorinated PEEK, the attached proteins must have changed their conformation so drastically that the cells

cannot adhere via specific receptors. Changed conformation of proteins upon adhesion has been noted by Grinnell & Feld (1982) who demonstrated that greater quantities of fibronectin adsorbed to hydrophobic polystyrene, but that cell adhesion and antibody binding was increased on hydrophilic polystyrene.

The increased wettability of the materials after oxygen and argon treatment was seen to lead to an increase in cell number and spreading which was more noticeable at the longer time periods of 24 and 48 hours. These observations could not be quantified due to the limited resolution of the image analysis system as discussed above.

The cell morphology was seen to change from rounded to spindle shaped as the cells spread during the experimental period. The fluorinated surface supported more elongated cells than the other surfaces; a lower circularity and higher object length was measured on this surface. Although more spindle shaped cells were seen on the hydrophobic surface, qualitatively they were not as flattened as those on the hydrophilic surfaces. This inhibition of spreading is in agreement with the seemingly unattractive nature of the surface with respect to the numbers of cells attached.

Experiments were performed in the absence of serum in an attempt to enhance the influence of the material surface, especially at the early time periods where the protein covering due to cell secretion would be minimal. Under these conditions $M^{c}Coy$ fibroblasts were found to adhere to all the PEEK surfaces. Fibroblasts have been shown to adhere and spread in the absence of serum by several groups including Schakenraad (1986), Curtis (1986b), and Bergethon (1989); although Brandley (1987) reported an absolute requirement for serum for the attachment and spreading of Balb/3T3 fibroblasts. It is likely that the necessity of serum proteins for cell attachment and spreading is dependent on the particular cell line and substratum used.

In the absence of serum, cell attachment may be mediated by cell adhesion proteins such as fibronectin secreted by the cell itself (Grinnell 1978). The possibility of direct attachment of the cell to hydroxyl groups on the surface has been shown by Curtis (1986b); in their system protein synthesis was inhibited and RGDS tetrapetptide was used to block any residual fibronectin sites present, yet cells still attached to a hydroxyl rich polystyrene surface. This group (1986a) has also demonstrated that in the absence of serum fibroblasts were able to modify appropriate surfaces by oxidation and hence increase the number of hydroxyl groups.

In the procedure used, the cells were conditioned to grow in serum and there was likely to be residual proteins attached to the cell surface on seeding. It is therefore most probable that the cells were attaching via proteins secreted or shed from the cell surface. If attachment was mediated by the secretion of cellular attachment proteins, conformational changes in these proteins might be expected, as for the serum proteins, upon adsorption to the hydrophobic substrate. The increase in cell numbers seen on the hydrophobic surfaces in the absence of serum indicates that if conformational change of cell secreted proteins is occurring, it's effects are not as detrimental as for the serum proteins. In the absence of serum, electrostatic attraction between the cell membrane and the substratum might be expected to play a larger part in cell attachment as the masking effect of serum proteins would be removed. If this mechanism was important cell adhesion would be higher on the hydrophilic surface, again this was not the case. Cells were less spread on all of the surfaces with few spindle shaped cells seen, even at 4 hours after seeding. The pattern of cell adhesion seen, with cell attachment increased on the hydrophobic surfaces in comparison to the hydrophilic surfaces is difficult to explain.

The wettabilities obtained after plasma treatment of the APC2 surface should be equivalent to those on the PEEK surface as the surface layer of APC2 is usually described as being resin rich. However, slightly different effects may have been obtained as the HFP treated surface was not as hostile to cell attachment in the presence of serum as the HFP treated PEEK surface was. In the absence of serum there was increased adhesion and spreading on the HFP treated surface, thus confirming the finding on the PEEK surfaces. In comparison to the other surfaces, a higher cell number was seen at the early time periods, and the cells were more spread after 3 hours of seeding.

On both the PEEK and APC2 plasma treated surfaces the differential adhesion and spreading of cells onto the hydrophobic surface in the absence of serum is perplexing. Measurement of contact angles gives an indirect assessment of the surface energy of a material; in general, the smaller the contact angle the higher the surface energy of the material. The preference of cells for the more hydrophilic surfaces in the presence of serum is in agreement with the work of Schakenraad et al. (1986) on the correlation between cell attachment and spreading and substrata surface energy. The findings in the absence of serum contradict results from this same study, where the adhesion and spreading was found to be more marked on the high surface energy substrata in serum free medium. As well as the surface wettability, the chemical groups and the nature and density of surface charges present may be influencing the cell adhesion (Chapter VII). It may be that the charge density on the hydrophilic surfaces was not optimal for cell attachment (Maroudas,1975b; Curtis 1986a). Electrostatic attraction and mediation via cell secreted proteins are probably the mode of attachment for cells on the hydrophilic surfaces in serum free medium; the mechanism for the increased attachment on the hydrophobic surfaces is unclear.

The results discussed above are only preliminary and need repeating to confirm the unusual results obtained. Although SEM of cells on the material surface gave useful results, the spreading of the cells on the treated surface would be better addressed using TEM (transmission electron microscopy) in conjunction with SEM. The gap between the cell membrane and the substratum could be measured and the type of contact identified. It may be that although the cells are present in higher numbers on the hydrophobic surface, they are not so closely apposed to the substratum and do not display the usual interaction sites; for example focal adhesion sites, which are the sites of integrin mediated attachment. Thin films of semicrystalline PEEK are available and preliminary studies by the author have shown that cells adhered in the same manner as in this study, and that the samples could be embedded and ultrathin sections obtained for examination using TEM. Single plies of APC2 were examined in the same way, but unfortunately ultrathin sections could not be obtained, even using a diamond knife.

The numbers of cells adhering to the treated surfaces could be better quantified using a methylene blue assay performed on the material surface, with the metabolic activity of adherent cells examined using an MTT assay. Conformational change of cell attachment proteins on the hydrophobic surface could be assessed by measuring the binding of anti-fibronectin and anti-vitronectin antibodies. If this was done in the presence of cells in serum supplemented and serum free medium, any differences in the degree of conformational change of cell secreted proteins as opposed to serum proteins could be assessed. To rule out adhesion by cell secreted or shed proteins, the RGDS tetrapeptide could be used to block any fibronectin or vitronectin binding sites and intracellular protein synthesis inhibited. If cells still attach it must be due to some aspect of the surface chemistry.

The effect of surface roughness on cell attachment and spreading was assessed using etched surfaces obtained by O_2 plasma etching of APC2. The roughness produced was related to the width of carbon fibres revealed on the surface (7μm) and was therefore on the cellular scale. The main difference seen was at the first time period, 30 minutes after seeding, where cells were seen on the etched but not the control surface. At the earlier time periods, cells were seen to be more spread on the etched surface, although by 6 hours, this difference was not noticeable. Contact guidance was seen on the etched surfaces with the fibroblasts preferentially aligning in the fibre direction. Contact guidance is thought to be an important mechanism *in vivo*, governing the migration of many different types of cells, for example neural crest cells along a neural tube; that it was more noticeable with the primary fibroblast line, HGF cells, may be due to their retaining more *in vivo* characteristics.

The cells observed on the etched surfaces at the 30 minute observation point were seen to display prominent surface blebs and microvilli indicative of membrane activation. These membrane protrusions are commonly seen on cell seeding and initial attachment and are also associated with cell locomotion. They were not limited to cells on the etched surfaces but were seen on cells on all the materials. Blebs are blisters of membrane filled with cytoplasm which are thought to arise either from herniation at weak points of the cell membrane caused by a rise in internal hydrostatic pressure (Harris, 1973) or they may be part of the continual cycle of membrane activity due to microfilament contraction, disassembly and reassembly (Dunn, 1980). Microvilli are thought to serve as a reservoir of excess surface membrane that is utilized as the cell becomes increasingly spread (Erickson & Trinkaus, 1976). The observations made on the PEEK and APC2 surfaces, both treated and control, support this view as few microvilli were seen on spread cells.

Initial experiments into the potential of the MTT and the MB assays in quantifying the cellular response to the modified surfaces showed a trend towards increased adhesion on the APC2 surface which was not significant with the small sample sizes used.

The reason for enhanced adhesion and spreading of cells onto roughened substrata is unclear, but has been noted by other workers. Textured surfaces have been utilised to enhance the function of various biomaterials in situations where apposition of a particular cell type was desired; for example, endothelial cells on vascular grafts. In the system used, the hydrophilicity of the surface was increased after etching and therefore the effect of roughness cannot be divorced from the effect of an increase in wettability. To discern the major influence on cell adhesion, samples of etched and hydrophilic APC2 both produced using an O_2 plasma but for different periods of time, should be examined simultaneously. It would also be interesting to see whether seeding cells in serum free medium affects the response of cells to the substrate. It may be that the differential attachment and spreading on the etched surface is enhanced under these conditions. To declare conclusively the etched surface to be more, less or no different with respect to cell adhesion, further experiments using the MB assay to quantify cell adhesion and the MTT assay to quantify cell metabolism would be expedient.

Fibroblasts were used in the *in vitro* studies as they had been used previously in the biocompatibility testing and were easy to maintain; they were therefore ideal to assess the general reaction, if any, of cells to the modified substrata. Obviously, the next stage would be to use osteoblasts in the test systems. Osteoblasts are believed to function in the control of *in vivo* calcification by synthesis and secretion of collagen, non-collagenous proteins and growth factors, and by regulation of the flux of calcium and phosphate

ions. They may also be involved indirectly in the osteoclast-mediated process of bone resorption (Barnes, 1987). The osteoblast cell membrane is thought to mediate many of these activities by specialized cell membrane domains which are cytochemically distinct, (Watson, 1989) such cells are termed polarized cells. With such a highly functionalized cell membrane, osteoblasts are likely to be more sensitive to substrate chemistry and texture than fibroblasts, which are not described as polarized cells. Matsuda & Davies (1987), demonstrated that although osteoblasts migrated onto the surface of both bioactive glass (45S5) and quartz, extracellular matrix was only elaborated on the bioactive surface. In conjunction with the methods described to examine further the effect of modified surfaces on fibroblasts, markers associated with osteoblast function could be used to assess the cell response to the material. Collagen Type I is secreted *in vivo*, and its secretion *in vitro* is used as a characteristic marker for osteoblasts; alkaline phosphatase levels could be monitored, this enzyme is widely used as a measure of bone cell activity; specific bone proteins such as osteonectin could also be measured.

The use of plasma treatments to enhance cell attachment and spreading under physiological conditions *in vitro* has important implications for the design of a low modulus or composite material for orthopædic applications. As discussed in Chapter I, the advantage of using composite materials such as APC2 is that the modulus of the implant can be matched closely to that of the bone, thus reducing the effect of stress shielding. With the higher modulus materials, bone cement (PMMA) has been used as a means of securing the implant, but it also acts to bridge the difference in modulus between the bone and the implant. With low modulus materials such a bridge would not be necessary and therefore a different method of securing the implant could be used, without the drawbacks associated with PMMA.

Ideally, the implant material would be secured by direct incorporation into the bone environment and would not be sequestered from the bony tissue by a fibrous capsule. The results from the biocompatibility studies on PEEK and PEEK / carbon composites inferred that the materials are osteoconductive, providing an extremely attractive surface for bone cells. In the case of a hip joint replacement or fracture fixation plate, the materials would be in a more loaded situation than in the intraosseous biocompatibility study (Chapter V) and therefore more likely to be subject to micromotion and disruption of the bone/implant interface. Early stabilization of the interface by enhanced cell adhesion and stimulation of bone formation would therefore be advantageous.

10.3 The cellular response to surface modifications *in vivo*

Chemically modified PEEK and etched APC2 discs together with controls were implanted intramuscularly to evaluate the *in vivo* cellular response to modified material surfaces. As with the biocompatibility studies, error was introduced into the analysis of the material/muscle interface by the necessary removal of the material prior to sectioning. The lack of a fibrous capsule made identification of the implant site more difficult than at the longer time periods used in the biocompatibility study. The implant site became clearer to identify at the later time periods where the granulation tissue was more organized and so immunocytochemical analysis was performed on tissue taken 7 days (APC2 O_2 plasma etched and control) and 14 days (HFP and O_2 plasma treated PEEK) post-implantation.

Sections were stained for resting and activated T-cells, B-cells and macrophages. The only lymphocytes observed were a few T-cells, closely associated with suture material; their presence was not therefore indicative of a cellular immune reaction to the material. Macrophages were observed

associated with the implant site of all the materials. Initially it was hoped to quantify the numbers of inflammatory cells seen associated with the material/host interface, but after examination of the sections it was felt that the error introduced by removing the material would make use of the term "quantification" deceptive, regardless of the number of sections analysed. To see if there was a noticeable difference between any of the samples, and as one section from each was already stained, the number of objects present was counted using the analysis system. Higher counts were recorded from the 7 day implants (APC2 etched and control) but no clear trends regarding the surface treatments could be discerned. In future, all *in vivo* studies would be designed on the premise that the implant site must be preserved by sectioning the material *in situ* using resin embedding of the material/tissue; use of a low temperature resin such as LRGold as discussed in Chapter VI would also enable immunocytochemical stains to be performed.

On implantation, proteins will adsorb to the material surface, and as shown by the *in vitro* work it is likely that protein conformation is changed on attachment to surfaces of different wettability - leading to changes in cell adhesion and spreading. Surface roughness was also observed to lead to differences in cell adhesion and spreading. *In vivo* other factors such as micromotion between tissue and material may be more important than degrees of surface wettability or roughness in determining the level of fibrous encapsulation or the apposition of a particular cell type. It may be argued that since wound healing is such a complex procedure involving many proteins, growth factors, hormones and cells, any surface effect may be masked - provided the material is non-toxic or non-degradable.

Conversely it can be claimed that to explain the differences in capsule thickness and differential adhesion of cells such as osteoblasts to implants, some aspect of the material surface must modulate the host response towards different materials; whether the surface roughness or the surface chemistry is most important is debatable. The close apposition of bone to titanium implants has been attributed to surface chemistry aspects (Albrektsson, 1985b), although for osseointegration to occur, the surface must be textured to allow for mechanical interlocking of the implant with the tissue. The effect of PTFE and titanium hollow chambers on early wound healing has been assessed by Eriksson (1990) by measuring levels of Il-1, LBT_4, and leukocytes harvested from the exudate in the chamber. Between two observation points at 24 hours and 6 days, the leukocyte number and LBT_4 concentration increased significantly in the PTFE chamber as compared to the titanium chamber. This increased inflammatory reaction was thought to be linked to the fibrous capsule formed after longer periods of implantation; that adjacent to PTFE was found to be thicker than that adjacent to titanium.

In vivo studies by other groups have shown that macrophage adherence can be dependent on the surface roughness of a material, with more macrophages found on rough rather than smooth surfaces (Salthouse, 1984). In cases where different materials were examined, the numbers of macrophages varied with the surface roughness and not with the material composition (Behling, 1986).

Future work using resin embedded specimens could address the problems and anomalies described above. The effects of wettability and roughness could be dissociated by simultaneously examining etched and hydrophilic APC2 produced using an O_2 plasma. The examination time could be increased to enable observation to be made of any modulation of the fibrous capsule formed. The effects of surface modifications on the response of bone tissue to

the materials could be examined using backscattered electron imaging and transmitted light microscopy, techniques already successfully demonstrated in the biocompatibility study. In fact, the results from the biocompatibility study indicate that surface roughness may modulate the bone response to a material. Uniformly treated rods for implantation may be obtained by standing the rods on end in the plasma reactor chamber ensuring an even treatment apart from one end. Rough and smooth surfaces may be obtained as described in Chapter VI.

10.4 Summary

Increasing the surface wettability or roughness enhanced early cell attachment and spreading *in vitro*, and may provide a basis for improved early attachment of cells leading to reduced micromotion and early stabilization of the tissue / implant interface; thus enhancing the fixation of orthopædic prostheses.

1. Little inflammatory reaction was seen to the test materials, PEEK, D150CA30 and APC2, implanted intramuscularly for periods of time up to 9 months. Examination of the bony response to the materials at 6 months showed no tissue necrosis and good healing around the implant with very close bone apposition. These observations indicate that the materials are appropriate for implantation within the body.

2. Backscattered electron imaging was found to be a useful method for examining the hard tissue response to the implants, allowing visualization of areas of remodelling.

3. The test materials were found to be non-cytotoxic using a range of qualitative and quantitative *in vitro* cytotoxicity tests and two cell types. This reinforces the comment in (1) concerning the good biocompatibility of these materials.

4. The MTT test was found to be a reproducible and fast method of assessing test material cytotoxicity in both solid and extracted form. It gave comparable results to the more conventional ^{3}H-Tdr uptake assay and more information than the simple assessment of cell number using the MB assay.

5. Mechanical tests performed after ageing of the materials both *in vitro* and *in vivo* showed no changes in the properties of PEEK; however, small but significant changes in the mechanical properties of the composites under "worst

case" conditions were recorded. As continual monitoring of the flexural modulus whilst being aged revealed no significant changes, it is concluded that the composites show good mechanical stability under physiological ageing conditions. The interfacial shear strength and stiffness developed by APC2 at the bone / implant interface was found to compare favourably with other materials reported in the literature.

6. Plasma treatments of the test materials were shown to change both the surface wettability and roughness of the materials depending on the treatment used. This glow discharge system provided an excellent model for systematically assessing the contribution of material surfaces to the host response both *in vitro* and *in vivo*.

7. The surface treatments were shown to modify the *in vitro* cellular response to the test materials. In comparison to controls, the hydrophilic surface was more attractive than the hydrophobic surface with respect to cell attachment and the plasma etched surface enhanced early cell attachment and spreading.

8. The quantitative assessment of the *in vivo* response to the materials was inconclusive but the test methods used, image analysis in conjunction with specific cell staining, were shown to be promising.

Adams, D., Williams, D.F., (1984) The response of bone to carbon-carbon composites. *Biomaterials* **5**:59-64

Agins, H.J., Alcock, N.W., Bansal, M., Salvati, E.A., Wilson, P.D., Pellicci, P.M., Bullough, P.G. (1988) Metallic wear in failed titanium-alloy total hip replacements. A histological and quantitative analysis. *J. Bone Jt. Surg.* **70A**:347-356

Albrektsson, T., Branemark, P.I., Hansson, H.A., Lindstrom, J. (1981) Osseointegrated titanium implants. *Acta Orthop. Scand.* **52**:155-170

Albrektsson, T., Albrektsson, B. (1987) Osseointegration of bone implants. A review of an alternative mode of fixation. *Acta. Orthop. Scand.* **58(5)**:567-77

Albrektsson, T. *CRC Crit. Rev. Biocompat.* 1 (1985) pp531

Allen, R.C., Loose, L.D. (1976) Phagocytic activation of a luminol-dependent chemiluminescence in rabbit alveolar and peritoneal macrophages. *Biochem. & Biophys. Res. Communications* **69(1)**:245-252

Amstutz, H.C. (1985) Arthroplasty of the hip: the search for durable fixation. *Clin Orthop.* **200**:342-361

Andrade, J.D. (1985) The contact angle and interface energetics. In: Surface and Interfacial Aspects of Biomedical Polymers pp 274-276

Andrew, T.A. Berridge, D., Thomas, A., Duke, R.N.F. (1985) Long-term review of Ring total hip arthroplasty. *Clin. Orthop.* **201**:111-122

Argraves, W.S., Pytela, R., Suzuki, S., Millan, J.L., Pierschbacher, M.D. and Ruoslahti, E. (1986) cDNA sequences from the alpha subunit of the fibronectin receptor predict a transmembrane domain and a short cytoplasmic peptide. *J. Biol. Chem.* **261**:12922-24

Attwood, T.E., Dawson, P.C., Freeman, J.L., Hay, L.R.J., Rose, J.B. and Staniland, P.A. (1981) Synthesis and properties of polyaryletherketones. *Polymer* **22**:1096

Baier, R.E., (1975) Applied chemistry at protein interfaces. *Adv. Chem. Ser.* **145**:1

Bancroft, J.D., Stevens, A. (1977) Theory and practice of histological techniques. Churchill Livingstone

Barnes, D.M. (1987) Close encounters with an osteoclast. *Science* **236**:914

Behling, C.A. and Spector, M.(1986) Quantitative characterization of cells at the interface of long-term implants of selected polymers. *J. Biomed. Mater. Res.* **20**:653-666

Ben-Ze'ev, A., Farmer, S.R., Penman, S. (1980) Protein synthesis requires cell-surface contact while nuclear events respond to cell shape in anchorage dependent fibroblasts. *Cell* **21**:211-236

Bergethon, P.R., Trinkaus-Randall, V. and Franzblau, C. (1989) Modified hydroxyethylmethacrylate hydrogels as a modelling tool for the study of cell-substratum interactions. *J. Cell Sci.* **92**:111-121

Bhuyan, B.K., Loughman, B.E., Fraser, T.J., Say, K.J. (1976) Comparison of different methods of determining cell viability after exposure to cytotoxic compounds. *Exp. Cell. Res.* **97**:275-280

Black, J. (1989) Editorial. *J. Biomed. Mater. Res.* **23**:1243-1245

Blundell, D.J., Osborn, B.N. (1983) The morphology of poly(aryl-ether-ether-ketone) *Polymer* **24**:953

Bozarth, M.J., Gillepsie, J.W., McCullough R.L. (1987) Fibre orientation and its effect upon thermoelastic properties of short carbon fibre reinforced poly(etheretherketone) (PEEK). *Polymer Composites* **8(2)**:74-81

Brandley, B.K., Weisz, O.A., and Schnaar, R.L. (1987) Cell attachment and long-term growth on derivatizable polyacrylamide surfaces. *J. Biol. Chem.* **262**:6431-6437

Branemark, P.I., Adell, R., Albrektsson, T., Lekholm, U., Lundqvist, S., Rockler, (1983) Osseointegrated titanium fixtures in the treatment of edentulousness. *Biomaterials* **4**:25

Briggs, D. Seah, M.P. (1983) Practical surface analysis by Auger and X-ray photoelectron spectroscopy. Wiley & Sons

Brown, S.A., Hastings, R.S., Mason, J.J., Moet, A. (1990) Characterization of short-fibre reinforced thermoplastics for fracture fixation devices. *Biomaterials* **11**:541-547

Buchanan, R.A, Rigney, E.D., Williams, J.M. (1987) Ion implantation of surgical Ti-6Al-4V for improved resistance to wear accelerated corrosion. *J. Biomed. Mater. Res.* **21**:355-366

Buck, C.A. and Horwitz, A.F. (1987) Cell surface receptors for extracellular matrix molecules. *Ann. Rev. Cell. Biol.* **3**:179-205

Bullough, P.G., DiCarlo, E.F., Hansraj, K.K., Neves, M.C. (1988) Pathologic studies of total joint replacement. *Orthop. Clin. North America* **19**:611-625

Burton, S.A., Petersen, R.V., Dickman, S.N., Nelson, J.R. (1986) Comparison of *in vitro* bacterial bioluminescence and tissue culture bioassays and *in vivo* tests for evaluating acute toxicity of biomaterials. *J. Biomed. Mater. Res.* **20**:827-838

Cahoon, J.R. (1978) Evaluation of a precipitation hardened wrought cobalt-nickel-chromium-titanium alloy for surgical implants. *J. Biomed. Mater. Res.* **12**:805-819

Cameron, H.U. (1982) The results of early clinical trials with a microporous coated metal hip prosthesis. *Clin. Orthop.* **165**:188

Cameron, H.U. (1986) Six year results with a microporous coated metal hip prosthesis. *Clin. Orthop.* **208**:81

Carmichael, J., DeGraff, W.G., Gazdar, A.F., Minna, J.D., Mitchell, J.B. (1987) Evaluation of a tetrazolium based semiautomated colorimetric assay: Assessment of chemosensitivity testing. *Cancer Res.* **47**:936-942

Charnley, J. (1960) Anchorage of the femoral head prosthesis to the shaft of the femur. *J. Bone Jt. Surg.* **42B**:28

Chen, L.B., Murray, A., Segal, A., Bushnell, A., Walsh, M.L. (1978) Studies on intracellular LETS glycoprotein matrices. *Cell* **14**:377

Chen, W.T. and Singer, S.J. (1982) Immunoelectron microscopic studies of the sites of cell substratum and cell-cell contacts in cultured fibroblasts. *J. Cell. Biol.* **95**:205

Christel, P., Meunier, A., (1987) Development of a carbon-carbon hip prothesis. *J. Biomed. Mater. Res.* **21(A2)**:191-218

Clemow, A.J.T. Weinstein, A.M., Klawitter, J.J., Koeneman, J., Anderson, J. (1981) Interface mechanics of porous titanium implants. *J. Biomed. Mater. Res.* **15**:73-82

Cogswell, F.N. (1983) Microstructure and properties of thermoplastic aromatic polymer composites. *28th National SAMPE symposium* **28**:528-533

Cook, S.D., Barrack, R.L., Thomas, K.A., Haddad, R.J. (1988) Quantitative analysis of tissue growth into human porous total hip components. *J. Arthroplasty* **3(3)**:249-262

Couchman, J.R., Hook, M., Rees, D.A. and Timpl, R. (1983) Adhesion, growth and matrix production by fibroblasts on laminin substrates. *J. Cell Biol.* **96**:177-183

Chehroudi, B., Gould, T.R. and Bruette, D.M. (1988) Effects of a grooved epoxy substratum on epithelial cell behaviour *in vitro* and *in vivo*. *J. Biomed. Mater. Res.* **22**:459-473

Chwirut, D.J. (1984) Long term compressive creep deformation and damage in acrylic bone cements. *J. Biomed. Mater. Res.* **18**:25

Curtis, A.S.G., Forrester, J.V., McInnes, C. and Laurie, F. (1983) Adhesion of cells to polystyrene surfaces. *J. Cell Biol.* **97**:1500

Curtis, A.S.G., Forrester, J.V. and Clark, P. (1986a) Substrate hydroxylation and cell adhesion. *J. Cell Sci.* **86**:9-24

Curtis, A.S.G., McMurray H. (1986b) Conditions for fibroblast adhesion without fibronectin. *J. Cell Sci.* **86**:25-33

Denizot, F., Lang, R. (1986) Rapid colorimetric assay for cell growth and survival. Modification to the tetrazolium dye procedure giving improved sensitivity and reliability. *J. Immunol. Methods* **89**:271-277

Dunn, G.A. (1980) Mechanisms of fibroblast locomotion. In: Cell adhesion and motility, ed. Curtis, A.S.G. and Pitts, J.D. pp409-423

Ekstrand, K., Ruyter, I.E., Wellendorf, H. (1989) Carbon/graphite fiber reinforced poly(methylmethacrylate): Properties under dry and wet conditions. *J. Biomed. Mater. Res.* **21**:1065-1080

Engh, C.A. (1983) Hip arthroplasty with a Moore prosthesis with a porous coating: A five year study. *Clin. Ortho.* **176**:52

Erickson, C.A., Trinkaus, J.P. (1976) Microvilli and blebs as sources of reserve surface membrane during cell spreading. *Exp. Cell. Res.* **99**:375-384

Eriksson, A.S., Bjursten, L.M., Ericson, L.E., Thomsen, P. (1988) Hollow implants in soft tissues allowing quantitative studies of cells and fluid at the implant interface. *Biomaterials* **9**:86-90

Eriksson, A.S., Thomsen, P. (1990) Leukocytes, LBT_4 and interleukin-1 content in titanium and PTFE hollow chambers implanted in the rat abdominal wall. In: Clinical Implant Materials, Ed. Heimke, Elsevier Science Publishers pp 25-30

Feigal, R.J., Yesilsoy, C., Meiser, H.H., Nelson, J. (1985) Differential sensitivity of normal human pulp and transformed mouse fibroblasts to cytotoxic challenge. *Archs. Oral Biol.* **30(8)**:609-613

Fernandez-Fairen, M., Vasquez, J.J. (1983) The ageing of polymethylmethacrylate bone cement. *Acta Orthop Belg.* **49**:512

Garvin, K.L., Salvati, E.A., Brause, B.D. (1988) Role of gentamicin-impregnated cement in total joint arthroplasty. *Orthop. Clinics North America* **19(3)**:605-610

Gillett, N., Brown, S.A., Dumbleton, J.H., Pool, R.P. (1985) The use of short carbon fibre reinforced thermoplastic plates for fracture fixation. *Biomaterials* **6**:113-121

Girzadas, D.V., Geens, S., Clayton, M.L. & Leidholt J.D. (1968) Performance of a hinged metal knee prosthesis. *J. Bone Jt. Surg.* **50A(2)**:355-364

Grayson, M.A., Wolf, C.J. (1987) The solubility and diffusion of water in poly(aryl-ether-ether-ketone) (PEEK). *J. Polym. Sci.:B: Polym Phys.* **25**:31-41

Grinnell, F. (1978) Cellular adhesiveness and extracellular substrata. *Int. Rev. Cytol.* **53**:65-144

Grinnell, F., Feld, H.K. (1982) Fibronectin adsorption on hydrophilic and hydrophobic surfaces detected by antibody binding and analyzed during cell adhesion in serum - containing medium. *J. Biol. Chem.* **257**:4888-4893

de Groot, K., Geesink, R., Klein, C.P.A.T., Serekian, P. (1987) Plasma sprayed coatings of hydroxylapatite. *J. Biomed. Mater. Res.* **21**:1375-1382

de Groot, K. (1989) Letters to the Editor. *J. Biomed. Mater. Res.* **23**:1367-1371

Guess, W.L., Rosenbluth, A., Schmidt B., Autian, J. (1965) Agar diffusion method for toxicity screening of plastics on cultured cell monolayers. *J. Pharmas. Sci.* **54**:1545-1555

Gunston, F.H. (1971) Polycentric knee arthroplasty. *J. Bone Jt. Surg.* **53B**:272

Haddad, R.J., Cook, S.D., Thomas, K.A. (1987) Biological fixation of porous coated implants. *J. Bone Jt. Surg.* **69A**:1459

Harris, A.K. (1973) Cell surface movements related to cell locomotion. In: Locomotion of tissue cells, Ciba Foundation Symposium. **14**:3-20

Harvey, W., Scutt, A., Meghji, S., Caniff, J.P. (1986) Stimulation of human buccal mucosa fibroblasts *in vitro* by betel-nut alkaloids. *Archs. Oral Biol.* **31(1)**:45-49

Hayman, E.G., Engvall, E., A'Hearn, E., Barnes, D., Pierschbacher, M.D. and Ruoslahti, E. (1982) Cell attachment on replicas of SDS polyacrylamide gels reveals two adhesive plasma proteins. *J. Cell Biol.* **95**:20-23

Hench, L.L., Splinter, R.J., Allen, W.C., Greenlee, T.K. (1971) Bonding mechanisms at the interface of ceramic prosthetic materials. *J. Biomed. Mater. Res. Symp.* **2**:117

Hench, L.L. (1978) Development of a new biomaterial-prosthetic device. In: Orthopædic Mechanics: Procedures and Devices. Ghista and Roaf, London Academic Press pp287

Herman, J.H., Sowder, W.G., Anderson, D., Appel, A. M,. Hopson, C.N. (1989) Polymethylmethacrylate-induced release of bone resorbing factors. *J. Bone Jt. Surg.* **71A(10)**:1530-1541

Ho, C.P., Yasuda, H. (1988) Ultrathin coating of plasma polymer of methane applied on the surface of silicone contact lenses. *J. Biomed. Mater. Res.* **22**:919-929

Hockley, K., Baxter, D. (1986) Use of the 3T3 cell - neutral red uptake assay for irritants as an alternative to the rabbit (Draize) test. *Proc. Chem. Toxic. Meeting* **24**:473-475

Hoffman, A.S. (1986) A general classification scheme for "hydrophilic" and "hydrophobic" biomaterial surfaces. *J. Biomed. Mater. Res.* **20**:ix-xi

Holmes, R.E., Hagler, H.K., Coletta, C.A. (1987) Thick section histometry of porous hydroxyapatite implants using backscattered electron imaging. *J. Biomed. Mater. Res.* **21**:731-739

Horbett, T.A., Schway, M.B. (1988) Correlations between mouse 3T3 cell spreading and serum fibronectin adsorption on glass and hydroxyethylmethacrylate-ethylmethacrylate coploymers. *J. Biomed. Mater. Res.* **22(9)**:763-793)

Horowitz, S., Frondoza, D., & Lennox, D.W. (1986) Effect of polymethyl methacrylate on a murine macrophage P388D1 line. *Transactions of the 32nd Annual Meeting of the Orthopædic Research Society.* **11**:287

Hynes, R.O., Destree, A.T. and Wagner, D.D. (1981) Relationship between microfilaments, cell-substratum adhesion and fibronectins. *Cold Spring Harbor Symp. Quant. Biol.* **46**:659.

ICI Victrex data sheet (1985) VKT3/0386

ICI Fiberite data sheet (1986) 3a

ICI Victrex data sheet (1988) VK2/0988

ICI Victrex PEEK data sheet (1990) VK7/0190

Inoue, T., Cox, J.E., Pilliar, R.M. and Melcher, A.H. (1987) Effect of the surface geometry of smooth and porous coated titanium alloy on the orientation of fibroblasts *in vitro*. *J. Biomed. Mater. Res.* **21**:107-126

Izzard, C.S., Lochner, L.R. (1976) Cell to substrate contacts in living fibroblasts: an interference-reflexion study with an evaluation of the technique. *J. Cell Sci.* **21**:129-159

Jarcho, M. (1981) Calcium phosphate ceramics as hard tissue prosthetics. *Clin. Orthop.* **157**:259

Jasty, M.J., & Floyd, W.E. (1986) Localized osteolysis in stable, non-septic total hip replacement. *J. Bone Jt. Surg.* **68A**:912

Johanson, N.A., Bullough, P.G., Wilson, P.D. (1987) The microscopic anatomy of the bone-cement interface in failed total hip athroplasties. *Clin. Orthop.* **218**:123

Johnson, H.J., Northup, S.J., Seagraves, P.A., Garvin, P.J., Wallin, R.F. (1983) Biocompatibility test procedures for materials evaluation *in vitro*. I Comparative test system sensitivity. *J. Biomed. Mater. Res.* **17**:571-586

Judet, R., Siguier, M., Brumpt, B. (1978) A noncemented total hip prosthesis. *Clin. Orthop.* **137**:76

Kang, I., Ito, Y., Masahiko, S. and Imanishi, Y. (1989) Attachment and growth of fibroblast cells on polypeptide derivatives. *J. Biomed. Mater. Res.* **23**:223-239

Kirkpatrick, C.J., Mittermayer, C. (1990) Theoretical and practical aspects of testing potential biomaterials *in vitro*. *Materials in medicine* **1**:9-13

Klebe, R.J., (1974) Isolation of a collagen -dependent cell attachment factor. *Nature (London)* **250**:248-251

Klebe, R.J., Bentley, K.L. and Schoen, R.C. (1981) Adhesive substrates for fibronectin. *J. Cell Physiol.* **109**:481-488

Kleinman, H. K., Klebe, R.J., and Martin, G. R., (1981) Role of collagenous matrices in the adhesion and growth of cells. *J. Cell Biol.* **88**:473-485

Korvick, D.L., Newbrey, J.W., Bagby, G.W., Pettit, G.D., Lincoln, J.D. (1989) Stress shielding reduced by a silicon plate-bone interface. *Acta Orthop. Scand.* **60(5)**:611-6

Korman, N.J., Sudilovsky, O. and Gibbons, D.F. (1984) The effect of humoral components on the cellular response to textured and nontextured PTFE. *J. Biomed. Mater. Res.* **18**:225-241

Krause, W.R., Krug, W., Eng, B., Miller, J. (1982) Strength of the cement-bone interface. *Clin. Orthop.* **163**:290

Lee, A., Ling, R., Pearson, G. Fixation. In: Introduction to the biomechanics of joints and joint replacement. pp 172-187. Edited by Dowson, D., and Wright, V. Mechanical engineering publications Ltd, (1981) London.

Lentz, A.J., Horbett, T.A., Hsu, L. and Ratner, B. (1985) Rat peritoneal macrophage adhesion to hydroxyethyl methacrylate-ethylmethacrylate copolymers and hydroxystyrene-styrene copolymers. *J. Biomed. Mater. Res.* **19**:1101-1115

Lindblad, B., Wright, S.W., Sell R.L., Burkel, W.E., Graham, L.M. and Stanley, J.C. (1987) Alternative techniques of seeding cultured endothelial cells to ePTFE grafts of different diameters, porosities, and surfaces. *J. Biomed. Mater. Res.* **21**:1013-1022

Linder L., (1989) Osseointegration of metallic implants. 1. Light microscopy in the rabbit. *Acta. Orthop. Scand.* **60(2)**:129-134

Looney, M.A., Park, J.B. (1986) Molecular and mechanical property changes during aging of bone cement *in vitro* and *in vivo*. *J. Biomed. Mater. Res.* **20**:555

Lombardi, A.V., Mallory, T.H., Vaughn, B.K., Drouillard, D.O. (1989) Aseptic loosening in total hip arthroplasty secondary to osteolysis induced by wear debris from titanium-alloy modular femoral heads. *J. Bone Jt. Surg.* **71A(9)**:1337-1342

Lord, G., Marotte, J.H. (1988) Cementless revision of failed aseptic cemented and cementless total hip arthroplasties. *Clin. Orthop.* **235**:67

Lydon, M.J., Minett, T.W., Tighe, B.J., (1985) Cellular interactions with synthetic polymer surfaces in culture. *Biomaterials* **6**:396-402

MacIntosh, D.L., (1958) Hemiarthroplasty of the knee using a space occupying prosthesis for painful varus and valgus deformities. *J. Bone Jt. Surg.* **40A**:1431

Marchant, R., Hiltner, A., Hamlin, C., Rabinovitch, ., Slobodkin, R., Anderson, J. (1983) In Vivo biocompatibility studies. I. The cage implant system and a biodegradable hydrogel. *J. Biomed. Mater. Res.* **17**:301-325

Marchant, R.E., Johnson, S.D., Schneider, B.H., Agger, M.P., Anderson, J.M. (1990) Hydrophilic plasma polymerized film composite with potential application as an interface for biomaterials. *J. Biomed. Mater. Res.* **24**:1521-1537

Maroudas, N.G., (1975a) Polymer exclusion, cell adhesion and membrane fusion. *Nature (London)* **254**:695-696

Maroudas, N.G. (1975b) Adhesion and spreading of cells on charged surfaces. *J. Theor. Biol.* **49**:417-424

Matsuda T., Davies J.E., (1987) The *in vitro* response to bioactive glass. *Biomaterials* **8**:275-283

McAuslan, B.R. and Johnson, G. (1987) Cell responses to biomaterials I: Adhesion and growth of vascular endothelial cells on poly (hydroxyethyl methacrylate) following surface modification by hydrolytic etching. *J. Biomed. Mater. Res.* **21**:921-935

McKellop, H, Clarke I, Markolf, K., Amstutz, H. (1981) Friction and wear properties of polymer, metal, and ceramic prosthetic joint materials evaluated on a multichannel screening device. *J. Biomed. Mater. Res.* **15**:619-653

McMillin, C.R., Meerbaum, S.O., Schmidt, S.P. (1990) Biocompatibility testing of PEKEKK. In: *22nd International SAMPE Technical Conference*, pp 127-132.

Minoura, N., Aiba, S., Fujiwara, Y., Koshizaki, N. and Imai, Y. (1989) The interaction of cultured cells with membranes composed of random and block copolypeptides. *J. Biomed. Mater. Res.* **23**:267-279

Mosmann, T. (1983) Rapid colorimetric assay for cellular growth and survival: application to proliferation and cytotoxicity assays. *J. Immunol. Methods* **65**:55-63

Muckle, D.S., Minns, R.J. (1990) Biological response to woven carbon fibre pads in the knee. *J. Bone Jt. Surg.* **72B**:60-62

Nguyen, H.X., Ishida, H. (1987) Poly(aryl-ether-ether-ketone) and its advanced composites: a review. *Polym. Comp.* **8(2)**:57-73

Noble, P.C., Alexander, J.W., Lindahl, L.J., Yew, D.T., Granberry, W.M., Tullos, H.S. (1988) The anatomic basis of femoral component design. *Clin. Orthop.* **235**:148-163

Obara, M., Kang, M.S. and Yamada, K.M. (1988) Site directed mutagenesis of the cell-binding domain of human fibronectin: Separable, synergistic sites mediate adhesive function. *Cell* **53**:649-657

Osborn, J.F., Willich, P., Meenen, N. (1990) The release of titanium into human bone from a titanium implant coated with plasma-sprayed titanium. In: Clinical Implant Materials, Ed. Heimke, Elsevier Science Publishers pp75-80

Peacock, J.A., Fife, B., Nield, E., Crick, R.A. (1986) Examination of the morphology of aromatic polymer composite (APC-2) using an etching technique. *Composite Interfaces* 299-306

Pick, E. (1986) Microassays for superoxide and hydrogen peroxide production and nitroblue tetrazolium reduction using an enzyme immunoassay microplate reader. In: *Methods in enzymology* **132**:417-419

Pierschbacher, M.D. and Ruoslahti, E. (1984) Cell attachment activity of fibronectin can be duplicated by small synthetic fragments of the molecule. *Nature* **309**:30-33.

Pizzoferrato, A., Ciapetti, G. Human lymphocytes (^{3}H) thymidine uptake test for the evaluation of alloplastic material bioçompatibility. In: Ceramics in Surgery, edited by Vincenzini, Elsevier Scientific Publishing Company, Amsterdam, 1983

Poss, R., Walker, P., Spector, M., Reilly, D.T., Robertson, D.D., Sledge, C.B. (1988) Strategies for improving fixation of femoral components in total hip arthroplasty. *Clin. Orthop. Rel. Res.* **235**:181-193

Pytela, R., Pierschbascher, M.D. and Ruoslahti, E. (1985) Identification and isolation of a 140kD cell surface glycoprotein with properties expected of a fibronectin receptor. *Cell* **40**:191-198

Robertson, D.D., Walker, P.S., Granholm, J.W., Nelson, P.C., Weiss, P.J., Fishman, E.K., Magid, D. (1987) Design of custom hip stem prostheses using three dimensional CT modelling. *J. Comp. Assisted Tomog.* **11(5)**:804-809.

Rushton, N., Rae, T., (1984) The intra-articular response to particulate carbon fibre reinforced high density polyethylene and its constituents: an experimental study in mice. *Biomaterials* **5**:352-356

Salthouse, T. (1984) Some aspects of behaviour at the implant interface. *J. Biomed. Mater. Res.* **18**:395-401

Saunders, S., Bernfield, M. (1987) Cell surface proteoglycan binds mouse mammary epithelial cells to fibronectin and behaves as an interstitial matrix receptor. *J. Cell Biol.* **106**:423-430

Schakenraad, J.M., Busscher H.J., Wildevuur, C.R.H., and Arends, J., (1986) The influence of substratum surface free energy on growth and spreading of human fibroblasts in the presence and absence of serum proteins. *J. Biomed. Mater. Res.* **20**:773-784

Schakenraad J.M., Kuit, J.H., Arends, J., Busscher, H.J., Feyen, J. and Wildevuur, Ch. R.H. et al. (1987) In vivo quantification of cell-polymer interactions. *Biomaterials* **8**:207-210

Schatzker, J. Smith, G., Clark, R., McBroom, R. (1978) Strain gauge analysis of bone response to internal fixation. *Clin. Orthop.* **132**:244-51

Schauer, U., Krolikowski, I., Rieger, C. (1989) Detection of activated lymphocyte subsets by fluorescence and MTT staining. *J. Immunol. Methods* **116**:221-227

Schmalz, G., Netuschil, L. (1985) A modification of the cell culture agar diffusion test using fluoresceindiacetate staining. *J. Biomed. Mater. Res.* **19**:653-661

Schmidt G., Robenek, H., Harrach, B., Glossl, J., Nolte, V., et al. (1987) Interaction of small dermatan sulfate proteoglycan from fibroblasts with fibronectin. *J. Cell Biol.* **104**:1683-1691

Seballe, K., Hansen, E.S., Rasmussen, H., Pedersen, C.M., Bunger, C. (1990) Hydroxyapatite coating enhances fixation of porous coated implants. *Acta. Orthop. Scand.* **61(4)**:299-306

Sgouras, D., Duncan, R. (1990) Methods for the evaluation of biocompatibility of soluble synthetic polymers which have potential for biomedical use: 1 - Use of the tetrazolium -based colorimetric assay (MTT) as a preliminary screen for evaluation of *in vitro* cytotoxicity. *Materials in Medicine* **1(2)**:61-68

Shelton, R.M., Rasmussen, A.C., and Davies, J.E. (1988) Protein adsorption at the interface between charged polymer substrata and migrating osteoblasts. *Biomaterials* **9**:24-29

Shirandami, R., Esat, I.I. (1990) New design of hip prosthesis using carbon fibre reinforced composite. *J. Biomed. Eng.* **12**:19-22

Skerry, T., Suswillo, R., Haj, A., Ali, N., Dodds, R., Lanyon, L. (1990) Load-induced proteoglycan orientation in bone tissue *in vivo* and *in vitro*. *Calcif. Tissue Int.* **46**:318-326.

Skondia, V., Davydov, A.B., Belykh, S.I., Heusghem, C. (1987) Chemical and physicomechanical aspects of Biocompatible Orthopaedic Polymer (BOP) in bone surgery. *J. Int. Med. Res.* **15**:293

Soltesz, U. Baudendistel, W. (1989) Concepts for determining the bond between implant materials and bone. Proceedings from: 8th European Conference on Biomaterials, Heidelberg.

Spector, M. (1987) Historical review of porous coated implants. *J. Arthrop.* **2(2)**:163-177

Spector, M., Cheal, E.J., Jamison, R.D. (1990) Composite materials for hip replacement prostheses. In: *22nd International SAMPE Technical Conference*, pp 1119-1130

Sipehia, R. (1990) The enhanced attachment and growth of endothelial cells on anhydrous ammonia gaseous plasma modified surfaces of polystryene and poly(tetrafluoroethylene). *Biomat., Art. Cells, Art. Org.*, **18(3)**:437-446

Tanner, K.E., Doyle, C. Bonfield, W. (1990) The strength of the interface developed between biomaterials and bone. In: Clinical Implant Materials, Ed. Heimke, Elsevier Science Publishers pp149-154

Taylor, S.R., Gibbons, D.F. (1983) The effect of surface texture on the soft tissue response to polymer implants. *J. Biomed. Mater. Res.* **17**:205-228

Tayton, K., Johnson-Nurse, C., McKibbin, B., Bradley, J., Hastings, G.W. (1982) The use of semi-rigid carbon-fibre reinforced plastic plates for fixation of human fractures. *J. Bone Jt. Surg.* **64B**:105-111

Thomas, K.A., and Cook, S.D. (1985) An evaluation of variables influencing implant fixation by direct bone apposition. *J. Biomed. Mater. Res.* **19**:875-901

Thomas, K.A., Kay, J.F., Cook, S.D., Jarcho, M. (1987) The effect of surface macrotexture and hydroxylapatite coating on the mechanical strengths and histologic profiles of titanium implant materials. *J. Biomed. Mater. Res.* **21**:1395-1414

Townley, C.O. (1988) Total knee arthroplasty: a personal retrospective and prospective review. *Clin. Orthop. Rel. Res.* **236**:8-22

Tran, C.N.B., Walt, D.R. (1989) Plasma modification and collagen binding to PTFE grafts. *J. Colloid Interface Sci.* **132**:373-381

Tullos, H.S. (1984) Total hip arthroplasty with a low modulus porous coated femoral component. *J. Bone Jt. Surg.* **66A**:888

Turner, R.M., Cogswell, F.N. (1986) The effect of fibre characteristics on the morphology and performance of semi-crystalline thermoplastic composites. *18th International SAMPE Technical Conference* pp32

Underwood, P.A. and Bennett, F.A. (1989) A comparison of the biological activities of the cell-adhesive proteins vitronectin and fibronectin. *J. Cell Sci.* **93**:641-649

Vallee, B.L., & Ulmer, D.D. (1972) Biochemical effects of mercury, cadmium, and lead. *Annual Rev. Biochem.* **41**:91

van der Valk, P., van Pelt, A.W.J., Busscher, H.J., de Jong, H.P., Wildevuur, Ch.R.H., Arends, J. (1983) Interaction of fibroblasts and polymer surfaces: relationship between surface free energy and fibroblast spreading. *J. Biomed. Mater. Res.* **17**:807-817

Vogler, E.A., and Bussian, R.W., (1987) Short-term cell-attachment rates: A surface sensitive test of cell-substrate compatibility. *J. Biomed. Mater. Res.* **21**:1197-1211

Wang, Q., Springer, G.S. (1989) Moisture absorption and fracture toughness of PEEK polymer and graphite fiber reinforced PEEK. *J. Composite Materials* **23**:434-447

Watson, L.P., Kang, Y., Falk, M.C. (1989) Cytochemical properties of osteoblast cell membrane domains. *J. Histochem. Cytochem.* **37(8)**: 1235-1246

Wayner, E.A. and Carter, W.G., (1987) Identification of multiple cell adhesion receptors for collagen and fibronectin in human fibrosarcoma cells possessing unique α and β subunits. *J. Cell Biol.* **105**:1873-1884

Weiss, P. (1941) Nerve patterns: the mechanics of nerve growth. *Growth* (suppl) **5**:163-203

Wenz, L.M., Brown, S.A., Moet, A., Merritt, K., Steffee, A. (1989) Accelerated testing of a composite spine plate. *Composites* **20(6)**:569-574

Wenz, C.M., Merritt, K., Brown, S.A., Moet, A. (1990) *In vitro* biocompatibility of polyetheretherketone and polysulfone composites. *J. Biomed. Mater. Res.* **24**:207-215

Williams D.F. (1987a) Definitions in biomaterials. Amsterdam, Elsevier.

Williams, D.F., McNamara, A., Turner, R.M. (1987b) Potential of polyetheretherketone (PEEK) and carbon-fibre-reinforced PEEK in medical applications. *J. Mat. Sci. Letters* **6**:3

Wright, T.M., Rimnac, C.M., Faris, P.M., Bansal, M. (1988) Analysis of surface damage in retrieved C-fibre reinforced and plain polyethylene tibial components from posterior stabilized total knee replacements. *J. Bone Jt. Surg.* **70A(9)**:1312-1319

Woo, S.L.Y., Akeson, W.H., Levenetz, B., Coutts, R.D., Matthews, J.V., Amiel, D. (1974) Potential application of graphite fibre and methyl methacrylate resin composites as internal fixation plates. *J. Biomed. Mater. Res.* **8**:321-338

Yamada, K.M. and Kennedy, D.W. (1987) Peptide inhibitors of fibronectin, laminin, and other adhesion molecules: Unique and shared features. *J. Cell Physiol.* **130**:21-28

Yasuda, H., Gazicki, M. (1982) Biomedical applications of plasma polymerization and plasma treatment of polymer surfaces. *Biomaterials* **3**:68-77

Yeh, Y.S., Iriyama, Y., Matsuzawa, Y., Hanson, S.R., Yasuda, H. (1988) Blood compatibility of surfaces modified by plasma polymerization. *J. Biomed. Mater. Res.* **22**:795-818

Yoda, O. (1984) The radiation effect on non-crystalline poly(aryl-ether-ether-ketone) as revealed by X-ray diffraction and thermal analysis. *Polym. Comm.* **25**:238-240